Investigation of Cochlear Disturbance Induced During Surgical Intervention

A thesis submitted for the degree of Doctor of Philosophy

By

Yu Zhang

College of Engineering, Design and Physical Sciences

Brunel University London

2018

Abstract

Hearing loss is a common impairment or disability for human beings, and is impacting an increasing amount of people, augmented by the growing aging population around the globe. Cochlear implantation, as one of the most effective ways to restore hearing, can only applied to profoundly deaf patients at the moment. In order to expand the group of people who can benefit from cochlear implantation to those with less severe hearing loss, endeavours need to be made to best preserve residual hearing and minimise trauma induced during cochlear implantation surgery.

In this thesis, the disturbance induced in the cochlea, i.e. the acoustic and mechanical energy transmitted into the cochlea, during cochleostomy drilling is studied – as well as establishing a comparison between a manually guided conventional technique and a manually supported tissue guided robotic drilling technique. The results show that by changing surgical techniques and how they are applied can have a significant impact on levels of disturbance induced – robotic-aided approach induced lower level of equivalent SPL for up to 86% of the time and can be as much as 39 dB lower than that generated by conventional surgical drilling.

This work is timely because trauma is an important consideration to clinicians and health care providers. Cochleostomy is one of the major and most disruptive

surgical process during cochlear implantation. With the increasing amount of cochlear implant electrode array designs that are shorter and less intrusive, and the increasing demand of electric-acoustic stimulation via cochlear implant to better resemble the human auditory system, the approach to reduce disruption during cochleostomy drilling is highly relevant to the progression in the hearing care industry and the benefits of the growing hearing impairment community.

Acknowledgements

I would like to thank Professor Peter Brett for giving me the opportunity to embark on this journey, for welcoming me as his student, extending his kindness, patience and understanding, and sharing his knowledge and wisdom. I would like to thank Dr Xinli Du for his invaluable guidance and support, intelligibly and emotionally, through every stage of my PhD research. I would also like to thank Dr Nikolaos Boulgouris for his enthusiasm and professionalism in supervision, for sharing his wealth of knowledge on signal processing, and for the stimulating and insightful discussions we had.

I'd like to express my sincerest gratitude towards our collaborating researchers from University Hospitals Birmingham NHS Foundation Trust: Professor Philip Begg, Mr Alistair Mitchell-Innes, Mr Chris Coulson and Mr Richard Irving, for their help in securing cadaver lab access, their full suite of acoustic measurement facilities and their clinical expertise. In addition, I would like to thank Queen Elizabeth Hospital Birmingham Charity for funding my research.

I would also like to thank people for their invaluable friendship and kindness throughout my years at Brunel Institute for Bioengineering: Ms Jenny Kume, Shima Abdullateef, Angel Naveenathayalan, Dr Madalina Negoita, Dr Ruth Mackay, Dr Nicola Pomella, Dr Shavini Wijesuriya, Lei Hou, Qunfang Jiang, Dr

Svetlana Ignatova and Dr Carola Koenig. A special thank goes out to Professor Colin Clark for being a wonderful friend and always a good listener.

Finally, I would like to thank my parents, Xingqiang Zhang and Tianzhu Jin, my parents-in-law, Wei Lin and Hong Guo, and my husband Yun, for their continuing support, encouragement and love.

I dedicate this work to my parents Mr Xingqiang Zhang and Ms Tianzhu Jin

for their unconditional love and care throughout my life.

Contents

Chapter 1 Introduction 1
1.1 Aims 3
1.2 Relevance of the Research.....4
1.3 The Mechanism of Hearing.....7
1.4 Considerations, Approach and Objectives 10
1.5 Thesis Layout 12
1.6 Outcomes of the Research.....13
Chapter 2 Background and Literature Review 15
2.1 Hearing Loss Treatment Landscape 15
2.1.1 Conventional hearing aids.....17
2.1.2 Implantable Hearing Aids 19
2.1.3 Cochlear Implants 21
2.2 Numerical Modelling of Cochlear Mechanics 24
2.3 Experimental Techniques to Study Cochlear Dynamics.....25
2.3.1 Laser Doppler Vibrometry 25
2.3.2 Historic techniques and latest development of tools and techniques……29
2.4 Literature Review on Measurement of Cochlear Noise Exposure during Ear Surgery.....30

2.4.1 Methods to Measure Cochlear Noise Exposure to Disturbance during Ear Surgery....32
2.4.2 Previous Findings of the Noise Exposure of the Inner Ear during Cochleostomy Drilling....39
2.5 Conclusions....48
Chapter 3 Mathematical Model of Cohclear Mechanics....49
3.1 Anatomy and Function of Cochlea....51
3.2 Formulation of the Problem....56
3.2.1 Abstraction and Assumptions....56
3.2.2 Hydrodynamics....59
3.2.3 Mathematical Formulation and Boundary Condition....61
3.2.4 Summary of Equations....65
3.3 Numerical Solutions and Results....66
3.3.1 Cochlear Frequency Sensitivity....67
3.3.2 Effect of Creating a TW....70
3.4 Discussion and Conclusions....76
Chapter 4 Experimental Study of Cochlear Dynamics using Porcine Cochlea....78
4.1 Use of Porcine Cochlea....79
4.2 Experimental Setup....80
4.3 Effects of Creating a Third Window on the cochlea....87
4.4 Conclusions....90
Chapter 5 Chapter 5: Experimental Methods to Study the Mechanical Energy Cochlea is Exposed to during Cochleostomy Formation....91
5.1 Importance of Hearing Preservation Study....92
5.2 Experimental Methods....96
5.2.1 Cadaveric Head Preparation for Acoustic Measurements....96
5.2.2 Calibration of Sound Conducting Qualities....97
5.2.3 Measurement of Round Window Velocity during Drilling Procedure....101

5.2.4 Calculation of Equivalent Sound Pressure Level.....107
5.3 Data Processing.....110
5.3.1 Algorithm for Signal Drop-off Recognition.....111
Chapter 6 Noise Exposure of Human Cochlea during Cochleostomy 121
6.1 Analysis and Results.....122
6.1.1 Time Series Analysis.....122
6.1.2 Determination of the Middle Ear Transfer Function.....127
6.1.3 Frequency Spectrum of Round Window Velocity.....132
6.1.4 Equivalent Sound Pressure Level Induced during Cochleostomy Formation.....139
6.1.5 Instantaneous Total Sound Pressure Level Induced during Cochleostomy Formation.....149
6.2 Discussion.....156
6.3 Concluding Section.....158
Chapter 7 Conclusions and Suggestions for Future Work 161
7.1 Summary and Conclusions.....161
7.2 Future Work.....166
Appendix A **.....168**
A.1 Removal of 'Off-target' Events.....169
A.2 Baseline Drift Correction.....171
Appendix B **.....173**
B.1 Spectral Analysis.....173
B.2 Equivalent Sound Pressure Level.....175
B.3 Equivalent Sound Pressure Level against Time.....176
Appendix C **.....179**
References **.....182**

List of Figures

Figure 1.3 -1 Anatomical diagram of the hearing system …… 8

Figure 1.3 -2 Corss section of one loop of the cochlea …… 9

Figure 2.1.1 -1 The typical construction of a behind-the-ear conventional hearing aid ……... 19

Figure 2.1.3 -1 The standard design of a cochlear implant ……..... 22

Figure 2.3.1 -1 Schematic layout of a Laser Virbometer ……..... 27

Figure 2.3.1 - 2 | An example of retro-reflective speckle noise …… 29

Figure 3.1 -1 Physiology properties of cochlea ……..…. 54

Figure 3.2.1 -1 Two-dimensional box model of cochlea …….…….. 57

Figure 3.3.1 -1 Magnitude of the basilar membrane displacement …….…... 68

Figure 3.3.1 -2 Phase of the basilar membrane displacement …….……69

Figure 3.3.2 -1 Basilar membrane displacement before and after a TW created at 2mm from stapes along the cochlear wall …….……. 73

Figure 3.3.2 -2 Basilar membrane displacement before and after a TW is created at 2mm, 15mm and 30mm from stapes along the cochlear wall ……..... 74

Figure 4.1 -1 A porcine cochlea with intact stapes and round window …..... 80

Figure 4.2 -1 Experimental setup ……... 81

Figure 4.2 -2 Microscopic view of the cochlea …….…. 83

Figure 4.2 -3 Illustration of cochlea mounting …….…. 86

Figure 4.2 -4 A close-up view of the experimental setup …….…. 84

Figure 4.2 -5 The experimental setup showing cochlea, robotic held piezo actuator and microscopic part of the laser vibrometer ……..…. 87

Figure 4.3 -1 Round window velocity before and after cochleostomy ……..… 89

Figure 5.2.2 -1 Schematic illustration of the calibration setup …….…… 99

Figure 5.2.2 -2 Calibration setup in the lab on the human cadaver head (proximal) …….…..… 99

Figure 5.2.3 -1 Round window vibration measurement using laser vibrometer while the surgeon was performing cochleostomy drilling …….….. 102

Figure 5.2.3 -2 Force and torque transients versus time during robotic drilling ……..... 104

Figure 5.2.3 -3 Surgeon's microscopy view showing two complete cochleostomy formation and the round window with retroreflective tape …….. 105

Figure 5.3 -1 Data processing flow chart: Time Series Analysis ……..... 111

Figure 5.3.1 -1 After Processing Stage A, data samples satisfying condition 1 get recognised as drilling signal and kept their original values …...…… …… 116

Figure 5.3.1 -2 After Processing Stage A, data samples satisfying either condition 1 or condition 2 get recognised as drilling signal and kept their original values …… 117

Figure 5.3.1 -3 A 3-millisecond recording before and after being processed .. 120

Figure 6.1.1 -1 Round window vibration velocity throughout the whole cochleostomy drilling procedure - Cochlea A ……..… 123

Figure 6.1.1 -2 Round window vibration velocity throughout the whole cochleostomy drilling procedure – Cochlea B ……..… 124

Figure 6.1.1 -3 Round window vibration velocity throughout the whole cochleostomy drilling procedure – Cochlea C ……. 125

Figure 6.1.1 -4 Comparison between conventional and robotic drilling methods – rms round window velocity over the whole cochleostomy procedure …….…. 127

Figure 6.1.2 -1 Middle ear transfer functions of Cochlea A, B, and C …… 131

Figure 6.1.3 -1 Frequency spectrum of the drilling signal covering the whole cochleostomy procedure - Cochlea A ……. 135

Figure 6.1.3 -2 Frequency spectrum of the drilling signal covering the whole cochleostomy procedure - Cochlea B ……. 136

Figure 6.1.3 -3 Frequency spectrum of the drilling signal covering the whole cochleostomy procedure - Cochlea C ……. 137

Figure 6.1.3 -4 3-D spectrogram of drilling-evoked round window vibration velocity ……. 138

Figure 6.1.4 -1 Mean equivalent sound pressure level - calculated at the corresponding METF-specified frequencies ……..... 141

Figure 6.1.4 -2 Mean equivalent sound pressure level – calculated over 1/3 octave band of the corresponding METF-specified frequencies ……..…. 141

Figure 6.1.4 -3 METF-RW after spline interpolation …….. 143

Figure 6.1.4 -4 Equivalent sound pressure level generated during conventional and robotic drilling – on Cochlea A ……. 145

Figure 6.1.4 -5 Equivalent sound pressure level generated during conventional and robotic drilling – on Cochlea B ……. 146

Figure 6.1.4 -6 Equivalent sound pressure level generated during conventional and robotic drilling – on Cochlea C ……. 147

Figure 6.1.4 -7 A comparison of the peak amplitude of the induced mechanical disturbance in terms of equivalent sound pressure level ……..…. 148

Figure 6.1.5 -1 Sound Pressure Level plotted against time, normalised by total drilling time on Cochlea A ……...……..... 153

Figure 6.1.5 -2 Sound Pressure Level plotted against time, normalised by total drilling time on Cochlea B……...…….……..... 154

Figure 6.1.5 -3 Sound Pressure Level plotted against time, normalised by total drilling time on Cochlea C……...…….……..... 155

List of Tables

Table 2.1.2 - 1 Operation time and cost for common hearing implants per ear ……... 20

Table 2.4.2 -1 Previous studies of cochlear noise exposure during ear surgery …… 46

Table 5.2.3 -1 Experiment sequence ……..... 107

Table 6.1.5 -1 Statistics for the equivalent sound pressure level over time 152

List of Abbreviations

BM	Basilar membrane
CI	Confidence interval
DB	Decibel
EAS	Electric acoustic stimulation
FFT	Fast Fourier transform
LDV	Laser Doppler Vibrometer
METF	Middle ear transfer function
OC	Organ of Corti
OW	Oval Window
RM	Reissner's membrane
RW	Round window
RWM	Round window membrane
SNR	Signal-to-noise ratio
SPL	Sound pressure level
SPL_eq	Equivalent sound pressure level
SV	Scala vestibule
SM	Scala media
ST	Scala tympani
VM	Vestibular membrane

Chapter 1

Introduction

Hearing loss is a common impairment or disability for human beings. The influence hearing loss has on patients and the wider society is profound. It not only significantly affects both the physical and mental fitness of patients, but also on the lives of their families. Among the alternatives to conventional hearing aids, cochlear implantation is a remedy with remarkably good hearing restoration. However it can only applied to profoundly deaf patients at the moment. In in recent years, residual hearing preservation has attracted increasing attention. One of the major reasons for this arising interest is to maximise the benefits of cochlear implantation for all prospective patients – with as little sacrifice of their residual hearing as possible. Endeavours need to be made to

best preserve residual hearing and minimise trauma induced during cochlear implantation surgery.

The principal aim of this research is to investigate the disturbance induced in the cochlea by surgical therapy. It focuses on the one of the major and most disruptive surgical process during cochlear implantation - cochleostomy. In the work, a non-contact experimental method was devised to achieve this aim and to enable an approach that has versatility for further investigations in future. To validate the approach, different techniques in cochleostomy were contrasted to identify causes of principal disturbance leading to trauma of tissues and to the hearing organ. The results show that by changing surgical techniques and how they are applied can have a significant impact on levels of disturbance induced.

It is important to state that the experimental techniques are intended to provide a better understanding for the therapies, and possibly new devices, where performance can be measured. Porcine and cadaver cochlea have been investigated by the techniques. This work is timely because trauma is a consideration currently viewed as important by clinicians and manufactures of hearing devices.

1.1 Aims

The principal aim of this research is to investigate the disturbance induced in the cochlea by surgical therapy, and through this, to develop a reliable and repeatable approach to quantify the level of disruption in a context that is more widely comprehensible.

To answer the question of how traumatic surgical therapy is to hearing is of course difficult to achieve at the causal stage as further evidence will be necessary with regard to patient post-operative performance. This will be a topic of further investigation following on from this work. In this work the interest is in the methods of reducing the amplitude of disturbance induced within the cochlea, on the basis that a lower amplitude poses reduced risk to preservation of patient residual hearing. Experimental measurement of the range of disturbances generated during surgical operation relative to natural sound has been important, particularly in terms of understanding how amplitudes compared with the normally applied thresholds of sound levels that lead to temporary and permanent deafness. Techniques to build the relationship with such data have to be developed. The focus on the cochlea, the central sensing organ, has been strategic as it is both a vital and sensitive point in the hearing mechanism. The cochlea organ is effectively a ‘sealed fluid volume’ and the ideal measuring technique has to be inert to the natural hearing process. Any modification to the cochlea has to be justified such that there is no effect strong enough to alter the conclusions that can be drawn on the parameters to be assessed.

Cochleostomy is chosen as the surgical therapy under investigation in this thesis because firstly cochlea is a delicate sensing organ within the hearing procedure; secondly there is a real need for cochleostomy in the treatment of significant hearing loss, as more details are presented in Section 1.2. Drilling into cochlea is also considered to be a possible starting point, in terms of devising a new measuring technique that is applicable to investigate along the length of the cochlea. However consistent exposure of the membrane underlying the bone capsule of the cochlea, without puncture, is a requirement and difficult to achieve in practice. Ideally the procedure should enable evaluation of disturbance of surgical techniques applied at other points of the hearing chain.

1.2 Relevance of the Research

The motivation for research into surgically induced disturbance is to meet the pressing challenges that arise from the increasing impact that hearing loss poses on the lives of individuals, families, society and the growing awareness, among clinicians and patients community, of the benefits of residual hearing preservation during surgery.

Hearing loss is a common impairment or disability for human beings. The percentage of people in western countries who have a hearing impairment that necessitates adoption of hearing aids is approximately 15% (Lunner, Rudner, & R??nnberg, 2009). In the UK alone, the number of people with a form of hearing loss exceeded 10 million by 2011 (Action On Hearing Loss, 2011). Similar to other senses, it is very common that hearing degrades with age. The percentage

of people over 70 years old in UK who have hearing loss is 71.1% (Action On Hearing Loss, 2011). With increasing life expectancy and consequently a growing aging population in the UK and around the world, the number of people suffering hearing loss is expected to soar. Inadequately controlled exposure to loud sound contributes to hearing loss. The growing variety of loud sound sources in our everyday life, including tools and machines in the work place, headphones and loudspeakers, places more people at greater risk of hearing impairment, and could contribute further to the statistics of hearing impairment.

The influence hearing loss has on patients and the wider society is profound. Hearing loss not only significantly affects both the physical and mental fitness of patients; it frustrates their social interaction and economic productivity. This has a significant impact on their potential of life and lives of their families. For patients suffering hearing loss since an early stage in their life, personal development can be extremely challenging with limited opportunities and resources, compared to their normal-hearing counterparts. In short, the increasing number of people at risk, the harm it brings to the patients and the care pressure it places on the family members of the patients and the community can lead to long-term negative social and economic consequences.

Residual hearing preservation has attracted increasing attention in recent years. Cochlear implantation is a remedy with remarkably good hearing restoration. However it is only applied to profoundly deaf patients. The reason for this discrimination relates to poor preservation of tissue and hearing preservation during the implantation process. The tier of patients above the threshold of

'Profoundly Deaf', are not considered for implantation as they would likely suffer a noticeable loss in residual hearing. The consistent and satisfactory performance of cochlear implants has aroused interest among patients with some residual hearing. The development of electroacoustic electrodes enables electric acoustic stimulation (EAS) - a combination of electric stimulation and preserved hearing amplification, which delivers enhanced speech perception for patients who have substantial hearing at certain frequencies especially in the low-frequency range (Gantz, Turner, Gfeller, & Lowder, 2005)(Turner, Gantz, Karsten, Fowler, & Reiss, 2010)(vonIlberg et al., 1999)(Kiefer et al., 2004)(Gantz, Turner, & Correspondence, 2003)(Gantz & Turner, 2004). To leverage EAS and maximise the benefits of cochlear implantation for all prospective patients, endeavours have to be made to best preserve residual hearing and minimise trauma induced during cochlear implantation. Among different stages in the surgical procedure of cochlear implantation, cochleostomy is considered crucial to hearing preservation (Lehnhardt, 1993). The reasons are two fold, the considerable chance of inadvertent perforation being the first. Inadvertent perforation is destructive as it exposes the cochlea to perilymph contamination – by bone dust and exotic fluid like blood, and the risk of drill bit entering scala vestibuli and potentially damaging the basilar membrane where sensory cells are located. Secondly, the action of drilling on the delicate central sensing organ can cause acoustic mechanical trauma - inner ear trauma resulted from excessive acoustic stimuli or in general mechanical disturbance. Drill-induced mechanical trauma is proven to be severe in middle ear surgery especially if the ossicular chain is drilled unintentionally (Jiang et al., 2007).

In this thesis, the mechanical disturbance generated during cochleostomy will be evaluated – by experimentally quantifying the mechanical energy the cochlea is exposed to, and contrasted to the energy exposure when a relatively atraumatic cochleostomy technique enabled by robotics is used instead.

1.3 The Mechanism of Hearing

To set the scene for discussion in this thesis, an introduction to the physiology of the auditory system is provided in this section.

The ear, or the peripheral auditory system, can be divided into three parts: outer, middle and inner ear as shown in Figure 1.3-1. The sensory organ of the ear is located in the inner ear – a snail-shaped bony structure called cochlea. Two intrinsic membrane-covered openings on cochlea called oval window (OW) and round window (RW), are both located at the basal end of the cochlea. Sound enters via pinna, travels through the external auditory canal and causes the eardrum to vibrate. The vibrations are then transmitted to the inner ear through the vibrating ossicles in a chain. The last part of the ossicular chain is the stapes. It is in direct contact with one of the openings on the cochlea mentioned above called OW. The vibration energy of stapes is transduced into motion in the fluid inside the cochlea called perilymph.

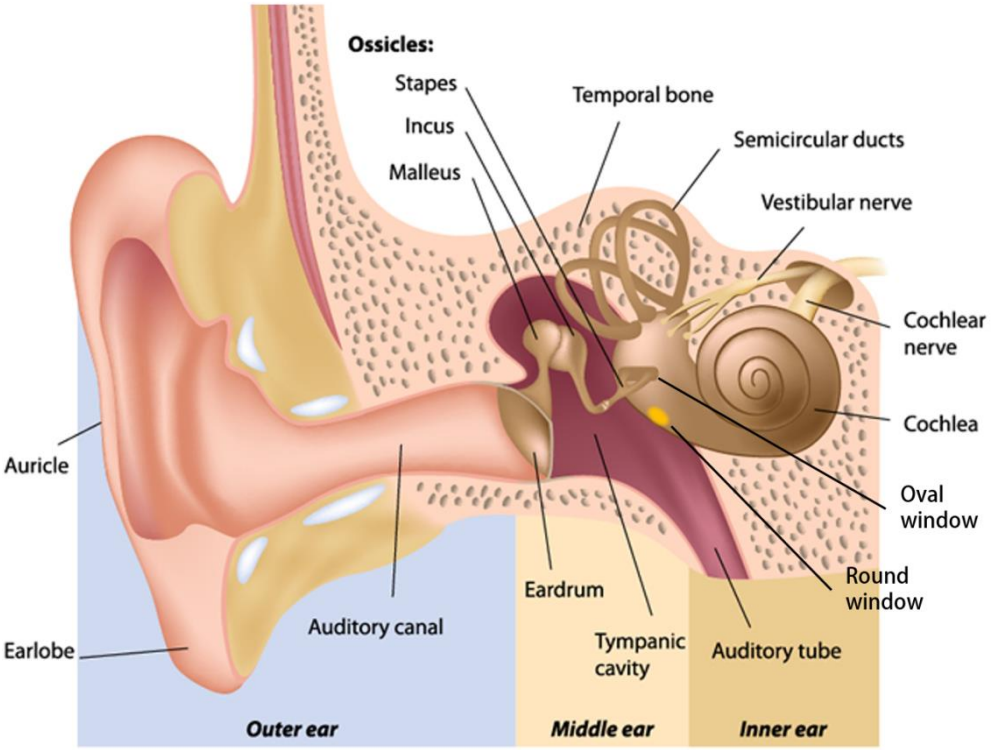

Figure 1.3 - 1 | Anatomical diagram of the hearing system. Adapted from Alila Medical Media Shutterstock [11]

Figure 1.3-2 is the cross-section of one loop of the cochlea. The diameter of one loop is approximately 1.5 mm. The motion in the fluid stimulates vibration of the basilar membrane (BM) where acoustic signal is processed and discriminated along the length of cochlea from the basal to the apical end. The outer and inner hair cells located on BM function as receptor cells. The mechanical movement is transduced into the electrochemical signal to stimulate the auditory nerve via hair cells. Due to the tapered shape and the graded stiffness of BM, each point on the BM has one particular frequency that it responds most significantly to. High-frequency sound stimulates mostly the part of BM close to the basal end of the

cochlea, while low-frequency sound causes stronger response towards the apical end of the BM.

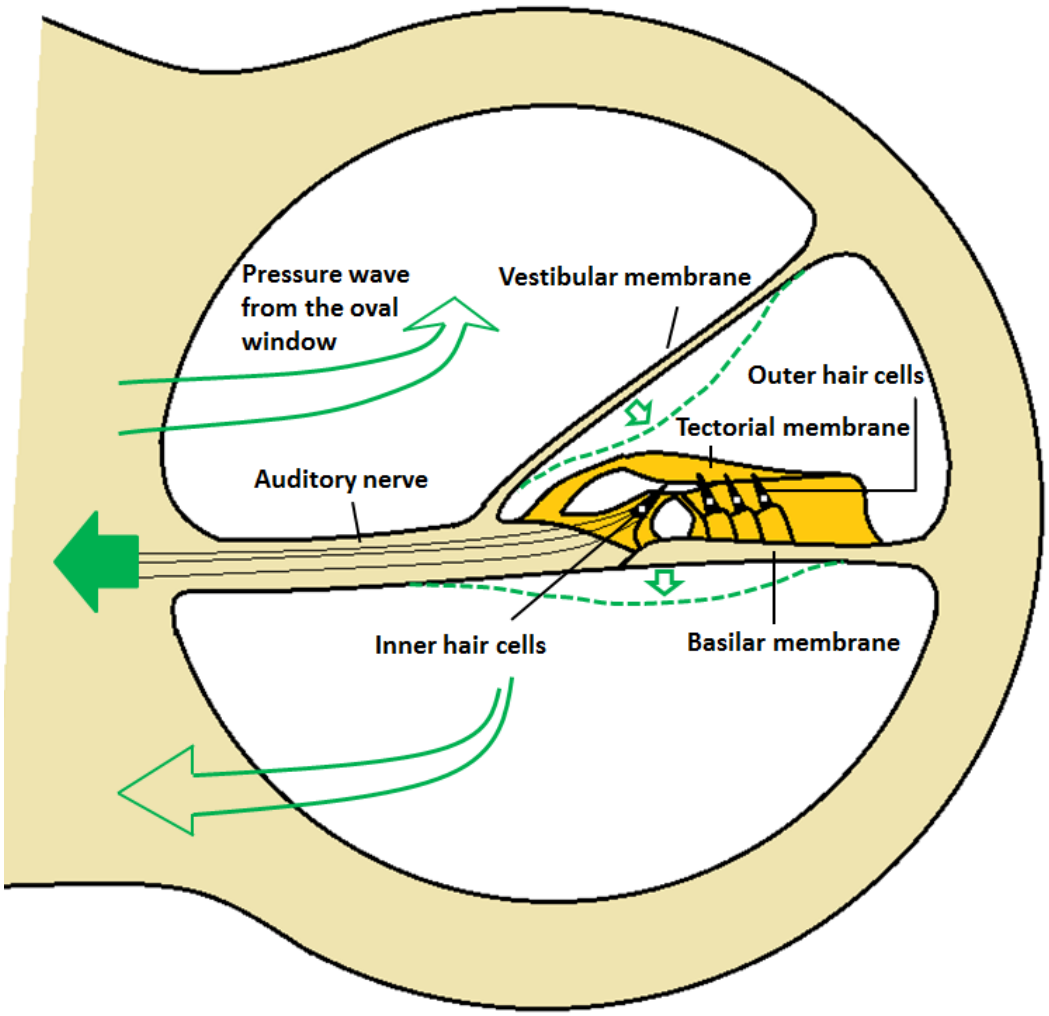

Figure 1.3 - 2 | Cross section of one loop of the cochlea. Adapted from Hohmann and Schmuckli [12]

The enclosure of the cochlea capsule and the limited size of it impose challenges on the design and execution of experimental measurements. To capture the natural response of the cochlea to disturbance induced by surgical intervention, a

non-contact method is adopted to satisfy both accuracy and integrity as the key considerations in biological sample manipulation and measurements.

1.4 Considerations, Approach and Objectives

To achieve the aims put across in Section 1.1, the following principal objectives had to be met:

- Obtain Experimental measurement of the range of mechanical disturbances generated during surgical operation of cochleostomy;
- Develop both the experimental and computational approach to relate the mechanical disturbance measured to natural sound levels;
- Measurement made on real cochlea, with as much close relevance to surgical reality as possible, along with control in place to isolate target from ambient noise or other sources of signal contamination.

To assist understanding of the objectives, the considerations and corresponding approach applied in the investigation are explained to offer reality in context.

Measurements have to be taken on real cochlea. It is ineffective and unproductive to set up measurements on an artificial replica since a range of tissue properties largely remain unknown and are difficult to find in any other way. Porcine cochlea was used to develop the experimental techniques in the

laboratory. This led to clinical investigations on human cadaver specimen. The use of human cadaver specimen within the head is to test the techniques in as a realistic situation as possible for surgical relevance.

The small size of cochlea offers limited scope for manipulation. Experiments are designed to enable access of measuring systems. The quantity to be measured – membrane vibration velocity, is in very small magnitude and prone to ambient noise. Measures have to be taken to enable isolation or control with respect to ambient noise.

As the cochlea is an enclosed bone tissue capsule, it requires a technique to expose endosteum without perforating it. The exposure also needs to be created consistently at each point along the cochlea bony wall and on each cochlea sample. Therefore a measure to create consistent windows is required to eliminate sources of distortion and to increase accuracy in the investigation.

The approach chosen is such that there is insignificant influence on the parameters to be measured. It was determined that the limited modification made by the experimental approach does not notably modify the dynamics of the cochlea, for example the effect of drilling at multiple points on the cochlea.

A model of cochlear dynamics yielding insights on the sensitivity of placement of measurement and the effects of modification to cochlear is a valuable tool. This helped to prepare the experimental approach, and reduced time spent on measurements for which there was no benefit toward the aims of the work.

Experimental measurement of the range of disturbances generated during surgical operation relative to natural sound has been important to understand how amplitudes impinge on thresholds that are normally applied to assess sound levels that lead to temporary and permanent deafness. Techniques to build the relationship with such data have to be developed.

1.5 Thesis Layout

This thesis is divided into 6 chapters following introduction.

Chapter 2 reviews previous experimental studies on cochlear mechanics and technologies and tools developed or deployed for defining the characteristics and properties of cochlea, either its static parameters or its dynamic response to mechanical stimuli. The state-of-art hearing aid technology is also reviewed at the beginning, which provides the context for the motivation for this study.

Chapter 3 describes the model developed to provide guidance on the planning and control in the experimental study on cochlea. The limited range of structural modification can be introduced on the cochlea without fundamentally altering its dynamics is simulated. Insights are also obtained on sites that cannot be gauged directly in the lab to deepen the understanding that can be achieved from experimental observation.

Chapter 4 describes work performed in the laboratory on porcine cochlea to assess the considerations and controls that need to be in place for a valid, consistent set of measurements on cochlea. The principles used, procedures

designed and tools deployed are presented in this chapter with the reasoning explained.

Chapter 5 describes work performed on human cadavers to obtain quantitative assessment of the effect that surgical intervention exerts on the cochlea, and to evaluate the benefits that the robotic surgical technique can offer.

Chapter 6 presents the results obtained from human cadavers and discusses the implications, especially those regarding to whether the robotic drilling approach would be helpful to preserving the residual hearing.

The conclusion of Chapter 7 summarises key outcomes and identifies areas where further work will help boost advancement in the topic of this work and expand the field of application to studies of other biological structures.

1.6 Outcomes of the Research

New knowledge and achievements arising from the work and presented in this thesis is summarised as follows:

1 In cochleostomy - one of the more tissue-sensitive procedures in surgical treatment of hearing loss, disturbances can be noticeably reduced by the robotic technique by up to 30%.

2 Quantitative insight into drilling disturbance is generated for both conventional and robotic drilling procedures, in terms of equivalent sound

pressure level, by comparing the mechanical disturbance level induced by drilling to that caused by acoustic stimulus on the same ear. Experimental techniques and considerations are also constructed in practice for contrasting disturbances generated during ontological surgical remedies.

3 Signal processing algorithms are developed, for identifying and removing spikes in signal due to contamination, in order to retrieve the true vibration signal of membrane. This signal processing technique can be valuable to future studies on cochlear membrane or other biological samples that suffer from weak or unstable laser reflection.

Chapter 2

Background and Literature Review

This chapter covers the state-of-art of technologies and devices available to treat hearing loss, and moreover, the intervention involved in these treatments. To devise a reliable method to assess the intensity of the intervention, tools and techniques for vibration measurement are reviewed, as well as the techniques to estimate the static and dynamic properties of cochlea.

2.1 Hearing Loss Treatment Landscape

Hearing loss can be categorised into conductive hearing loss and sensorineural hearing loss. Conductive hearing loss, as implied by the name, is a loss of signal

conduction between the outer and inner ear. In addition to the problems with ossicles in the middle ear, disorders in either the outer ear or the middle ear can lead to conduction failure, for example ear canal blockage, tympanic membrane rupture and middle ear infection. Conductive hearing loss can be treated with medication or minor reconstruction surgery therefore are normally temporary.

Sensorineural hearing loss normally represents malfunction in the inner ear or the auditory nerve. This type of hearing loss can develop with aging, especially at the high frequency band of hearing range. This trauma in the inner ear is caused by the condition when the sensitive hair cells inside the cochlea become degraded or damaged. Sensorineural hearing loss are usually permanent, except for some cases of sudden sensorineural hearing loss (SSHL) from which people can recover at least some of their hearing spontaneously – usually within one or two weeks if treated promptly. Therefore, hearing aids are needed to retain the ability to conduct daily communication and other activities for patients suffering from sensorineural hearing loss.

Various types of hearing loss treatments have been developed in correspondence to the different nature of hearing impairment. For mild or moderate sensorineural hearing losses with fully functional middle ear structure, amplification of the acoustic signal in the ear canal is a sensible and by far the most prominently used solution. For hearing loss related to abnormal middle ear bone structure, surgical reconstructions would be engaged. For patients with trauma in their inner ear, cochlear implantation is currently considered the most effective rehabilitation method. In the following sections, different types of hearing aid devices and their

recent advances are introduced and briefly reviewed. Less sophisticated treatments like medication or ossicular chain reconstruction are not considered here.

2.1.1 Conventional hearing aids

Conventional hearing aids are the most prevalent device among patients with some form of hearing loss. However, though being recommended to be fitted with one, quite a number of patients do not wear it or give up using the hearing aid after a certain amount of time. The main reasons behind the underuse of conventional hearing aids can be summarised as the non-ideal hearing correction – i.e. feedback and distortion, discomfort caused by occlusion and the stigma of disability. Recent studies show that the complexity in care and maintenance can also be considered as an important reason for elderly patients (Cohen-Mansfield & Taylor, 2004) (Vuorialho, Karinen, & Sorri, 2006) (Öberg, Marcusson, Nägga, & Wressle, 2012) (Tomita, Mann, & Welch, 2001). Insertion and manipulation of hearing aids require considerable manual dexterity, which is especially undesirable for the elderly who are dominant prospective hearing aid benefiters. Detailed reasons can be different for specific devices and the health condition, common listening environment and cognitive ability of the individual. However the poor sound quality and the lack of capability to distinguish specific voices from noise in the background remain the primary reasons for its less than expected popularity.

Figure 2.1.1-1 shows an example of the conventional hearing aids, revealing key components and their functionalities. The fundamental principle of the conventional hearing aid is the amplification of acoustic signal entering the external ear canal. It collects sound from the environment, processes and amplifies the signal with the embedded computer chip and transmits the processed signal to the earpiece. The earpiece sits in ear canal and sends the tuned and amplified sound down the ear canal. The conventional hearing aids thus only work if the middle and inner ear part of the auditory system retain at least a certain degree of functionality. With the advances in technology especially in microelectronics, it becomes possible to make the device a great deal smaller, enabling new types of devices and wearing experiences like in-the-ear and completely-in-canal. However problems like discomfort in the ear canal still remain one of the many issues that make it less than ideal as a long-term solution to hearing impairment.

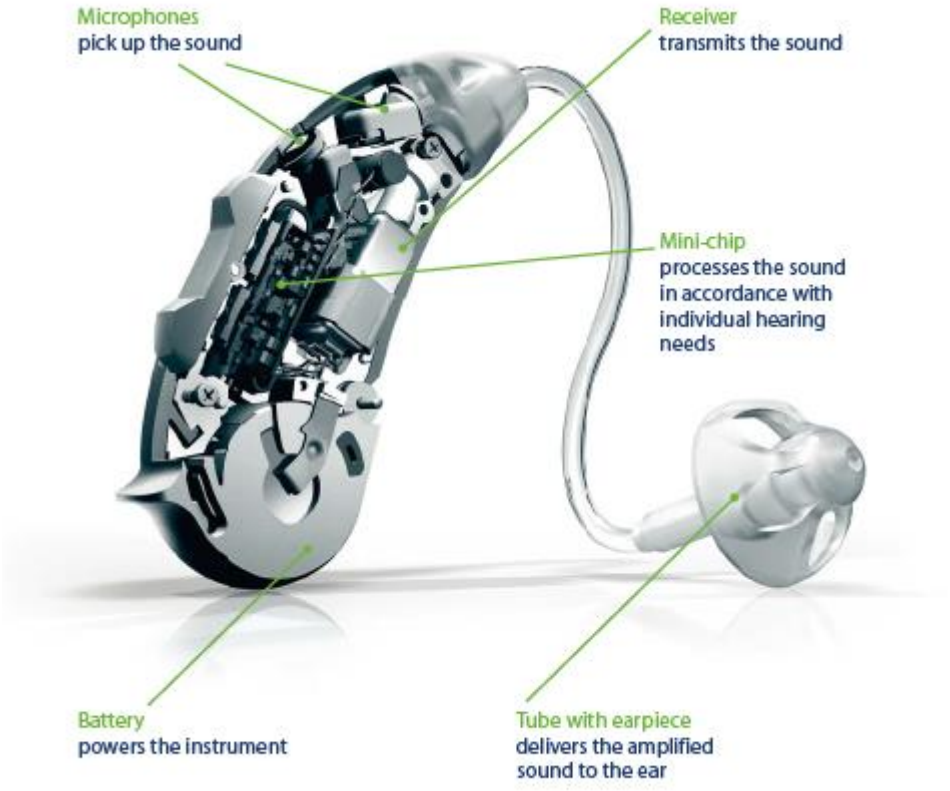

Figure 2.1.1 - 1 | The typical construction of a behind-the-ear (BTE) conventional hearing aid. The microphones pick sound from the environment which is processed by the mini- or micro-chip. The processed signal is transmitted by the receiver to the earpiece where the amplified sound is transmitted further along the ear canal. The whole system is powered by the embed battery.

2.1.2 Implantable Hearing Aids

In response to the unsatisfactory features of conventional hearing aids, research on implantable hearing aids has been conducted since the emergence in the 1930s (Haynes, Young, Wanna, & Glasscock, 2009). Instead of amplifying the sound vibration into outer ear, implantable devices stimulate deeper into the auditory system, which reduces the probability of energy loss along the path of

stimulation reaching the cochlea. Contemporary implantable hearing aids are often referred to as active middle ear implants (AMEI). The working principal for the majority of middle ear implants is to stimulate the ossicular chain. The main drawback of ossicular stimulating is that energy can be dissipated back to the ear drum and outer ear instead of being completely transmitted into the inner ear. Apart from that, the difficulty in placing such a mid-ear implant on delicate ossicular bone makes the implantation extremely challenging and time-consuming. Other hearing aid implant worth to be mentioned is the bone anchored hearing aid (BAHA) which is simple to implant and more cost-effective compared to middle ear implant. The problem of BAHA is mainly low power efficiency and poor frequency response.

The table below summarises the cost and operation time incurred in the three most commonly used hearing implantation methods. Compared to those, though conventional hearing aids have lower upfront cost between £300 and £3000 (Action on Hearing Loss, 2012), the need of repair, replacement and regular supply of battery would stretch the budget in the long term.

Table 2.1.2 - 1 | Operation time and cost for common hearing implants per ear

Hearing Implant	**Operation Time**	**Cost**
Bone Anchored Hearing Aid	45 – 60 mins	£4,000
Middle Ear Implant	2.5 hours	£12,000
Cochlear Implant	2.5 hours	£25,000

2.1.3 Cochlear Implants

Cochlear implants accommodate the rehabilitation needs for patients with severe to profound sensorineural hearing loss. It has become a standard treatment for bilateral severe to profound hearing loss. It bypasses almost the entire auditory system and directly stimulates the auditory nerve. Its functioning does not rely on any part of the original mechanism – delivers remarkable performance and improves the life quality of people with hearing loss especially those whose hearing is too severely impaired to be able to benefit from any alternative types of hearing aids.

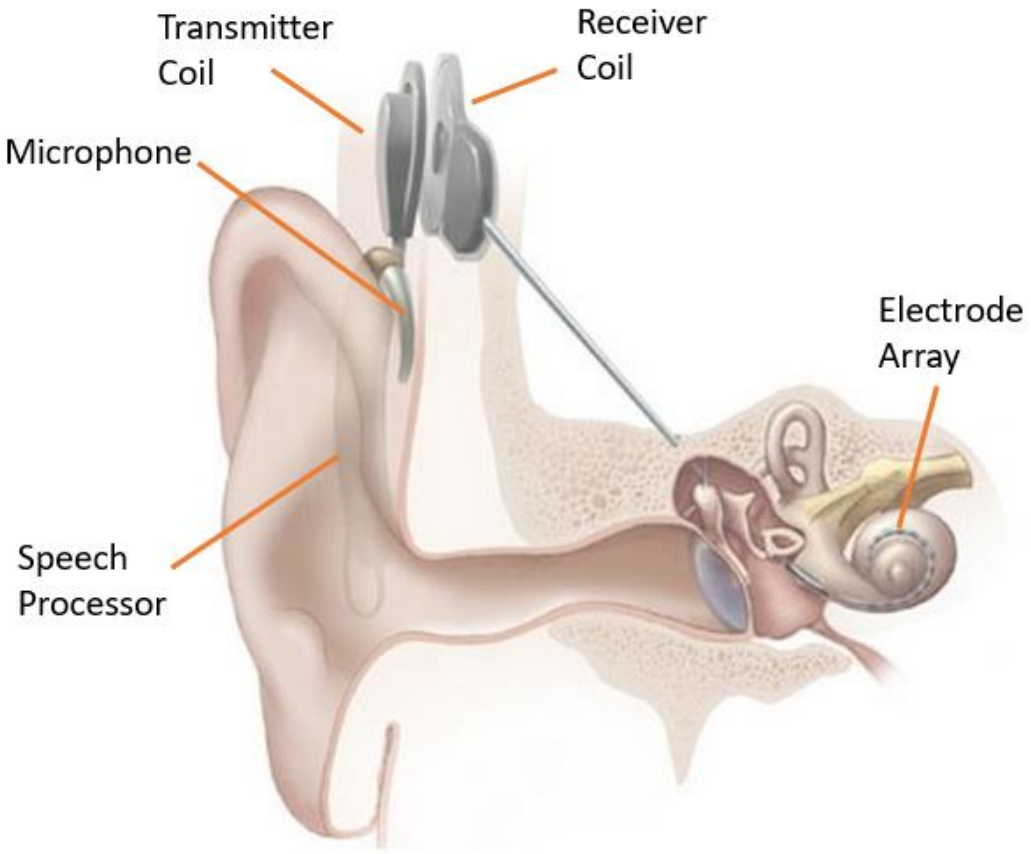

Figure 2.1.3 - 1 | An illustration of the standard design of a cochlear implant (over ear)

As shown in Figure 2.1.3-1, the cochlear implant consists of microphone, sound processor, transmitter coil and the fully electrode array. Natural hearing mechanism works by converting sound waves entering the ear to the movement of hair cells, which generates electric current in the inner ear. Likewise, the cochlear system converts acoustic signal into electric currents. The electric currents then stimulate the auditory nerve in the cochlea, from where nerve impulses get transmitted to the brain.

Since the working mechanism does not rely on the hair cell or any other part of the cochlea, the structure as well as the implantation procedure of cochlear implant was designed to replace the entire hearing system - with no intention to preserve any residual hearing. This makes sense for the current major recipients of this therapy - people who have very little hearing. However the quality of the performance of cochlear implant makes it a compelling choice of treatment for people with less severe hearing loss as well (Gifford, Dorman, Shallop, & Sydlowski, 2010). To enable patients with residual hearing to benefit from cochlear implantation, attempt has been made to lower the risk of losing residual hearing. This is related to the concept of electric acoustic stimulation (EAS) – combining the natural or amplified acoustic hearing with the electric stimulation of the cochlear implant. This is especially suitable for people have considerable residual hearing at lower frequency, as lower frequencies are sensed at the apical end of the cochlea where it is harder to be reached by the electrodes. Utilising the residual auditory functionality at the apical end also potentially avoids inserting further into the cochlea and reduces the risk of damaging any remaining healthy tissue.

To preserve the hearing, apart from using new types of electrode arrays which are thinner, shorter and more flexible (Lenarz et al., 2009) (Dalchow, Hagemeier, Muenscher, Knecht, & Kameier, 2013) (Dhanasingh & Jolly, 2017)(Brant & Ruckenstein, 2016), a better controlled, atraumatic surgical procedure can also make paramount contribution (Friedland & Runge-Samuelson, 2009). This thesis looks into whether using the robotic drilling can reduce inner ear trauma by

quantifying the mechanical disturbance generated during cochleostomy drilling. The mechanical disturbance generated during cochleostomy will be evaluated – by experimentally measuring the mechanical energy the cochlea is exposed to, and contrasted to the energy exposure when a relatively atraumatic cochleostomy technique enabled by robotics is used instead.

In the following sections, both theoretical and experimental techniques are briefly reviewed with an aim to aid the evaluation of noise exposure to cochlea, following by more detailed and specific, closely related, literature review focusing on assessing mechanical disturbance induced during cochleostomy.

2.2 Numerical Modelling of Cochlear Mechanics

Models are simplified expression of the complex physiological activities in cochlea. Models should be able to replicate key principles of cochlear dynamics, though construction of one can be tailored to purposes. One of the most critical criteria to identify the validity of a cochlear model is the frequency response mapping, i.e. high frequency tone prompts peak at basal locations on the BM while low frequency peaks occur more apical.

Multiple approaches towards cochlear modelling have been developed. Apart from physical models built from plastics or electronics [42] [43] [44], numerical models have been developed and progressed tremendously over the last century. Steel first applied Liouville-Green method [45] [46] to cochlear mechanical process in 1974 [47]. This mathematical analysis method was used widely and

intensively in two- and three- dimensional models [47] [48] [49] [50] on the assumption that the cochlear response is linear and passive. Numerical solutions including the finite-difference method from Neely [51] and the integral-equation method from Allen [52], offer a good insight and reference which is still popular among hearing researchers. With advancing measurement techniques and animal preparation methods, the understanding of nonlinearity and active process in cochlear signal transmission has been developed and recognised. This complements previous modelling works and accommodates considerations on frequency sharpening and backward transmission which was evidenced in experimental measurements [53] [54] [55]. Although there are arguments about the effect of spiral shape of cochlea on amplifying low frequency signals [56] [57], it is widely agreed that the spiral shell has no effect on the hearing process. Therefore uncoiled rectangular (2D) or box (3D) model are prevalent in the research field of cochlear dynamics.

2.3 Experimental Techniques to Study Cochlear Dynamics

Laser Doppler vibrometry, as the most popular tool used to study cochlear dynamics and the tool used through this thesis, will be introduced. It is followed by a brief review of other vibrational measurement techniques and other tools that have been used in the study of cochlear dynamics.

2.3.1 Laser Doppler Vibrometry

The working principle of laser Doppler vibrometry (LDV) is that the velocity of a moving object can be calculated from the Doppler frequency shift of the laser light after being reflected back from the moving object. As shown in Figure 2.3.1-1, the laser beam is split into two by the first beam splitter (BS 1). The objective beam is incident on the vibrating object where the light is scattered back. The reflected beam is then deflected by the second beam splitter (BS 2), and merged with the reference beam on the third beam splitter (BS 3). The merged beam is passed onto the photo detector. The superposition of the reflected and reference beam creates a modulated signal containing the Doppler frequency shift of the laser light. Through analysing the modulated signal, the velocity of the moving object can be obtained. Here f_0 is the frequency of the original laser beam, i.e. object beam; f_b is the carrier frequency added by the Bragg Cell. The acousto-optic modulator, i.e. Bragg Cell, is added before the reference beam reaches the detector in order to help determine the direction of movement. The Bragg Cell shifts the baseline frequency of the original reference laser beam f_0 to $f_0 + f_b$. The direction of the movement of the object can therefore be indicated by the decrease or increase of the modulation frequency by comparing $f_b + f_d$ against f_b. f_d is the frequency shift of the reflected beam compared to the original object beam. Due to the Doppler effect, f_d is proportional to the velocity of the object moving away or towards the laser souce and therefore enables quantifying the vibration of the object.

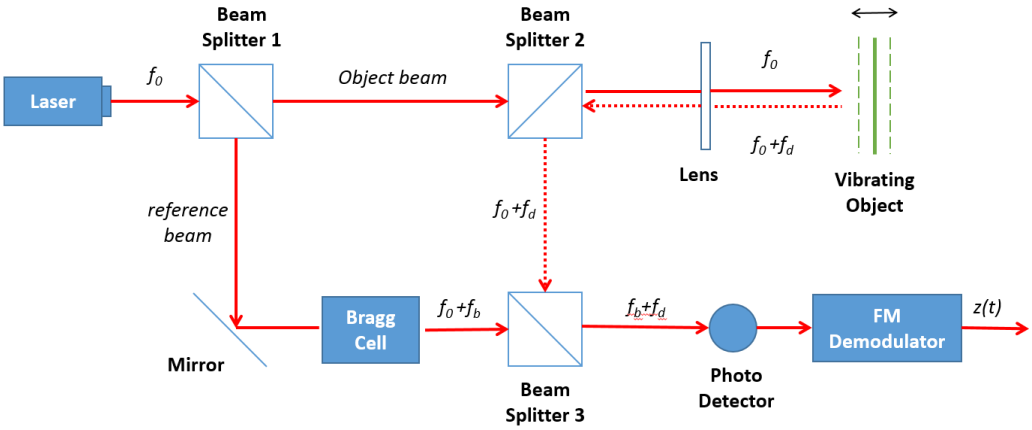

Figure 2.3.1 - 1 | Schematic layout of a Laser Virbometer showing the flow of laser beam which is key to the working principle of laser vibrometery

Laser Doppler vibrometry enables the non-invasive measurement of characteristics of vibration. It avoids influence on the observing object such as mass-loading the sample, which makes it particularly useful in characterising the mechanical properties of extremely small and extremely lightweight structures. It also enables the measurement on target that is too difficult to reach or be attached to by other sensors. It offers femtometer–level resolution and the performance is consistent in both microscopic scale and over large measurement distance. Hence, it has been a popular tool in many areas of scientific research and industry, for instance acoustic, automobile, aerospace, microfabrication and biomedical.

In the experimental study of cochlear dynamics, one typical consideration would be the need for angle correction. If the angle between the laser beam and the direction of vibration to be measured is numerically significant, a cosine

correction is normally required to be applied to the measured data, usually with a visually estimated angle (Nakajima et al., 2009) (Verhaert, Walraevens, Desloovere, Wouters, & Gérard, 2016) (Kwacz, Marek, Borkowski, & Mrówka, 2013).

Another yet-to-be-solved challenge in the use of laser Doppler vibrometer is the speckle noise. When the relative positions of retro-reflective speckles attached on the target to the laser vibrometer change due to movement not inline with the direction of the measured movement, such as subtle tilt or rotation, it results in changes in the output measurement data that are sometimes periodic and hard to be distinguished from the genuine vibration to be measured - 'pseudo-vibration' (Rothberg, Baker, & Halliwell, 1989). The non-organic change to amplitude can also lead to occasional drop of signal amplitude to a very low level, evident by spikes in signal that are abnormal to the general trend of genuine measurement data due to failure of demodulation (Hosek, 2012). In Chapter 5, the characteristics and effects of 'signal drop-out' in the measurement data is discussed. An algorithm tailored to the target vibrational characteristics to be measured, i.e. round window dynamics, is proposed and implemented with desirable results.

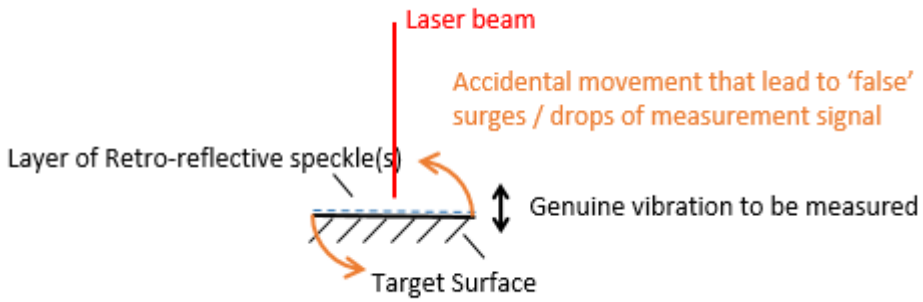

Figure 2.3.1 - 2 | An example of retro-reflective speckle noise

2.3.2 Historic techniques and latest development of tools and techniques

Since von Békésy's first direct measurement of BM motion via a combination of stroboscopic illumination and standard microscopy (von Békésy & Peake, 1990), various techniques for the measurement of cochlear dynamics have been developed, including capacitive probe method (Wilson & Johnstone, 1975) (LePage, 1987) , electronic speckle pattern interferometry [18], fibre-optic laser interferometry [19], fibre optic lever [20], laser homodyne interferometry [21] [22], laser heterodyne interferometry [23], and the very productive Mössbauer technique [24] [25] [26] [27] [28] [29] [30]. Among them, laser heterodyne interferometry and the Mössbauer technique are the most commonly used, both based on the Doppler effect in electromagnetic radiation.

Ruggero and Rich made a comparison between laser Doppler vibrometry and the Mössbauer technique in their 1991 paper [31] and recognised laser vibrometry a compelling replacement for the Mössbauer technique, though the latter led to

significant discoveries in cochlear dynamics including the nonlinearity in BM [25]. The main drawbacks of the Mössbauer technique are the nonlinearity in input-output transduction and the long data-sampling time required for quality measurements, limited by the nature characteristics of gamma radiation. The spherical glass micro beads for laser vibrometry are settled easily on the membrane since they have smaller surface area per unit weight; while the metal foil used to reflect gamma photons in the Mössbauer technique has the problem of floating in the perilymph.

Apart from laser vibrometry, other contemporary vibration measurement techniques include accelerometers and Near Field Acoustic Holography (NAH). Accelerometers are particularly relevant in measuring the vibration of large, heavy solid structures like airplanes and automobiles due to its need of attaching a sensor to the object. Same as LDV, NAH is a non-contact vibrational measurement technique. It determines the velocity at the target surface via mathematical transformation from the sound pressure measured in the nearfield, using Green's Functions. The capability of reflecting information in three dimensions makes it especially useful in locating the vibration source. Though as a technique to determine surface vibration velocity, LDV remains a faster and more direct method with consistency in accuracy (Martarelli & Revel, 2006) (Potter, VanKarsen, DeClerck, & Sklanka, 2012).

2.4 Literature Review on Measurement of Cochlear Noise Exposure during Ear Surgery

During cochlear implantation surgery, cochleostomy and electrode insertion are the two procedures that expose cochlea to the highest possibility and amount of trauma. To assess the trauma that surgical intervention like cochleostomy or electrode insertion, post-operative clinical study such as measuring the shift of pure-tone hearing thresholds after the operation (James et al., 2005) is a convincing and easy to implement method if the proper resource is available. Even though the results are generally more direct and more comprehensible, the clinical studies are quite expensive to run – requiring access to patient group and rigorous ethical approval procedure. This makes it not always suitable for testing a hypothesis at a primary stage. Besides, a multiplex of reasons can contribute to the hearing performance post-operative, for instance, acoustic trauma caused during cochleostomy drilling, tissue damaging caused during electrode insertion or the individual capability to recover after an operation. Since there is hardly any way to assess the hearing performance during the surgery, it is therefore very difficult to identify the source of trauma and quantify the trauma caused by each individual source or factor, via this approach.

Another approach worth mentioning is the histologic assessment (Sikka et al., 2017). It looks at the damage caused after the surgical intervention, by examining and grading the condition of intracochlear tissue on sectioned cochlea samples. It shares the same benefits as the clinical study mentioned above by providing a set of comprehensible results. However, the grading procedure can be subjective. Moreover, the conclusion is based on an underlying assumption

that caution has been taken during the fixation, decalcification, section procedure and no further damage has been introduced after the surgical intervention.

Several studies have been conducted to assess the noise exposure of cochlea in situ, i.e. the level of mechanical disturbance induced in the cochlea during surgery when a particular surgical technique is applied. The methods used and conclusions drawn are summarised and discussed in this section, to formulate a guideline for the design of the study in this thesis.

2.4.1 Methods to Measure Cochlear Noise Exposure to Disturbance during Ear Surgery

In the context of inner ear noise measurement, there are in general two approaches: the laser approach and the microphone approach. In this section, these two most popular approaches are reviewed, along with other measurement methods that were designed to measure specific parameters and serve particular research interests.

Due to the limited surface area on the cochlea - about the size of a pea with approximately 2.5 mm^2 membranous exposure at round window, it has been particularly challenging to accurately observe and quantify the vibration on or within the cochlea, especially before the immense advances in microelectronics and applications of laser became ubiquitous.

Microphone Approach

The microphone approach measures the acoustic pickup in decibel (dB) at the round window. The value measured is then calibrated against a reference measurement. The reference measurement is conducted by measuring the acoustic noise in dB at the same point of interest, i.e. round window when the specimen is exposed to a stimulus of a known acoustic noise level in dB SPL.

Pau et al. (Pau, Just, Bornitz, Lasurashvilli, & Zahnert, 2007) conducted experimental measurements of sound pressure levels at major steps of cochleostomy drilling on four fresh human temporal bones using a microphone. The recordings were performed with a tube inserted in the slightly widened round window niche and connected to a microphone. A 1 mm diamond burr was used at rotation speed of 24,000 to 27,000 rev/min. Bone conduction, similar to that applied by Kylén et al. (Kylén, Stjernvall, & Arlinger, 1977), was used for calibration in this study. Using the bone conduction calibration curve in frequency domain, the value of the equivalent sound pressure (p_A) can be calculated from the microphone measurements. This pressure value can be further converted to an equivalent sound pressure level (SPL) to offer an insight into the sound perception by the human ear, using the following equation described in sound level meter standard (IEC 61672-1: 2002):

$$L_{AF}(t) = 20 \cdot log_{10}\left(\frac{\sqrt{\frac{1}{\tau}\int_{-\infty}^{t} p_A^2(\zeta) e^{-\frac{t-\zeta}{\tau}} d\zeta}}{p_0}\right) \qquad (2.4.1\text{-}1)$$

Where $L_{AF}(t)$ is the fast exponential-time-weighted and A-weighting filtered sound pressure level at t when SPL is calculated; $\tau = 0.125s$ is the time constant for the fast exponential-time-weighting function; ζ is the time integration variable from the beginning of measurement to time point t; $p_A(\zeta)$ is the instantaneous A-weighted equivalent sound pressure; p_0 is a constant equal to 20 μPa representing sound pressure at 0 dB SPL.

The results indicate a tolerable noise level not exceeding approximately 110 dB as long as the membranous endosteal layer is not exposed. However, the SPL eq. exceeds 130 dB when the membranes are in touch with the running burr, which expose the cochlea to disturbance at the same level of drilling onto the ossicular chain. In middle ear surgery, drilling onto the ossicular chain is widely believed to cause dramatic trauma to the cochlea and can lead to permanent sensorineural hearing loss (Hallmo & Mair, 1996)(Urquhart, McIntosh, & Bodenstein, 1992).

Several other researches (Yu, Tong, Zhang, Zhu, & Duan, 2014)(Yin, Strömberg, & Duan, 2011)(Strömberg, Yin, Olofsson, & Duan, 2010) have achieved similar findings applying similar principles, with the end of the silicone tube of ER7C probe microphone system held firmly in the round window niche in parallel to drilling. However, microphone readings alone do not reflect the actual inner ear noise load, unless correlated with measurements that correspond to natural airborne sound pressure level. The effectiveness of capturing round window vibration via a microphone close to the round window membrane is subject to reservation. On the other hand, attaching the end of the tube straight onto round

window surface can alter the dynamic response of the membrane, which too leads to discrepancies in gauging the vibration elicited inside the cochlea. Some researchers (Yin et al., 2011) adopted this method and admitted that using a laser Doppler vibrometer to measure the membrane vibration could provide information more relevant to determining the actual cochlear noise load.

Laser Approach

The laser approach measures the vibrating velocity in mm/s at the point of interest. The value measured is then calibrated against a reference measurement. The reference measurement is conducted by measuring the vibration amplitude in mm/s at the same point of interest when the specimen is exposed to a stimulus of a known acoustic noise level in dB SPL.

Eze et al. (Eze, Jiang, & Fitzgerald O'Connor, 2014) investigated the noise that the cochlea was exposed to during different stages in drilling a cochleostomy using a laser Doppler vibrometery. Stapes velocity could be obtained directly from the laser vibrometer processor. The calibration was conducted based on air conduction principles, with stapes velocity measured by laser vibrometry when 100 dB SPL tones of 100 Hz to 10 kHz were delivered into the ear canal. Drill-induced stapes velocities were measured at selected stages of the cochleostomy formation. Integrity of the model, i.e. the sound conducting quality of the middle ear of each specimen was checked against standard middle ear transfer function (J. J. Rosowski, Chien, Ravicz, & Merchant, 2007)(*ASTM F2504 - 05, Standard Practice for Describing System Output of Implantable Middle Ear Hearing*

Devices, 2005) before drilling. Stapes velocities at different stages of cochleostomy were plotted in the frequency domain and compared between each other. There was a 2 kHz peak on the curve corresponding with drilling onto endosteal membrane, coinciding with the 2 kHz peak when the running drill touched the ossicular chain and a similar peak on the response curve to 100 dB sound conduction. The equivalent sound pressure levels were calculated by taking root mean square of the stapes velocity over a limited frequency bandwidth that contains the maximal velocity and converting using the middle ear transfer function obtained in calibration. Before touching the endosteum, recording SPL eq. ranged from 80 to 85 dB. It increased to an average level of 130 dB when the running burr hit the membranous labyrinth.

Laser vibrometry has been predominantly used as a standard method in research to study cochlear dynamics (Jorge, Zenner, Hemmert, Burkhardt, & Gummer, 1997), assess middle ear functionality (Aibara, Welsh, Puria, & Goode, 2001), and quantify the output of a middle ear implant system (J. J. Rosowski et al., 2007)(Gross??hmichen, Salcher, Kreipe, Lenarz, & Maier, 2015)(*ASTM F2504 - 05, Standard Practice for Describing System Output of Implantable Middle Ear Hearing Devices*, 2005). This method enables highly accurate and non-intrusive vibrational measurement. It provides a straightforward quantification of the drilling-evoked noise levels purveyed inside the cochlea.

Other Approaches

Microphones have also been used, in combination with a sound level meter, to directly measure the sound pressure levels generated at external and middle ear during mastoid surgery (Luxenberger, Lahousen, & Walch, 2012)(Parkin, Wood, Wood, & McCandless, 1980)(Spencer & Reid, 1985). The measurement is achieved by either placing the tip of the sound meter probe at 3mm lateral to the tympanic membrane (Parkin et al., 1980), or replacing the tympanic membrane with a microphone which has a diaphragm of the same size as a human tympanic membrane (Luxenberger et al., 2012).

Accelerometers have also been used as the major sensing element in noise measurement during ear surgery (Kylén et al., 1977)(Spencer & Reid, 1985)(Kylén & Arlinger, 1976). Accelerometers work by generating or modifying an electrical output proportional to the vibratory acceleration to which the accelerator is subjected. Before the maturity of laser technology and the prevalent use of lasers in vibration measurement due to non-intrusiveness, accelerometers have been the major tool to pick up vibration. Kylén et al. (Kylén et al., 1977) investigated the impact of different variables that affect the drill-generated noise levels in ear surgery using a miniature accelerometer. In an attempt to overcome the limited surface area available on the cochlea, the vibration was transmitted from the cochlea to the accelerometer via a 35mm long, 1.8mm diameter brass rod (Kylén et al., 1977)(Kylén & Arlinger, 1976) with one end cemented into a bony hole drilled in the promontory and the other end screwed on to the accelerometer. A force transducer coupled to a balance underneath the sample holder to eliminate the effect of changes in static force

applied manually. The SPL eq. was obtained by calibrating the accelerometer measurements during drilling against during stimulation by a bone conductor at specific frequencies at specific energy levels. The drilling was performed on the cortical bone of the intact human cadaver skulls. In analysis, the results were plotted over octave bands and compared to reference noise levels produced by a 6mm, type 3 burr at a rotation speed of 20000 rev/min, which provided an insight into the influence of varying drilling variables.

The measured signal was calibrated against the signal picked up by accelerometer when a bone vibrator was attached to the sample and driven by a series of pure tones within hearing frequency range (Kylén et al., 1977)(Spencer & Reid, 1985)(Kylén & Arlinger, 1976).

Electrocochleogram enables in-vivo evaluation of the impact of drilling in ear surgery. The change of the electrocochleogram during drilling can give us a hint of the sound level of the trauma generated. Electrocochleography (ECochG) is a technique used in clinics to record the electrical potentials generated in the cochlea and the auditory nerve when sound stimulus is present. To perform an ECochG, an electrode is inserted into the ear canal, and placed on the surface of either the ear canal or the TM. Clicks at intensities spanning from 10 dB HL to 100 dB HL at every 10 dBHL were fed to patients via an earphone. By contrasting ECochG traces (Hickey & O'Connor, 1991) before, during and after drilling on the mastoid in response to click-stimulus, the level below which the drilling noise starts to mask the click-stimulus can be obtained. The amplitude obtained is the equivalent noise level corresponding with drilling noise.

Optical fibre pressure sensor developed by Elizabeth S. Olson (Olson, 1998) offers an alternative way to gauge intracochlear pressure, which can be used to indicate the level of trauma caused inside cochlea during drilling. The optical fibre pressure sensor is made up of a gold-coated reflective thin-film diaphragm, optical fibres, a LED light source and a photodiode. The diaphragm at the tip of the optical fibre flexes in response to the change of pressure; the photodiode detects the light reflected off the diaphragm. To the author's best knowledge, there has not been any application of this sensor in drilling noise or other human intervention noise measurements. However, the optical fibre pressure sensor has been widely used to study dynamics inside the cochlea (P. Mittmann, Ernst, & Todt, 2014)(Kale & Olson, 2015)(M. Mittmann, Ernst, Mittmann, & Todt, 2016). A controversy over the use of optical fibre sensor as an accurate quantitative tool is that to insert the sensor into the cochlea, the cochlear membranous chamber has to be punctured and thus disturbing the enclosed liquid environment. Although measures are taken to minimise the effect of perforation for example liquid leakage, it remains questionable if this pressure measurement presents a true undistorted picture of the internal mechanics of the cochlea.

2.4.2 Previous Findings of the Noise Exposure of the Inner Ear during Cochleostomy Drilling

In this section, findings from previous research, particularly measurements taken while a cochleostomy is being drilled are examined, along with the approach adopted to acquire the level of mechanical disturbance the cochlea is exposed to.

Cipolla et al. (Cipolla, Iyer, Dome, Welling, & Bush, 2012) compared the usages of CO_2 laser and standard otologic drill in cochleostomy formation, in terms of their contributions to both acoustic and thermal cochlear trauma. The average intracochlear sound level measured when using the laser was 54.9 dB, compared to 89.9 dB when using the drill to perform cochleostomy. Maximum levels of intracochlear disturbance levels ranged from 75 to 118 dB for the laser, compared to the 95 - 136 dB range when the drill was in use. However, both thermal couple and acoustic probe were inserted into the cochlea fluidic space, through lifting the round window membrane and creating an extra cochleostomy. This incurs the leakage of normal cochlear fluids which was replaced by saline solution. This measurement technique impairs the integrity of the cochlea and thus evokes queries on the quantitative accuracy of the measurements.

Pau et al. (Pau et al., 2007) used a microphone to obtain a quantitative evaluation of the acoustic noise exposed to inner ear when a cochleostomy is being drilled. A microphone was used to capture the sound pressures at round window membrane via a tube inserted into the carefully milled round window niche. The microphone was calibrated to a selection of equivalent airborne sound pressure level. A bone vibrator, coupled with an audiometer, was applied to the temporal bone samples to deliver stimulus at the selected equivalent sound pressure levels, on the assumption that drilling generated noise was transmitted into cochlea mostly in the form of bone conduction. Maximum equivalent SPLs were approximately 110 dB before penetrating the bony shell and exceeded 130 dB when the running drill touched the membrane. Apart from the concerns that

attaching the plastic tube on the membrane may alter the dynamics of the membrane, the efficiency of energy transmission between membrane and tube-connected microphone is worth further discussion, especially if the end of the tube was not firmly attached to the membrane surface. In particular, microphone can pick up acoustic energy transmitted through the air rather than the signal of interest, i.e. the mechanical disturbance induced in the cochlea and transmitted through the cochlear fluid and round window membrane.

Yin et al. (Yin et al., 2011) measured the noise induced by drilling and during suction process in otologic surgery using a an ER7C probe microphone system. For cochleostomy drilling, the peak noise levels ranged from 116 to 131 dB SPL while drilling in cortical bone and the mastoid cavity exposed the cochlea to noise levels around 120 dB SPL. The probe microphone was placed in the round window niche, with the open end of the probe tube almost touching the round window. 10-second recording was done for each case investigated. Apart from the concerns aforementioned in reviewing the study of Pau et al. (Pau et al., 2007), there was no calibration conducted to relate the microphone pickups to actual levels of damage to hearing, though comparison between different types of drills and suction tips using the same experimental setup can be effective.

Kylén et al. (Kylén & Arlinger, 1976) used accelerometry as the main sensing technique in the measurements of drill-generated noise levels in ear surgery. Isolated temporal bones were placed on the scale of a balance, with a transducer coupled to the pan of balance to monitor the static vertical force applied on the specimen while vibration was being recorded in parallel. The vibration levels

reach a saturated value when the static force increase beyond 4 N. Similar measuring technique was applied on intact skulls, where vibrational levels were measured while drilling in cortical bone and mathematically converted to equivalent air-borne sound pressure level. Calibration was conducted using a bone conductor driven by a pure tone audiometer. The maximal noise levels measured ipsilaterally are 92-106 dB between 2 and 4 kHz bands for a cutting burr; for a diamond burr the noise level is 5 dB less in the 250, 2000 and 4000 Hz bands, and about 13 dB less in the 500 and 1000 Hz bands . A further study (Kylén et al., 1977), using the same measuring technique, investigated the drill-related contributing factors to noise generated during ear surgery. It concluded that size of the burr was the primary factor that influenced the noise levels while both rotation speed and location of the drilling had negligible effects. Here coarseness of the bone surface was considered consistent, due to all drillings were performed on the same part of body - cortical bone. Diamond burrs were 'quieter' than their cutting counterparts - by approximately 5 -11 dB. This is one of the first studies that evaluated the disturbance induced by surgical drilling and translated the results into equivalent air-borne sound pressure levels. With more advanced sensing technology, such as laser now available, disturbance can be gauged in a less invasive manner, removing the complexity of attaching accelerometer and the associated parts to the specimens under investigation.

Eze et al. (Eze et al., 2014) used laser Doppler vibrometry to measure the noise levels in cochlea during cochleostomy. Stapes velocity was recorded at six different stages of cochleostomy formation. The equivalent noise level was

calculated via taking the root mean square of the measured velocity over a certain frequency bandwidth and comparing it with the reference velocity measured during calibration at the same frequency. The mean equivalent sound level exceeded 130 dB when the burr touched or breached the membranous labyrinth. In an earlier study, Jiang et al. (Jiang et al., 2007) studied the risk of hearing deterioration if the ossicular chain is accidentally drilled on, with a similar experimental setup. Peak-to-peak stapes displacement was measured over short drilling episodes and converted into the equivalent sound pressure level via comparing to the stapes footplate displacement induced by a known acoustic signal. The equivalent noise levels generated were 93 to 125 dB SPL, comparable to those known to produce acoustic trauma. The cutting burr produced higher levels of noise than its diamond counterparts; drills with larger diameter create higher levels of vibration compared to ones with smaller diameter. This trend corresponds to the conclusions drawn by Kylén et al. (Kylén et al., 1977) when drilling on the cortical bone.

Previous works on cochlear noise exposure measurements mentioned above are summarised here in Table 2.4.2-1. The table shows sources of work in the left column and the corresponding results in the rightmost column. Parameters for setting up these measurements are indicated in the columns in between. Entries in the table are listed in the sequence of burr diameter from low to high. As reckoned by Kylén et al. (Kylén & Arlinger, 1976), a drill burr with larger diameter is very likely to generate a higher level of mechanical disturbance in the inner ear. By contrast, drilling speed is less influential on the level of disturbance

induced. Probably due to the different methodologies used in each study though, there is no obvious increase in SPL_{eq} with the increase of burr diameter in Table 2.4.2-1. Nevertheless, it is safe to conclude from the table that the peak sound pressure levels distribute in a restrained range from 80 dB to 136 dB among the reviewed studies. This provides a practicable scope for estimating the expected results of drilling disturbance measured on cochlea, and for identifying abnormalies in the experimental measurements.

It is worth noting that, there has not been a full, uninterrupted as well as non-invasive recording of whole cochleostomy formation procedure using laser vibrometry. In previous studies, only a maximum of 10 seconds of continuous drilling was captured non-invasively using laser Vibrometer, possibly mainly restricted by the processing power available on the analysing equipment. The whole drilling procedure has only been recorded by inserting microphone into the cochlea, risking losing the cochlea fluid, altering the cochlear dynamics and affecting the mechanical impedance between the drill bit and the RW.

Capturing the whole drilling procedure is particularly important in this study, primarily because it is not only the disturbance during contact time that is of interest, but also the fact that robotic drill enables less, if not none, interruptions during cochleostomy compared to using conventional drill - if the same drill burr and rotation speed is applied and assuming no difference in the bone thickness and condition. This reduced possibility of interruptions leads to reduced exposure to mechanical shock, surge of pressure and other events related to human intervention. In other words, the main difference between robotic and

conventional cochleostomy drilling is the more consistent and controlled techniques engaged in robotic drilling, which can be reflected properly in mechanical energy only when the entire drilling procedure is taken into consideration. Continuous recording facilitates a fuller coverage of the mechanical events, especially those that are particularly meaningful to the purpose of the study - comparison and contrast the two drilling methodologies.

Table 2.4.2 - 1 | A Summary of Previous Studies of Cochlear Noise Exposure during Ear Surgery

Source	**Main Surgical Procedure**	**Sample Type**	**Sample Size (no. of ears)**	**Location of Drilling/Intervention**	**Surgical Tool**	**Drill Rotation Speed**	**Location of measurement**	**Recording Technique**	**Drilling Episode Length**	**SPL_{eq} (peak)**
(Cipolla et al., 2012)	Cochleostomy	Temporal bone	8	Promontory	Drill - 1mm diamond	60,000 rev/min	Anterior TW *(INTRACOCHLEAR)*	Probe microphone	Whole Procedure	95 - 136 dB
(Pau et al., 2007)	Cochleostomy	Temporal bone	4	Promontory	Drill - 1mm diamond	24,000-27,000 rev/min	RW	Microphone + tube	At separate stages	>130dBA
(Eze et al., 2014)	Cochleostomy	Temporal bone	8	Promontory	Drill - 1mm diamond	15,000 rev/min	Stapes	Laser Doppler Vibrometer	At several points	80 - 132 dB
(Yin et al., 2011)	Cochleostomy	Temporal bone	12	Promontory	Drill - cutting (5.7, 3.6, 2.5 mm) diamond	25,000 rev/min	RW	Probe microphone	10 seconds	116 - 131 dB

					(4.1, 3.6, 2.2, 1.0 mm)					
(Kylén et al., 1977)	Tympanomastoid	Intact skull	10	Cortical bone	Drill – 6mm cut and diamond	22 000 rev/min	Promontory	Accelerometer	Short bursts	92 - 106 dBA (5 - 13 dB less for diamond)
(Kylén & Arlinger, 1976)	Tympanomastoid	Intact skull	11	Cortical bone	Drill – various specs	Various	Promontory	Accelerometer		100 dBA range
(Jiang et al., 2007)	Tympanomastoid	Temporal bone	5	Ossicular chain	Drill – various specs	16,000-25,000 rev/min	Stapes	Laser Doppler Vibrometer	10 seconds	93 - 102 dB (1mm diamond) 96 - 108 dB (1mm Cutting)

2.5 Conclusions

In this chapter, an overview of the contemporary hearing loss treatments shows that cochlear implantation remains the most important hearing loss treatment in terms of its effectiveness and unique ability to function without depending on the outer and middle ear to work. Drilling, as an essential part of cochlear implantation, can create a considerable amount of disturbance. This is supported by various pieces of research reviewed in Section 2.4.2. Despite the endeavour in measuring noise during different types of drillings in ear surgery, no study has measured and traced the noise, i.e. the mechanical disturbance generated in the cochlea, throughout the entire procedure of cochleostomy drilling. It is also interesting to have an evidence-based view about whether with the help of the robotic technique, the disturbance can be reduced due to the enhanced consistency and continuity that it provides.

The experimental study on the impact of robotic drilling is covered in Chapter 5 and Chapter 6. Before getting into the detailed experimental setup and result analysis of robotic drilling noise study on cadaver heads, Chapter 3 and Chapter 4 will guide us through the theoretical and experimental validation of the assumption that have been made for the cadaver experiments in the latter chapters – that creating a third window does not significantly affect the cochlear dynamics.

Chapter 3

Mathematical Model of Cochlear Mechanics

The cochlea is an important organ in the hearing of mammals. The fundamental functionality of it is a spectral analyser. In cochlea, different parts along the length of the basilar membrane (BM) respond differently according to frequency contents of stimulus signal. With the current measurement technologies, it is still extremely challenging to obtain a direct measurement of vibration inside cochlea without intruding on the fluid-filled capsular environment of cochlea. This, coupled with the complex functionality and extraordinary sensitivity of cochlea, makes it one of the most scientifically interesting and relatively less well understood components of the hearing chain. Multiple theories have been

developed or experimentally discovered for the mechanical process of signal transmission in cochlea within the last five decades (von Békésy & Peake, 1990) (Rhode, 1971) (Kemp, 1978) (R. F. Lyon, 1990) (R. R. Lyon & Mead, 1989) (Wilson, 1980), while multiple subjects remain open for debate (Ni, Elliott, Ayat, & Teal, 2014) including the mechanical effects of the coiling shape of cochlea. Constructing numerical models helps generate an in-depth understanding of the physics behind cochlear functionality, which is crucial and valuable to the development of medical treatment strategies for people with hearing loss. A model, apart from enabling verification of assumptions when compared to experimental findings, can also predict results of different experiments that can sometimes be difficult to conduct with sufficient level of consistency or within a limited time frame.

The first part of the chapter describes the anatomy of the cochlea in detail and explains how it functions based on the current well-accepted theory. In the second part, a two-dimensional box model is constructed computationally following classical assumptions - predominantly the two-dimensional model work of Neely (S T Neely, 1978). In the final part, the model is tested against the principal characteristics of cochlear mechanics and applied to evaluate if some structural modification can be made on cochlea without affecting the characteristics of interest by introducing some changes to the boundary condition of the model. It is important to obtain this knowledge because it helps determine whether two valid measurements can be achieved on the same cochlea as implemented on cadaver study in Chapter 5 and 6.

3.1 Anatomy and Function of Cochlea

The human cochlea is a snail-shell shaped structure where mechanical vibrations are transduced into neural signals. The cochlea sits in the inner ear part of the whole hearing system. Via tympanic membrane, i.e. ear drum, the acoustic signal in air is translated into vibrations of mechanical structures of the hearing system. The ossicular chain, consisting of malleus, incus, stapes, is attached to a membrane-covered opening on the inner ear called oval window (OW), as shown in Figure 3.1-a and b. Vibrations of the tympanic membrane couple into ossicles and force the stapes and the attached oval window to vibrate, thus converting the sound energy from pressure wave in the air into motion in the fluid of inner ear. The sound-induced wave propagates through the fluid along the length of cochlea, while interacting with the membranes inside the cochlea. Since the inner ear fluid is considered highly incompressible (Egbert De Boer, 1996), the pressure in the fluid induced by the volume displacement at the basal end needs to be relieved. Round window (RW), another elastic membrane at the basal end of the cochlea serves this purpose.

The cochlea coil is about 7 mm across (Escudé et al., 2006), formed by 2.75 spiral turns (Hardy, 1938). If unrolling the cochlea spiral, as illustrated in Figure 3.1-b, the cochlea can be viewed as a fluid-filled tube, containing into three channels. The top and bottom main channels are jointed at the apical end of the cochlea. As the cross-sectional view shows in Figure 3.1-c, the three fluid-filled chambers that constitute the cochlea are: scala vestibule (SV), scala media (SM) and scala tympani (ST). Both SV and ST are filled with perilymph – a fluid that

has high sodium content and low potassium content. The fluid inside SM is endolymph which is, on the contrary, low in sodium but high in potassium. The three chambers are separated by Reissner's membrane (RM) or Vestibular membrane (VM) and basilar membrane (BM) respectively. The longitudinal length of BM is generally believed to be approximately 35mm (Benesty, Sondhi, & Huang, 2007). From base to apex, both width and stiffness of the basilar membrane deviate - from stiff and narrow to flexible and wide. The reduction of stiffness is quite quantitatively significant, almost in an exponential manner

along the length of basilar membrane. In contrast, Reissner's membrane is thin and flexible. It is believed that Reissner's membrane barely has any impact on the mechanics in the cochlea. Neither does the spiral shape of the cochlea (Steele & Zais, 1985). The coiling of the cochlea is believed to offer compatibility and probably benefit the cochlea with centralised blood supply and nerve connection (Ni et al., 2014) . Whether there is any mechanical effect is yet to be resolved.

Also shown in Figure 3.1-c, the organ of Corti (OC) sits on the BM. OC is the sensory element of hearing, consisting of sensory receptors called the inner hair cell (IHC) and outer hair cell (OHC). There are three rows OHCs and one row of IHCs, all attached to BM. The IHC is responsible for transducing basilar membrane motions into neural impulse and pass it to the brain through the auditory nerves. The OHT does not transmit nerve impulse but is believed to regulate OC's sensibility to basilar membrane motions, given its ability to change shape according to the amplitude of voltage pulse generated in response

to motions (Fettiplace & Hackney, 2006) (Nam & Fettiplace, 2010) (Russell, 2008).

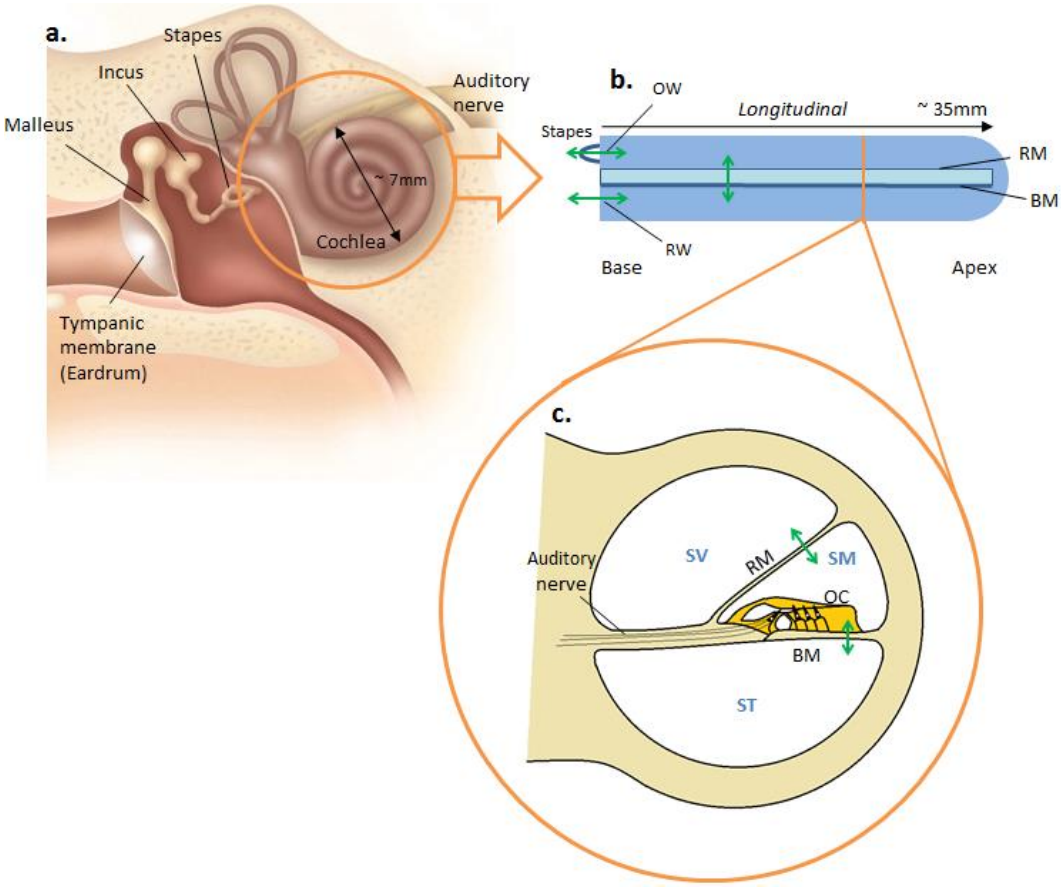

Figure 3.1 - 1 | Illustration of the physiology properties of cochlea at different degree of magnification. (a) A sectional diagram of the ear showing the middle ear and inner ear structures. (b) A unrolled cochlea with simplification showing the fluid tube with cochlear partition Reissner's membrane and basilar membrane. Note the tube shown is surrounded by otic bone apart from the two membrane-covered openings: oval window and round window. (c) A cross-sectional view of one turn of the cochlea coil with some simplification to emphasise the correlation between the motion of basilar membrane and the neural impulse generated.

As mentioned above, the physiological properties of basilar membrane vary along its length, especially the membrane stiffness. This leads to the frequency selectivity of basilar membrane vibration. As discovered in the classic experimental work by von Békésy in the 1940s (von Békésy & Peake, 1990), the magnitude of basilar membrane vibration increase as the wave travels along the length of cochlea until it reach a peak point and the vibration quickly diminishes. The place where the peak occurs is determined by the frequency of input signal. The higher the frequency, the more basal the peak occurs, and vice versa. This behaviour is core to the signal processing functionality of the cochlea and therefore is the most critical criteria to evaluate a cochlear model.

Since the excitation of sensory organ is a result of BM vibration, the motion of BM is a good indicator of the sound transmission within cochlea. In this chapter, BM is used as the main reference to evaluate the cochlear mechanics and its change in correspondence to alteration introduced.

3.2 Formulation of the Problem

The acoustic signal entering the ear canal causes the eardrum to oscillate, which leads to the mechanical vibration of middle ear bony structures. At the medial end of the ossicular chain, this mechanical vibration is transmitted into motion in cochlear fluid through the vibrating stapes footplate on the flexible oval window. This displacement at basal end of the cochlea causes pressure difference between chambers on either side of the basilar membrane and leads to deflection on the basilar membrane where the receptors organ of hearing reside. Therefore the vibration of BM is at the core of the mechanical process in the cochlea.

The objective of this model is to calculate BM displacement magnitude at a multitude of places along its length in response to a simple sinusoidal stimulus at the basal end and the impact of TW on this response. To be able to achieve this, a simple classical two-dimensional model is described in detail, majorly based on the model and numerical solutions established by Neely (S T Neely, 1978). In Section 3.3.2, by changing the boundary condition of the model, the creation of TW is introduced to the model to allow the exploration of the effect of TW on cochlear dynamics. A series of reusable MATLAB functions are created to allow instant computation of BM displacement magnitude for any input frequency.

3.2.1 Abstraction and Assumptions

The real structure of the cochlea can be complicated. There are components involved in the mechanical processes and the electrical processes, all

contributing to the functionality of the cochlea and sense of hearing. In order to reflect the basic physical principles of cochlear functions, the structure of the real cochlea has to be simplified to make the numerical calculation practical without sacrificing the determinant properties.

In this study, the focus is on the macro-mechanics of the cochlea. In this context, BM vibration is the core product of the mechanical process within cochlea. The factors that determine the BM vibration at each point along its length is the inertia of the fluid and the stiffness of the BM. The relationship between these factors can be replicated using a simple two-dimensional box model, as shown in Figure 3.2.1-1.

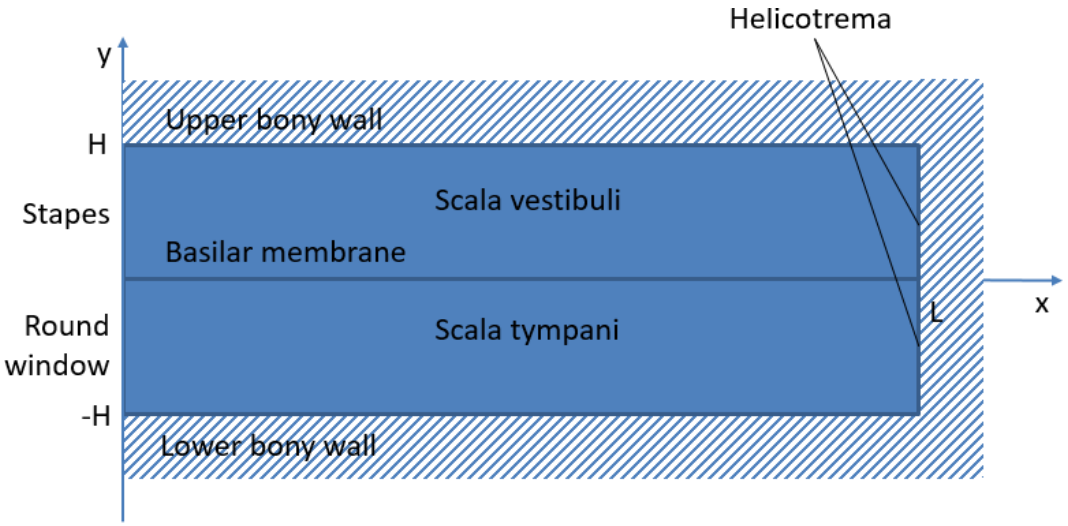

Figure 3.2.1 - 1 | Two-dimensional illustration of the box model of cochlea. Both upper and lower chambers, i.e. scala vesibuli and scala tympani, are filled with fluid, separated by basilar membrane and bounded by bony structure apart from the membrane-covered opening at the basal end.

The cochlea coil is unrolled since the coiling is believed irrelevant to cochlear mechanics (Steele & Zais, 1985). The x axis runs along the basilar membrane in

the longitudinal direction of the unrolled cochlea, from the base to the apex. The y axis is perpendicular to the x axis and thus perpendicular to the basilar membrane, in the direction from the bottom chamber scala tympani to the top chamber scala vestibuli. This simplification also takes into account the assumption that there is no variation of any physical quantity in the direction that is perpendicular to both x and y axes.

The two chambers are assumed to be identical in dimension – the distances from the basilar membrane to both upper and lower walls are denoted by H. L defines the distance from the stapes to the helicotrema, i.e. the length of the BM. It also implies that the cross-sectional area of the two chambers is assumed to be rectangular, enabling simpler calculation in two dimensions. This underlying assumption is supported by the fact that semi-circular assumption gives the similar results (E de Boer, 1991). Tapering is also believed not to affect the essential qualities of the cochlea (Kagawa, Yamabuchi, Watanabe, & Mizoguchi, 1987) therefore not considered in this model.

Assumptions are made on the relevant mechanical properties of components in the model. The upper and lower bony walls of the cochlea are assumed to be perfectly rigid. The viscosity of the cochlear fluid is negligible therefore no energy is dissipated into the fluid. This assumption is supported by viscosity's lack of impact on cochlear input impedance at frequencies higher than 500Hz (Koshigoe, Kwok, & Tubis, 1983) (Puria & Allen, 1991). The compressibility of the fluid is also considered negligible (Egbert De Boer, 1996). The cochlear partition, in this case simplified as BM, is elastic and deflects due to the pressure

difference between the upper and lower chambers. Due to the incompressibility of the fluid and the BM (Egbert De Boer, 1996), the flexible RW membrane is required to deflect by the same amount in the opposite direction of stapes.

Round window membrane, oval window, basilar membrane and the fluid inside cochlea are all assumed to be lossless. Therefore all energy is considered to be dissipated into motion of the membrane. The model is assumed to be linear, time-invariant to allow frequency response analysis. There is no longitudinal coupling along the length of the BM. The motion of each point on BM is induced by fluid pressure difference only. Fluid flows freely at the helicotrema therefore the pressure difference is zero at this point.

3.2.2 Hydrodynamics

The development of the hydrodynamics in this section follows Neely (S T Neely, 1978)(Stephen T Neely, 1981). At any point in the fluid at any time t, the velocity of the bulk fluid element is $\vec{\boldsymbol{V}}(x, y, t)$, and the pressure is P(x,y,t). Applying conversation of mass on the incompressible fluid with constant and uniform density ρ, by continuity, the velocity satisfies:

$$\nabla \cdot \vec{\boldsymbol{V}} = 0 \tag{3.2.2-1}$$

According to conservation of momentum, by Newton's second law, the rate of change of momentum equals to the total force. Considering the negligible viscosity and impact of gravity, the motion of the fluid satisfies:

$$\rho \frac{D\vec{\boldsymbol{V}}}{Dt} = -\nabla P$$

(3.2.2-2)

in which $\frac{D\vec{\boldsymbol{V}}}{Dt}$ is the material or substantial derivative (Huebner, 2001). If for any point in the fluid at any time t, the velocity $\vec{\boldsymbol{V}}$ has an x-component u and a y-component v, the material derivative can be expressed as:

$$\frac{D\vec{\boldsymbol{V}}}{Dt} = \frac{\partial \vec{\boldsymbol{V}}}{\partial t} + u\frac{\partial \vec{\boldsymbol{V}}}{\partial x} + v\frac{\partial \vec{\boldsymbol{V}}}{\partial y}$$

(3.2.2-3)

Since the flow speed is assumed to be very small in cochlea, the Equation 3.2.2-3 can be linearised into:

$$\frac{D\vec{\boldsymbol{V}}}{Dt} = \frac{\partial \vec{\boldsymbol{V}}}{\partial t}$$

(3.2.2-4)

Substitute Equation 3.2.2-4 into Equation 3.2.2-2 and take the divergence of both sides, the left-hand side transits into:

$$\nabla \cdot \left(\rho \frac{\partial \vec{\boldsymbol{V}}}{\partial t}\right) = \nabla \cdot \left(\rho \left(\frac{\partial u}{\partial t} + \frac{\partial v}{\partial t}\right)\right) = \rho \left(\frac{\partial}{\partial x}\frac{\partial u}{\partial t} + \frac{\partial}{\partial y}\frac{\partial v}{\partial t}\right) = \rho \frac{\partial}{\partial t}\left(\frac{\partial u}{\partial x} + \frac{\partial v}{\partial y}\right) = 0,$$

since by continuity, $\frac{\partial u}{\partial x} + \frac{\partial v}{\partial y} = \nabla \cdot \vec{\boldsymbol{V}} = 0$.

The following equation can therefore be obtained:

$$\nabla^2 P = 0$$

(3.2.2-5)

Equation 3.2.2-5 indicates that the pressure applied on any point in the fluid at any time satisfies Laplace's equation.

3.2.3 Mathematical Formulation and Boundary Condition

It has been established that it is the pressure difference between the two chambers above and below the cochlear partition that drives the vibration of the BM. The pressure difference function is defined as:

$$\mathrm{P_d}(\mathrm{x},\mathrm{y}) = \mathrm{P_{sv}}(\mathrm{x},\mathrm{y}) - \mathrm{P_{st}}(\mathrm{x},-\mathrm{y})$$

(3.2.3-1)

where $\mathrm{P_{sv}}(\mathrm{x},\mathrm{y})$ is the total pressure in the scala vestibuli at point (x,y) given there is no variation in this quantity in the z-dimension; $\mathrm{P_{st}}(\mathrm{x},-\mathrm{y})$ is the scala tympani counterpart at the mirror point across x-axis. It is assumed that the pressure distributions satisfy an anti-symmetric relationship such that:$\mathrm{P_{sv}}(\mathrm{x},\mathrm{y}) = -\mathrm{P_{st}}(\mathrm{x},-\mathrm{y})$. This is substantiated by numerous experimental observations (von Békésy & Peake, 1990) (Stenfelt, Hato, & Goode, 2004a) that the volume displacements of RW and OW are at exactly the same amplitude but in opposite direction.

The pressure difference function satisfies Laplace's equation as determined by Equation 3.2.1-5, given the fluid is assumed to have negligible compressibility:

$$\frac{\partial^2}{\partial \mathrm{x}^2}\mathrm{P_d}(\mathrm{x},\mathrm{y}) + \frac{\partial^2}{\partial \mathrm{y}^2}\mathrm{P_d}(\mathrm{x},\mathrm{y}) = 0$$

(3.2.3-2)

The boundary conditions of the model are defined by Equation 3.2.3-3 to Equation 3.2.3-6. They are the mathematical representation of the motions at the edges of the rectangular region, corresponding to assumptions made in Section 3.2.1. The upper and lower walls are assumed to be perfectly rigid therefore no motion at the upper and lower wall boundaries:

$$\frac{\partial}{\partial y}\mathrm{P_d}(x,\mathrm{H}) = 0$$

(3.2.3-3)

Basilar membrane has an unknown motion in y direction which can be defined by the acceleration of BM $a_b(x)$ and the volume density of the fluid ρ:

$$\frac{\partial}{\partial y}P_d(x,0) = 2\rho a_b(x)$$

(3.2.3-4)

where $a_b(x)$ is the acceleration of basilar membrane at point x and ρ is the density of the fluid. $a_b(x)$ only reflects the fluid motion at the BM boundary as a result of the motion in one of the fluid chambers while the factor 2 here on the right-hand side of the equation accounts for the reciprocal motion on the other side of cochlear partition. $a_b(x)$ here is set to be positive for downward acceleration.

Similarly, the boundary condition at the basal end can be defined as:

$$\frac{\partial}{\partial x} P_d(0, y) = -2\rho a_s$$

(3.2.3-5)

where a_s is the acceleration of stapes and is set to be positive for acceleration towards the positive side of x-axis.

The apical end has no pressure difference along the y axis, according to the assumption introduced in Section 3.2.1 about the helicotrema. The boundary condition is thus defined as:

$$P_d(L, y) = 0$$

(3.2.3-6)

Since the input signal to this linear system is simplified to be sinusoidal only, the field parameters in the system are considered as time-harmonic fields. The displacement response can be represented by a complex function such that:

$$w(x, y, t) = W(x, y)e^{i\omega t}$$

(3.2.3-7)

where $\omega = 2\pi f$ is the angular frequency.

The velocity and acceleration can thus be defined as:

$$v(x, y, t) = \dot{w}(x, y, t) = i\omega W(x, y)e^{i\omega t}$$

(3.2.3-8)

$$a(x, y, t) = \ddot{w}(x, y, t) = -\omega^2 W(x, y)e^{i\omega t}$$

(3.2.3-9)

Using Equation 3.2.3-7 and Equation 3.2.3-9, the relationship between basilar membrane displacement amplitude $w_b(x)$ at any time at point x and the corresponding acceleration is defined as:

$$w_b(x) = -a_b(x)/\omega^2$$

(3.2.3-10)

The passive cochlear partition is regarded as a single degree of freedom system containing mass, stiffness and damping, given the assumption that there is no direct mechanical coupling between neighbouring elements on basilar membrane. The basilar membrane acceleration can be defined by:

$$a_b(x) = \frac{iw}{\frac{K(x)}{iw} + R(x) + iwM(x)} P_d(x, 0)$$

(3.2.3-11)

where $K(x), R(x), and\ M(x)$ are the stiffness, damping, and mass of basilar membrane at position x.

Assume constant stapes displacement for all frequencies, and consider the need to normalise the solution to stapes displacement, the stapes is set to have unit displacement amplitude. From the relationship defined by Equation 3.2.3-7, 3.2.3-8, and 3.2.3-9, the acceleration can be defined as:

$$a_s = -\omega^2$$

(3.2.3-12)

3.2.4 Summary of Equations

A summary of equations that define the model of the motion within cochlea is presented as following.

In the fluid,

$$\frac{\partial^2}{\partial \mathrm{x}^2}\mathrm{P_d}(\mathrm{x},\mathrm{y}) + \frac{\partial^2}{\partial \mathrm{y}^2}\mathrm{P_d}(\mathrm{x},\mathrm{y}) = 0 \tag{3.2.4-1}$$

At the cochlea wall,

$$\frac{\partial}{\partial y}\mathrm{P_d}(x,\mathrm{H}) = 0 \tag{3.2.4-2}$$

At the helicotrema,

$$P_d(L,y) = 0 \tag{3.2.4-3}$$

Stimulus to the model at the stapes,

$$\frac{\partial}{\partial \mathrm{x}}P_d(0,y) = 2\rho\omega^2 \tag{3.2.4-4}$$

Response of the model along the basilar membrane,

$$\frac{\partial}{\partial y}P_d(x,0) = \frac{2\rho i\omega}{\frac{K(x)}{i\omega} + R(x) + i\omega M(x)}P_d(x,0)$$

(3.2.4-5)

With the Solution for $P_d(x,0)$ can be obtained from Equation 3.2.4-1 to Equation 3.2.4-5, the displacement of basilar membrane along its length can be calculated by

$$w_b(x) = \frac{1}{K(x) + i\omega R(x) - \omega^2 M(x)} P_d(x,0)$$

(3.2.4-6)

For any point along the length of basilar membrane, the BM displacement calculated using this model is a normalised value against stapes displacement.

3.3 Numerical Solutions and Results

Discretising the model of cochlea along the x and y dimension into a 256*8 grid points, the solution of the differential equations can be formulated into the matrix equations and solved numerically using Gaussian Block Elimination technique. It follows closely Neely's solution for the relationship between fluid pressure and membrane displacement (Stephen T Neely, 1981) and Gerald and Wheatley's guidance on solving a partial-differential equation (Gerald & Wheatley, 2004). The calculation and plotting process is programmed in MATLAB. The values of physical parameters were chosen in accordance to Steele & Taber's work (Steele & Taber, 1979) and are listed below:

Stiffness of BM at x mm from the stapes

$$K(x) = 1.0 \times 10^7 e^{-x/d}\ gs^{-2}mm^{-2}$$

where $d = 5\ mm$, equal to 1/7 total length of the cochlear uncoiled tube.

Damping of BM at x mm from the stapes

$$R(x) = 2\ gs^{-1}mm^{-2}$$

Mass of BM at x mm from the stapes

$$M(x) = 1.5 \times 10^{-3}\ gmm^{-2}$$

Distance from basilar membrane to either side of the cochlear bony wall

$$h = 1\ mm$$

Total length of the uncoiled cochlear tube

$$L = 35\ mm$$

Fluid density inside cochlea

$$\rho = 1.0 * 10^{-3}\ gmm^{-3}$$

3.3.1 Cochlear Frequency Sensitivity

The simulated displacement of basilar membrane is plotted against the longitudinal distance from the stapes. The results are presented in the form of the magnitude of the basilar membrane displacement relative to stapes displacement. For instance, 0 dB indicates the same displacement at both the stapes and the corresponding point on BM. The responses to pure tone stimuli at different frequencies across the hearing range of human are plotted together in Figure 3.3.1-1. The phase of displacement, i.e. the relative phase difference between the BM displacement and the stapes displacement is plotted in Figure 3.3.1-2. Zero

or the multiples of 2π denotes that at this frequency, BM vibrates in phase with the stapes, at the specific point indicated by its value on x-axis.

As anticipated, there is a place-dependent frequency sensitivity, i.e. high frequency signals have their peak response at relatively basal parts of the basilar membrane while low frequency signals have their peaks at relative apical positions. This is the principal characteristic of the cochlea as a frequency analyser: for every pure tone input, the location of where the peak motion occurs on BM is determined by the frequency of input pure tone, and the vibration decays exponentially post the peak location along the length of BM.

In short, this model satisfies the critical criteria of a model of cochlear mechanics. In the following section, some modification of the cochlear structure is introduced to the model and the results are used to determine the implication and impact of such change - a new addition to the study and conclusion can be accomplished using this classical model.

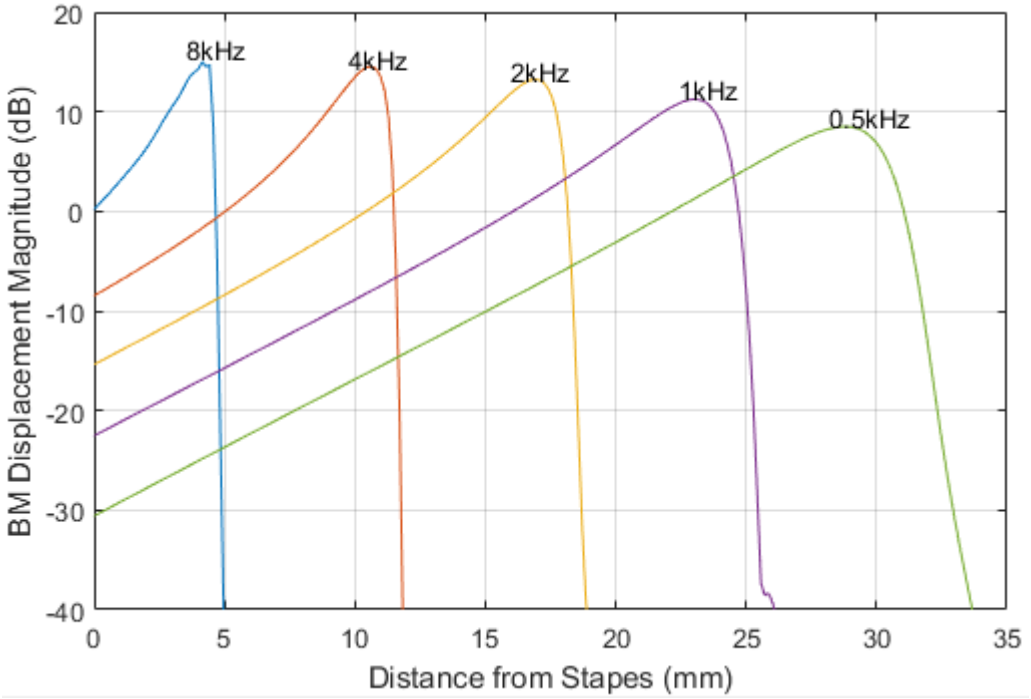

Figure 3.3.1 - 1 | Magnitude of the basilar membrane displacement *re* the stapes displacement, plotted against the distance from the stapes.

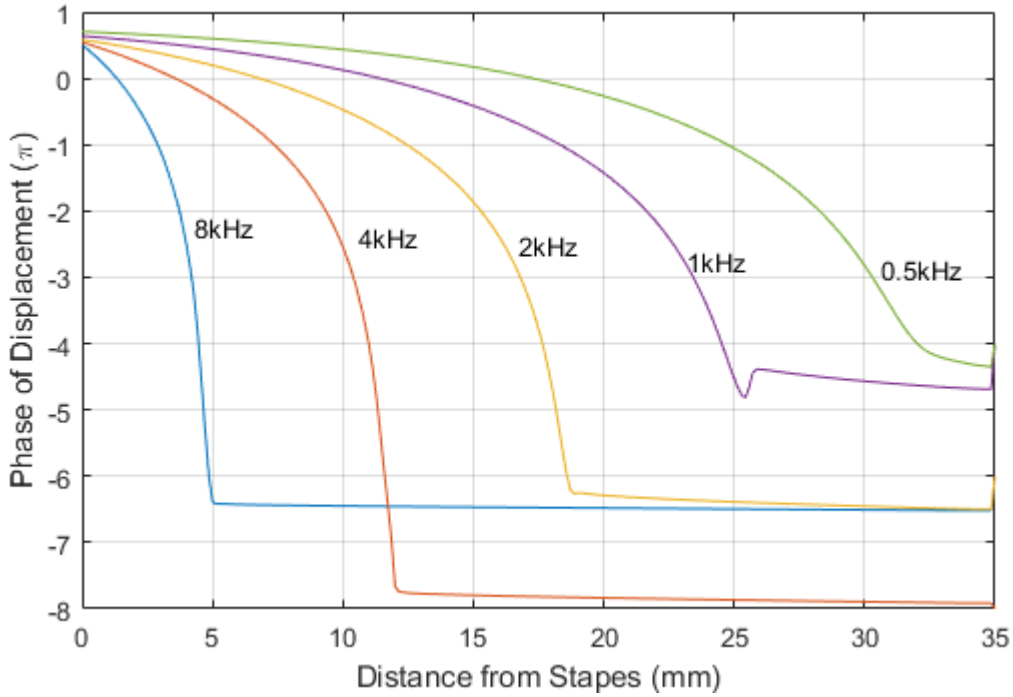

Figure 3.3.1 - 2 | Phase of the basilar membrane displacement *re* the stapes displacement, plotted against the distance from the stapes.

3.3.2 Effect of Creating a TW

The effect of TW can be simulated by changing the boundary condition at the upper and lower bony wall, via splitting Equation 3.2.3-3 into two equations to represent the rigid wall and elastic endosteal membrane exposure respectively. Assume the distance between the third window and the stapes along the length of cochlea is x_{TW} , the boundary condition of the rigid bony wall with third window can be defined as:

$$\frac{\partial}{\partial y}\mathrm{P_d}(x,\mathrm{H}) = 0, \;\; 0 < x < x_{TW} \; or \; x_{TM} < x < L$$

(3.3.2-1)

$$\frac{\partial}{\partial y}\mathrm{P_d}(x,\mathrm{H}) = 2\rho a_e(x), \;\; x = x_{TW}$$

(3.3.2-2)

$$where \; a_e(x) = \frac{iw}{\frac{K(x)}{iw} + R(x) + iwM(x)} P_d(x_{TW},\mathrm{H})$$

(3.3.2-3)

Stiffness of EM is constant long the length of cochlea and assumed to be equal to that of BM at the basal end:

$$K(x) = 1.0 \times 10^7 e^0 \; gs^{-2}mm^{-2}$$

Damping of EM, same as that of BM, is assumed to be constant:

$$R(x) = 2 \; gs^{-1}mm^{-2}$$

Mass of EM at x mm from the stapes is assumed to be half of that of BM, given that EM is a thin layer connective tissue while mass of BM here include the hair cells and other tissues that sit on it:

$$M(x) = 1.5 \times 10^{-3}\ gmm^{-2}$$

In Figure 3.3.2-1, the predicted BM displacement magnitude is plotted against the distance from the stapes, to simulate the scenario before and after a TW is created at 2mm from the base of the cochlea. This approximates the situation when cochleostomy is performed at the basal end on the cochlea – as in a normal cochlear implantation surgery. The results provide useful information to support the assumption in Chapter 5 that the presence of a TW on cochlea does not significantly affect its response to mechanical stimulus.

As denoted in Figure 3.3.2 -1, the solid orange line represents the BM response to pure tone stimulation before the presence of a TW, while the dotted green line represents the BM response after the creation of a TW. The comparison is conducted at different frequencies of the input signal: 0.5, 1, 2, 4 and 8 kHz.

Across the whole frequency spectrum, the simulated BM responses follow the same trend before and after the creation of a TW. The BM displacement in dB, indicating the sensitivity of BM to stimulus at OW, increase along the length of BM, until reaching its peak value and quickly decrease beyond the place where it peaks. Same as in a cochlea without the existence of a TW, higher-frequency input signal stimulates maximum response closer to the basal end on BM. Moreover, there is no noticeable change to the place where displacement peaks on the BM in terms of distance to stapes.

The biggest difference between ‘With TW’ and ‘No TW’ traces is at 4kHz. There is a 15% drop, approximately 2 dB difference between the peak values before and after cochleostomy. The creation of a TW has a higher impact at higher frequencies, compared to the lower-frequency counterparts. This can be related to the fact that higher frequency signals have their peaks close to where TW is created – 2mm from the basal end of the cochlea. The creation of TW has no significant impact at lower frequencies - the traces for ‘No TW’ and ‘with TW’ are almost identical when stimulus frequency is below 2kHz.

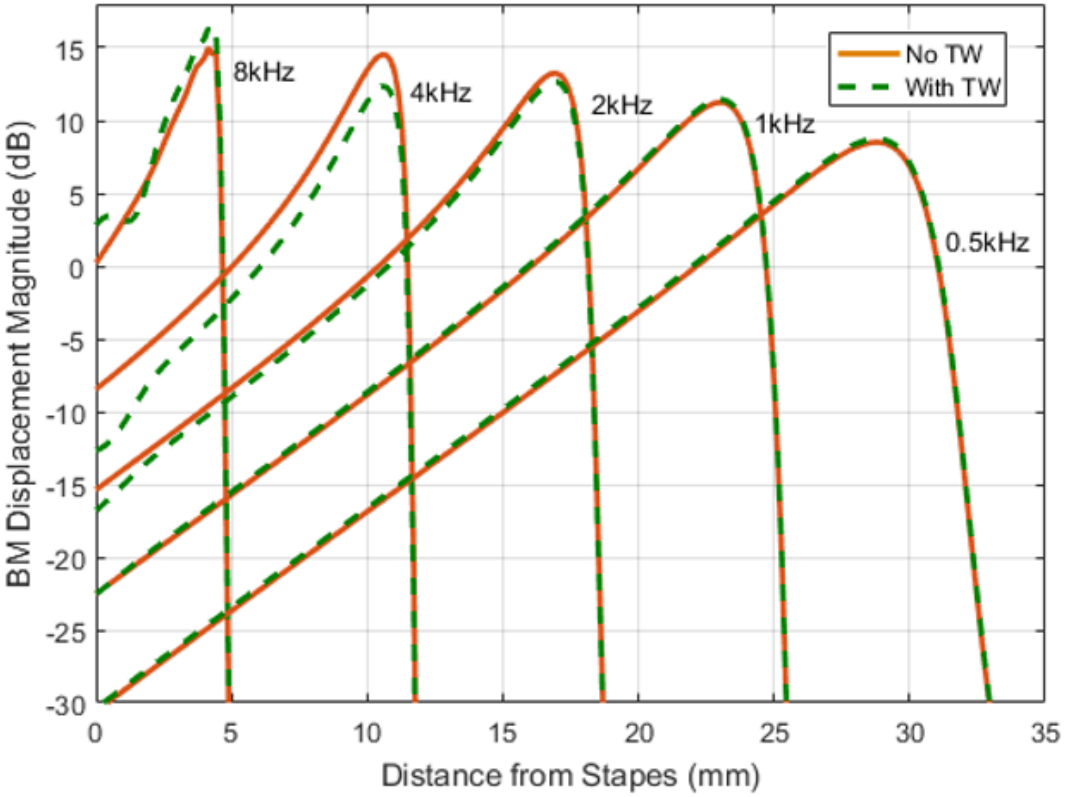

Figure 3.3.2 - 1 | Magnitude of the basilar membrane displacement *re* the stapes displacement, plotted against the distance from the stapes, before (black solid line) and after (orange dotted line) a TW is created at 2mm from stapes along the cochlear wall

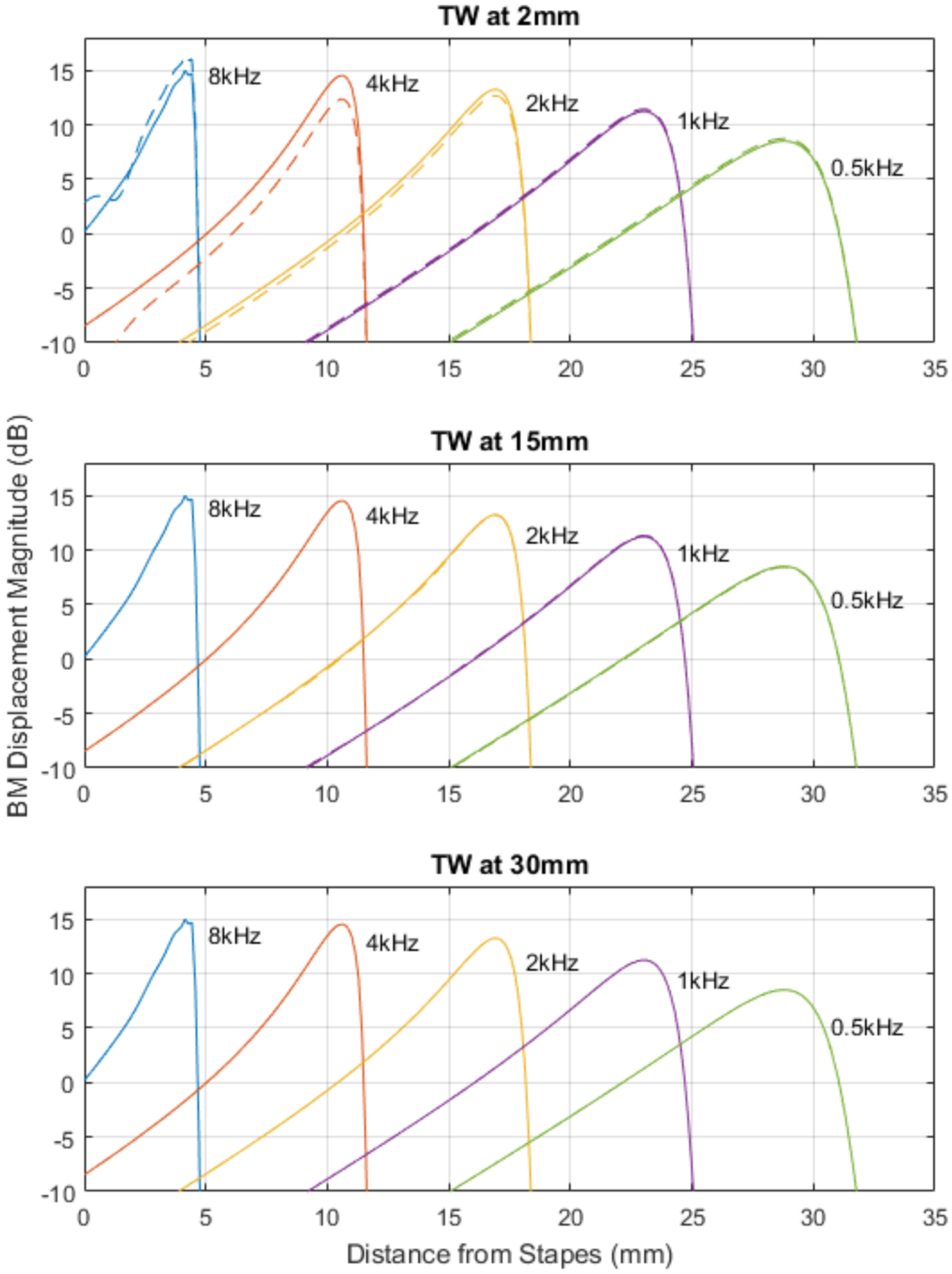

Figure 3.3.2 - 2 | Magnitude of the basilar membrane displacement *re* the stapes displacement, plotted against the distance from the stapes, before (solid line) and after (dotted line) a TW is created at 2mm, 15mm and 30mm from stapes along the cochlear wall.

Figure 3.3.2 -2 demonstrates the predicted displacement of basilar membrane along its length after a 1mm-diamter TW is created at 2mm, 5mm and 30mm respectively away from the stapes. The total length of the cochlea in this model is 35mm. The BM displacement prior to creation of a TW is represented by solid line, while the broken line depicts the BM displacement when a TW exists on the cochlea wall. The traces obtained for the same input frequency are plotted using the same colour to illustrate if there is an exact match between the pair.

By comparing the three sets of results, it can be noticed that the TW at the basal end (2mm) of the cochlea has a higher impact on BM displacement across all frequencies. Since the input stimulus is introduced to the system at basal end, the existence of an elastic membrane close to the basal end affects the total energy that is transmitted along the length of the cochlea.

Although the impact of creating a TW is significantly reduced for both cases when TW is created at 15mm and at 30mm away from the stapes respectively, there is distinction between the two sets of responses. In the scenario when TW is created at 30mm, the BM displacement after the creation of a TW is almost identical to that before the existence of TW, across all frequencies. This only applies to 8kHz and 4kHz when TW is created a 15mm from the stapes. The before and after curves are not as closely matched at lower frequencies –2kHz, 1kHz and 0.5kHz, when compared to their counterparts in the scenario when TW is created at 30mm.

As stated in the last paragraph, there is no significant impact on the BM displacement at 8kHz and 4kHz if the TW is created at 15mm from the stapes.

However there is noticeable change in BM displacement amplitude at 2kHz, 1kHz and 0.5kHz – all frequencies that have their characteristic peak further along the cochlea than 15mm from the stapes. This shows that the longitudinal position of TW along the length of the cochlea is related to the frequencies at which the existence of TW is most likely to impact. For frequencies with their peak BM response placed closer to stapes than TW, the BM displacement are less likely to be impacted subsequent to the creation of a TW. This is evident in plot 'TW at 30mm'. All frequencies have their original peak response at places less than 30mm from the stapes, hence at all frequencies the BM displacement is almost identical before and after the creation of a TW.

3.4 Discussion and Conclusions

A finite-difference method is utilised to solve this two-dimensional, passive cochlea model. The displacement of basilar membrane in response to sinusoidal stimulation at the oval window is plotted as a function of distance from the stapes. Cochlea's frequency distinguisher functionality is successfully demonstrated by the simulation results - the BM displacement increases along the length of BM, until reaching its peak value and quickly decreasing beyond the distinct, frequency-related place where it peaks. The higher the input frequency, the closer to base that the BM response peaks. This is a repeat of the classic mathematical solution to cochlear dynamics, predominately based on Neely's 1978 work (S T Neely, 1978), aided with modern computational tools like MATLAB. By modifying the boundary condition, the effect of TW is

studied - a new addition to the conclusions that can be reached using this classic model - and is concluded as follows.

TW created at basal end of the cochlea has a higher impact on the cochlea dynamics than TW created at the middle or apical part of the cochlea. The frequencies that have their peak response place further than where TW is positioned is more likely to be affected by the creation of TW. In other words, a TW that is created towards the apical end of the cochlea is least likely to impact the cochlea dynamics, in this case BM displacement. This can be a useful indication for future experimental studies of cochlear dynamics. A TW created close to the apical end of the cochlea can be an effective point of observation with minimum impact on cochlear dynamics if applicable. However, the creation of TW does not qualitatively alter how BM responses to stimulus introduced into cochlea. There is overall little impact on cochlear dynamics when a TW is created on the cochlear wall.

The next chapter will cover the experimental method used in the lab to study cochlear dynamics including the impact of the creation of TW, using porcine cochlea.

Chapter 4

Experimental Study of Cochlear Dyanmics using Porcine Cochlea

Using porcine cochlea as a physical model, one of the assumptions made for cadaver study in Chapter 5 can be tested: there is no significant change in RW velocity after the creation of a TW on cochlea. In this chapter, the experimental setup and procedure for vibrational response measurement on porcine cochlea is described in detail. This also serves as an opportunity to formulate some considerations that need to be taken into account of in the vibrational measurement on human cadaver heads.

4.1 Use of Porcine Cochlea

Porcine is an effective and economical alternative to cadaver head or temporal bone in the study of hearing mechanics. Porcine cochlea is very similar to human cochlea in terms of size and functionality (Pracy, White, Mustafa, Smith, & Perry, 1998) and is considered a useful model in ontological research (HaiJin et al., 2013) especially when there is limited access to human models due to ethnical complexities.

The porcine cochleae were harvested in the lab from porcine heads sourced directly from a local butcher. A porcine head was dissected into two halves to allow access to the cochlea from the medial side of the head. The brain was then removed to provide a clear visual and direct access to the cochlea which sits in the superior corner of the skull and is covered by dura mater. Dura is outermost layer of meninges – a membranous covering that surround the brain and protect it from being directly pressed against the skull surface. The dura matter covering the cochlea was cut along the edge of the cochlea with a scalpel and was lifted with surgical forceps. Considerable caution was then taken to extract the cochlea - by prying gently at several positions along the edge of cochlea until it is fully separated from the skull.

Figure 4.1-1 shows a fully detached cochlea, demonstrating the round window and the intact stapes.

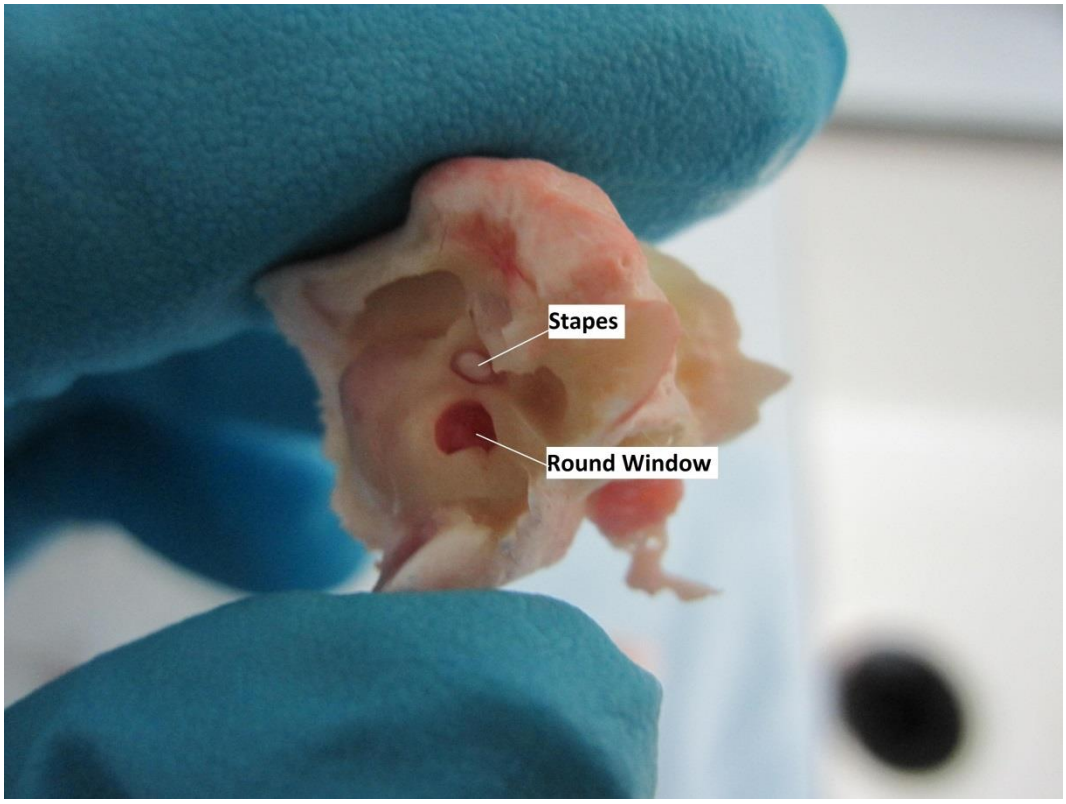

Figure 4.1 - 1 | A porcine cochlea with intact stapes and round window

4.2 Experimental Setup

The experimental setup for the measurement on porcine cochlea is illustrated by the following block diagram shown in Figure 4.2–1.

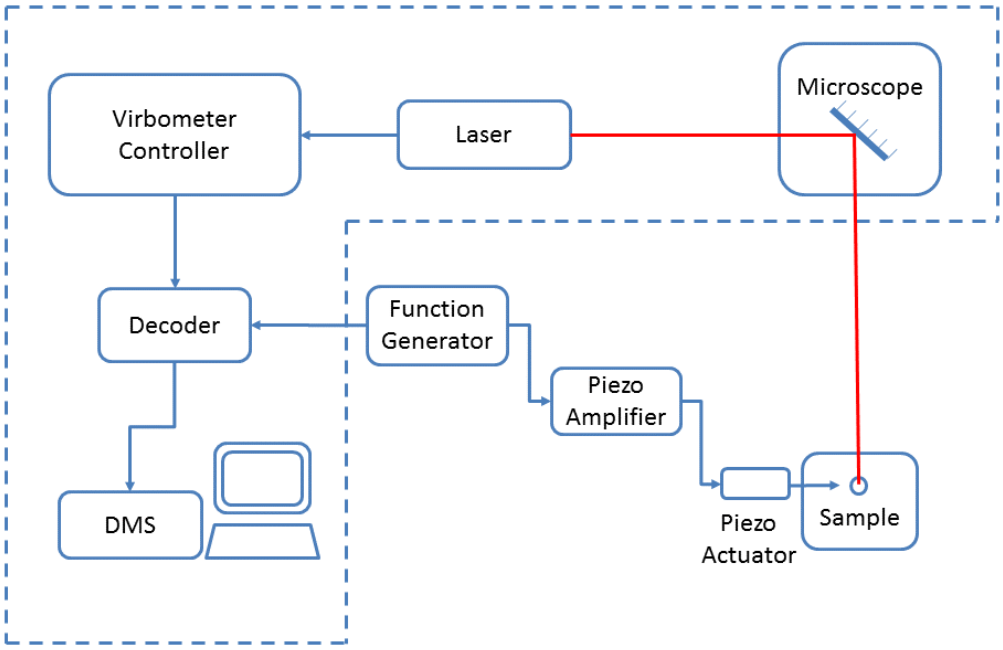

Figure 4.2 - 1 | Experimental setup illustrating key components and the flow of information

Actuation

A stimulation was imposed onto the cochlea through a 1-mm diameter custom-made pin that is attached to a PI P-820.10 Preloaded Piezo Actuator (Physik Instrumente GmbH & Co. KG, Karlsruhe, Germany) while the response was recorded from the round window (RW) to reflect the impact caused within the fluid-filled capsule. The piezo actuator was driven by an array of pure tones generated by TTi TGA1241 40MHz Arbitrary Waveform Generator (Aim-TTi Huntingdon, Cambridgeshire, United Kingdom). The signal was amplifiled through a matching Piezo Amplifier PI E-617 (Physik Instrumente GmbH & Co. KG, Karlsruhe, Germany) to ensure consistently equal amplitude applied to the

piezo actuator over the frequency band of interest in the study. The piezo actuator was driven at 0.125, 0.25, 0.5, 1, 2, 3, 4, 6, 8 and 10 kHz. The driving voltage was fed through the Polytec MSA-E-401 Junction Box and MSA-W-400 Data Management System (Polytec GmbH, Waldbronn, Germany) which offers decoding and data acquisition functionality and allows the signal to be monitored at its central data management system (DMS).

Laser Vibrometry

The vibration on the round window membrane (RWM) is captured by a laser Doppler vibrometer (LDV) – MSA 400 Micro System Analyzer (Polytec GmbH, Waldbronn, Germany). The components within the dashed lines in Figure 4.2 – 1 are all part of the laser vibrometer system, including OFV-5000 Vibrometer Controller and OFV-551/552 Fiber-Optic Interferometer. The laser beam was coupled into the microscopy system via OFV-072 Microscope Adapter and OFV-073 Microscope Scanner Unit. Along with the adapter and the scanner unit, there was also a video camera that was mounted on the microscope - a ZEISS SteREO Discovery.V8 microscope (Carl Zeiss Microscopy GmbH, Jena, Germany). This provides a live image feed through the objective lens, which allows monitoring of the status of the sample throughout the entire measurement process. The microscopic view of the stapes is shown in Figure 4.2-2.

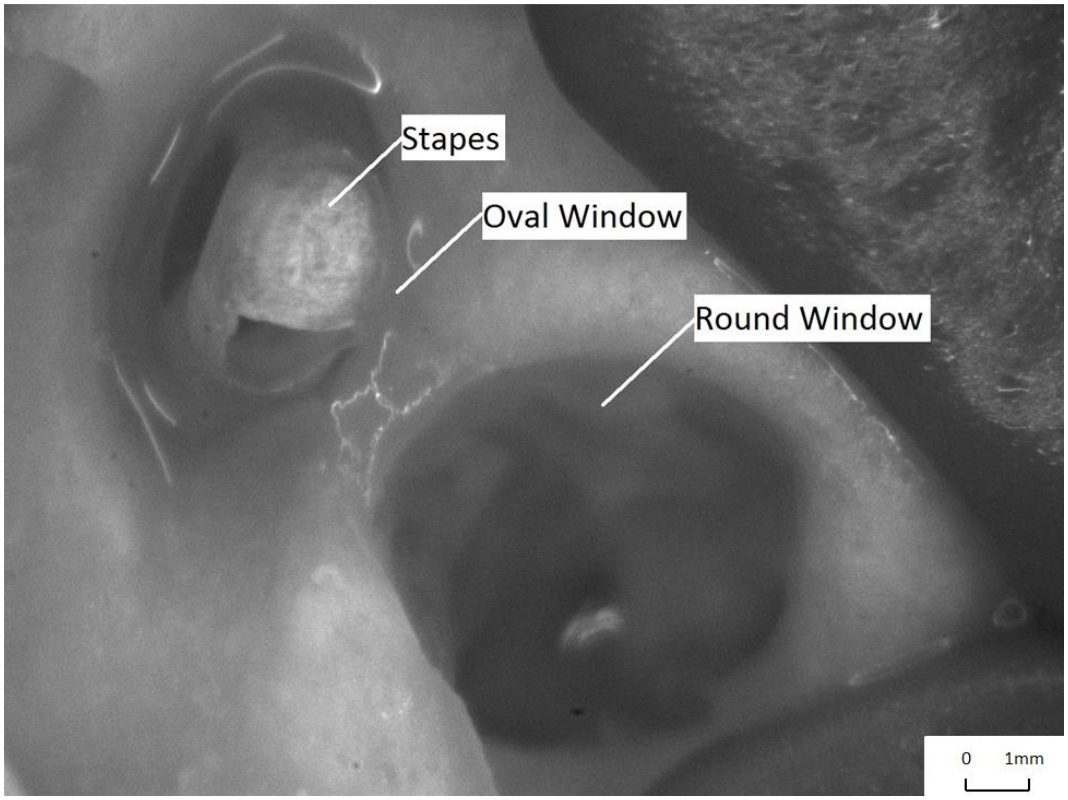

Figure 4.2 - 2 | Microscopic view of the cochlea showing key features of the cochlea that are relevant to the study: stapes, the membrane underneath stapes – oval window (OW), and round window (RW)

To ensure a consistently stable signal sensed by the laser vibrometer, the reflectance of RWM surface was increased by depositing a layer of microbeads (<1mg). In light of the knowledge that the level of vibration varies if observed at different positions on the round window membrane when subjected to the same level of stimulation(Stenfelt et al., 2004a)(Stenfelt, Hato, & Goode, 2004b), caution was taken to take measurements at a constant point on membrane – at the approx. centre of the RWM.

Other considerations

The cochlea was held in a custom-made cochlea holder that can be screwed onto the observation stage of the microscope. While the holder itself can be fixed on the stage firmly, it was found that the support it provided to the sample was insufficient for consistent measurements, given the irregular surface of a cochlea. Dental impression putty (Ivoclar Vivadent, Schaan, Liechtenstein) was applied to fill the gap between the cochlea and holder to eliminate the movement of cochlea during measurement, as illustrated in Figure 4.2-3. This simulates the cochlea mounting in head where the surrounding material closely follow the shape of the cochlea which sits tight within the skull. A properly supported porcine cochlea specimen under measurement is shown in Figure 4.2-4. Caution was also taken to set the cochlea such that the Round Window (RW) faced straight up. In other words, laser beam projected from the LDV through the microscope was kept inline with RW normal. The need for making cosine correction to the measurement data was therefore removed. Vibrational measurement could then be conducted with precision and consistency. The physical property of the putty ensures quick setting while allowing adequate time for adjusting the position cochlea until correct. After measurement, the mould can be removed from the holder, along with the cochlea, with no residue left.

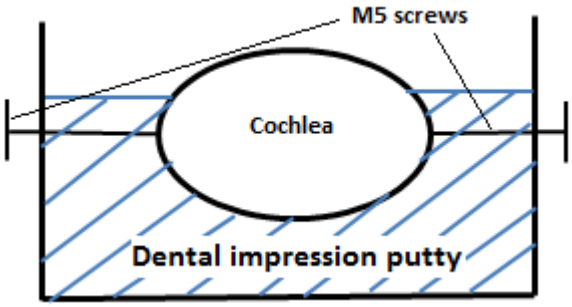

Figure 4.2 - 3 | An illustration of how cochlea is supported – simulates the cochlea in head where the surrounding material closely follows the shape of the cochlea

A snake-arm supported robotic drill was deployed to facilitate the right level of contact between stapes and the tip of the actuator. A custom-made surgical drill bit, with M3 thread at the tip instead of the standard drilling burr, was used to hold the piezo actuator which has a matching thread at one end. A fuller picture of the setup is shown in Figure 4.2-5. Thanks to the force and torque sensibility of the robotic drill, the drill bit automatically stops moving forward once there is a change of properties of media that the tip is in contact with – in this case a change from air to bone tissue upon piezo tip touching the stapes.

The porcine cochlea sample under measurement was placed on an Anti-Vibration table (Thorlab, New Jersey, United States), along with the microscopy system, optics of the laser vibrometer and other main elements of the experimental setup that do not provide pure monitoring and analysis functionalities.

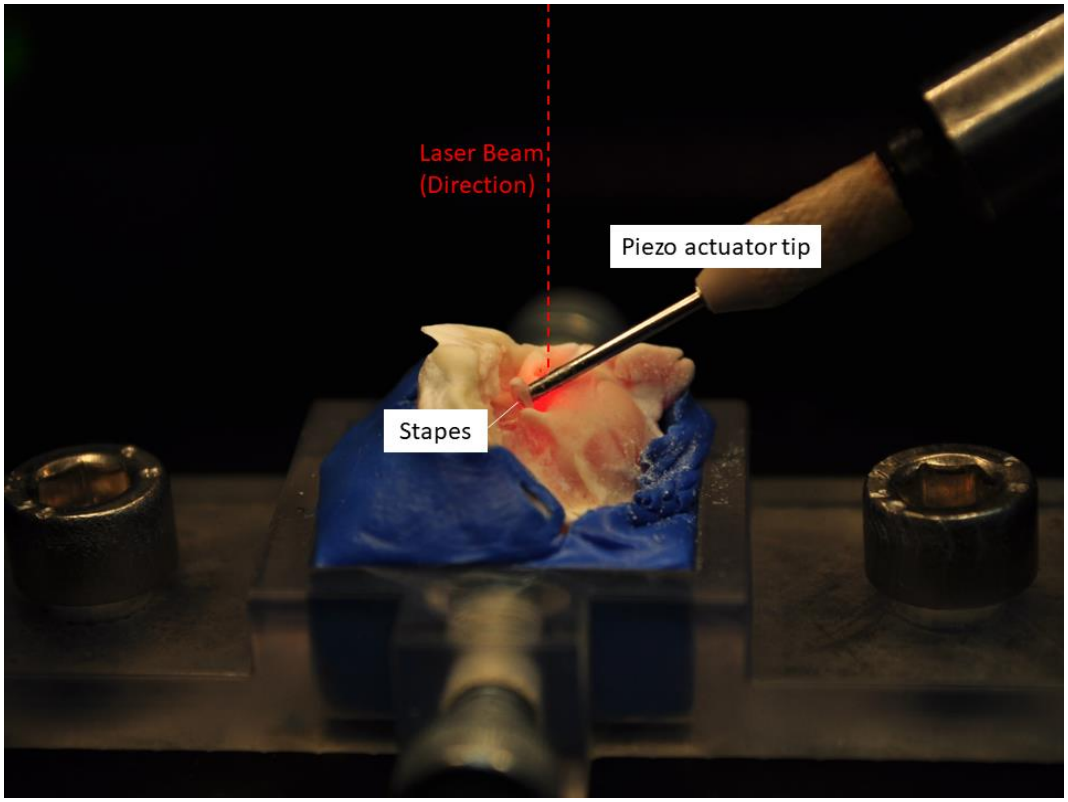

Figure 4.2 - 4 | A close-up view of the experimental setup showing piezo actuator in contact with stapes and the laser beam pointing on the round window which is located further away from the camera

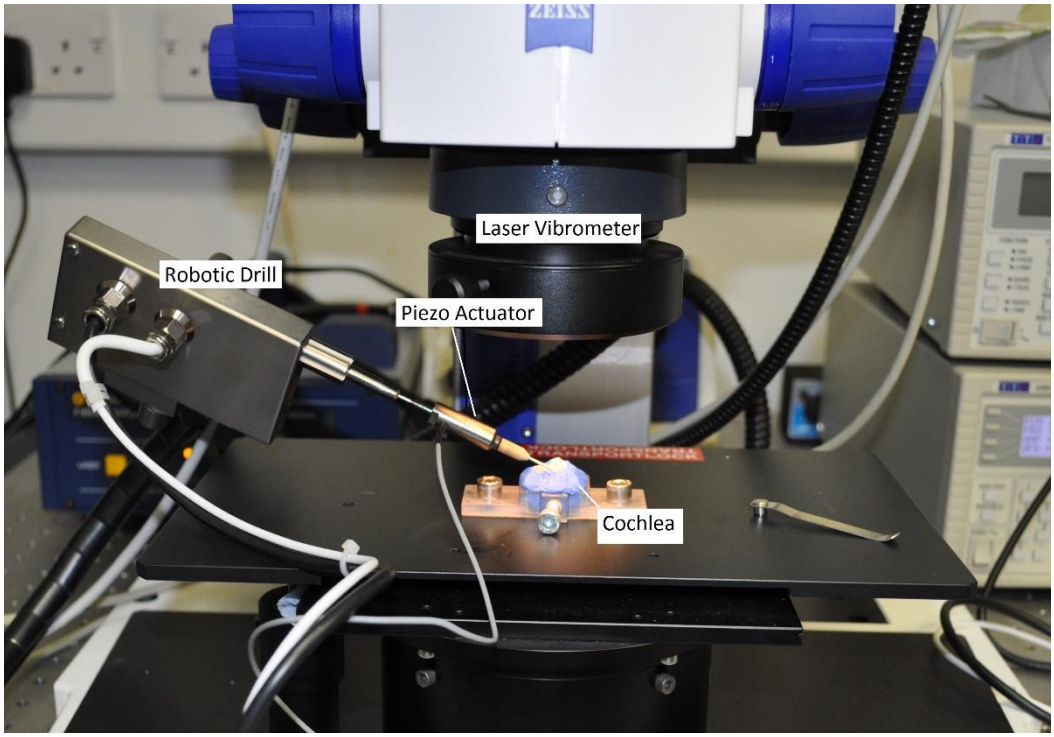

Figure 4.2 - 5 | The experimental setup showing cochlea, robotic-held piezo actuator and microscopic part of the laser vibrometer

4.3 Effects of Creating a Third Window on the cochlea

To investigate how the existence of a Third Window (TW) affects cochlear dynamics, the velocity of round window was measured before and after the creation of a TW. Stimulation was applied on the stapes while the response on the Round Window (RW) was measured. A TW was created on the cochlea with the smart hand-held robotic drill in between two measurements. Here a RW response is used as an indication of the mechanical motion inside the fluid-filled cochlea capsule, in order to minimise the intrusion and alternation to the physical structure of the cochlea. It was confirmed before recording started that the

velocity on cochlea bone was negligible compared to the velocity that can be measured on RW therefore no correction or reference was taken.

As mentioned in Section 4.2, as the energy source introduced into the cochlea, the stimulus on the stapes was applied at 0.125, 0.25, 0.5, 1, 2, 3, 4, 6, 8 and 10 kHz. The vibration on RW in response to stapes stimulus was converted into frequency domain using data acquisition module of the laser vibrometer system. The data was exported as an ASCII file and processed in Excel for analysis.

The measurements of the RW response to stimulus on stapes were conducted immediately before and after the TW was made to minimise the alteration of properties due to biological deterioration between two measurements. In an attempt to avoid discrepancies associated with Rigor Mortis, all data was collected from samples within 12 hours post slaughter.

A set of results was shown in Figure 4.3 - 1. The RW response before and after the creation of a TW show considerable similarity. This verifies the observation by (Masoud Zoka Assadi, 2011). The two curves follow the same trend, the general trend of both RW velocity curves correspond to other findings - RW velocity is lower at higher frequencies compared to that at the lower end of the frequency spectrum (Stenfelt et al., 2004b). This property applies to both curves in Figure 4.3-1. After the creation of a TW, there is no change of trend, nor continuous lower or higher values at more than two consecutive frequencies. It is therefore not a significant change to RW response in terms of its velocity after the creation of a TW on cochlea compared to when in its original state. The RW

velocity here were measured against the velocity magnitude of the piezo actuator tip in unit of dB. This normalisation was implemented at each of the frequency that RW velocity was measured at. The velocity measured at piezo actuator tip can be found in Appendix C.

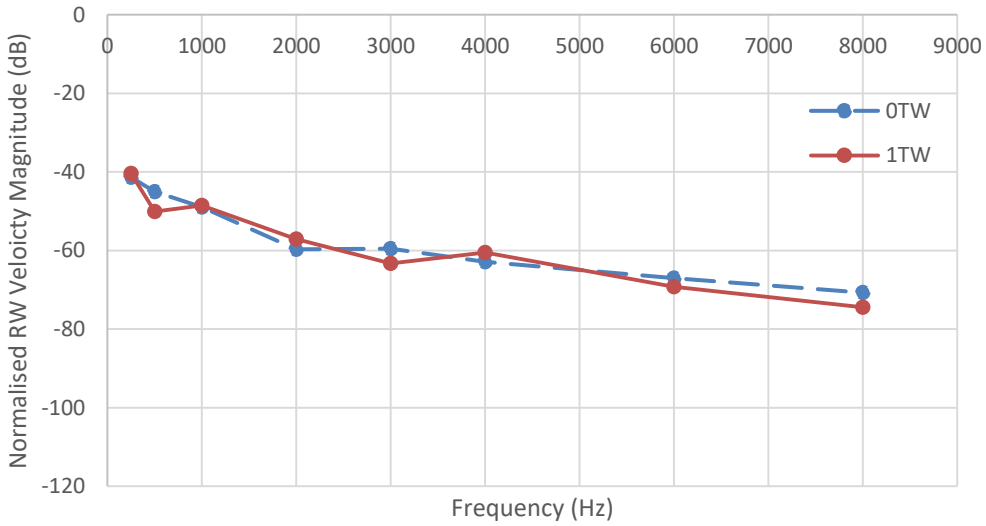

Figure 4.3 - 1 | Round window velocity before (blue dashed line) and after (red solid line) cochleostomy, i.e. creation of a TW, when the stapes is mechanically stimulated at selected frequencies within hearing range. The value is normalised against the magnitude of velocity of piezo actuator tip movement.

4.4 Conclusions

In this study, the methodology to conduct a vibrational measurement on cochlea was explored and practiced in order to answer the following question: whether the creation of a TW leads to significant change to cochlear dynamics that is measurable on RW.

Although equivalent subject is discussed in Chapter 3 using the mathematical model, an expectation is only achieved in terms of basilar membrane's behaviour. There is no direct assertion about the implication on RW velocity.

From this study, it can be concluded that there is no significant impact on RW velocity after the creation of a TW compared to before. This is a particularly relevant statement, since it provides a direct, experimental evidence to support one of the assumptions underlying the experimental procedure set up for human cadaver study. This study is covered in Chapter 5 and 6.

Chapter 5

Experimental Methods to Study the Mechanical Energy Cochlea is exposed to During Cochleostomy Formation

Preserving residual hearing for patients is an important aspect during ear surgery. Cochlear implant surgery (CIS) is a remedy for profoundly deaf patients. However, the remarkable performance achieved indicates potential benefit to a wider range of hearing impediment, including patients with hearing at low frequencies. To investigate, measurements were taken on the reduction in vibration induced in the hearing organ when using an acclaimed new surgical robotic drilling technique. Drilling is a fundamental process in ear surgery and

the robotic technique enables preservation of critical delicate membranous tissues, another cause of tissue trauma. Controlling conventional drill penetration is beyond human capability in perception and dexterity, whereas the new technique offers consistent results, predictable outcome, reduced vibration trauma and reduced complications.

Reported here is the contrasting acoustic and mechanical energy transmitted into the cochlea when drilling a cochleostomy when using a (1) Manually guided conventional technique (2) Manually supported tissue guided robotic drilling technique.

The vibration induced was measured at the round window – a naturally exposed membrane on the cochlea. It is a useful indicator of the mechanical movement of the fluid inside the cochlea. The mechanical movement of the fluid inside the cochlea causes the vibration of basilar membrane, and triggers the sense of hearing. Therefore measurement of the vibration at the round window is considered an effective way to gauge the mechanical energy transmitted into the cochlea and to assess potential damage to hearing induced during surgical drilling. Most importantly, this enables nonintrusive observation without introducing structural modification to the cochlea.

5.1 Importance of Hearing Preservation Study

Preserving the residual hearing function of the cochlea is an important factor to consider when conducting ear surgery. This caution also applies to cochlear

implant surgery, especially for patients who still have substantial hearing at low frequencies where acoustic signals can be perceived authentically by hair cells at the apical part of the cochlea.

The enhanced post-surgery hearing performance following cochlear implantation indicates potential expansion of the patient group able to benefit people who have residual hearing. The opportunity has increased focus on preserving residual hearing, driving innovations in inner-cochlear stimulation mechanisms and electrode design. A good example is electroacoustic stimulation (EAS). EAS leverages the residual active sensorial function at the apical region while injecting electric current via electrodes placed at the basal part of the cochlea. More importantly, it reduces exposure to trauma caused during placement of the electrode by limiting the electrode length and insertion depth. Bimodal stimulation is believed to improve hearing performance after cochlear implantation (Cipolla et al., 2012).

Apart from effort in refining electrode characteristics, attention has focused on the surgical procedure, more specifically exposure to acoustic and mechanical trauma during cochlear implant surgery. Among the steps of cochlear implantation, drilling is a significant contributor to trauma caused by both the potential high level of disturbance induced and the relatively long period of drilling during surgery. A normal cochlear implant surgery takes approximately 2 hours (“Royal National Throat Nose and Ear Hospital: Cochleaer implants for adults,” 2014). The average period of drilling directly on the cochlea to prepare

the cochleostomy is 8 minutes (Cipolla et al., 2012). Cochlea can be exposed to an average sound pressure level of 89.9 dB SPL, maximal 118 dB SPL during the approximately 8-minute continuous drilling period (Cipolla et al., 2012). According to information provided by The American Hearing Research Foundation (The American Hearing Research Foundation, 2008), persistent sound vibration louder than 85 dB SPL can cause permanent hearing loss. The hearing mechanism of the ear cannot tolerate sound levels greater than 140 dB SPL and the maximum duration the ear can be exposed to a 115 dB sound without permanent hearing loss is 15 minutes. When measured on temporal bones, the noise level during cochleostomy was found to range from 116 to 131 dB SPL and exceeded 130 dB SPL when the endosteal membrane was touched by the burr (Pau et al., 2007)(Yin et al., 2011).

Contemporary cochleostomy formation is performed by ENT surgeons using a conventional surgical drill. Inevitably there is the risk for endosteal membrane perforation by the completely manually controlled drill during cochleostomy drilling (Coulson, Reid, Proops, & Brett, 2007). The perforation could lead to severe trauma induced by the rotating burr touching basilar membrane and other intra-cochlear tissues. In addition, the leakage of perilymph will degrade residual hearing sensitivity and contribute to postoperative hearing loss.

The robotic surgical drill (Taylor et al., 2010) developed by researchers at Brunel University provides a consistent cochleostomy formation and was successfully trialled in the operating theatre (Brett et al., 2009). This surgical robotic drill will

detect membranous surfaces; stop drilling automatically and avoiding penetration. The approach avoids controlling this critical process using the inadequacies of human perception for feedback and enables the surgeon to make informed decisions during drilling on the state of the tissue, drill bit and process. The drilling force and torque transients coupled through the tissue are used to inform the robot of conditions in real-time such that precision is achieved with respect to the tissue and that force values are applied within an acceptable range. Consistent drilling results are achieved and the ability to sense at the tool-point in the tissue avoids the need to lift and reapply the drill such that progress can be checked visually. Previous studies show correlation between forces applied and the disturbance generated during drilling (Masoud Z Assadi et al., 2013). Limiting the period when the running burr is in contact with the endosteum is also reported as critical for reducing trauma, and is reported by independent researcher groups (Pau et al., 2007)(Yin et al., 2011)(Eze et al., 2014).

The objective of this study is to evaluate the acoustic and mechanical energy transmitted into the cochlea while drilling a cochleostomy. On human cadaveric heads, the decibel equivalent sound pressure level (dB SPL eq.) induced within the cochlea during cochleostomy drilling is quantified experimentally. Comparison between the conventional manual surgical drilling technique, that is prone to human intervention, and a consistent technique using an autonomous robotic drill was achieved.

5.2 Experimental Methods

5.2.1 Cadaveric Head Preparation for Acoustic Measurements

The cadaver experiments were carried out on two adult cadaveric human bodies bequeathed for medical education and research purposes, obtained at Keele Anatomy & Surgical Training Centre at University of Keele. Specimens were obtained within 120 hours of death and frozen at -20 °C. It was agreed by both (Pennings, Ho, Brown, Van Wijhe, & Bance, 2010) and (John J. Rosowski, Davis, Donahue, Merchant, & Coltrera, 1990) that the freezing and thawing process has no significant effect on the mechanical properties of the cochlea and is a common approach to collect specimens when the availability of fresh specimens is often limited and random. Experiments were carried out in a room temperature environment while a thawing procedure similar to that described by (Pennings et al., 2010) was followed before use.

Otoscopy and tympanometry was carried out prior to temporal bone drilling to confirm that both outer and middle ear were in good condition. To achieve easy access to the promontory and the basal turn of the cochlea, a wide cortical mastoidectomy and posterior tympanotomy was performed on each side of the head of each specimen. Care was taken to retain the ear canal wall intact throughout the whole experimental procedure to ensure that middle ear transfer function can be measured at different stages. The ossicular chain and the inner ear were examined carefully and no abnormality was found. Although the

purpose of experiments was not to investigate middle ear mechanisms, care was taken to keep tympanic membrane, ossicular chain and all ligaments and tendons intact throughout the whole experimental process, and to eliminate any effect of an incomplete sound conducting system, to cochlear dynamics.

For each specimen, the head and chest was resting on an anti-vibrational table, while the abdomen and below rested on a locked-in-position cadaver trolley, with the top surface of equal height to the anti-vibrational table. A small gap was left between table and trolley to minimise energy transmission from the floor via the trolley to the cadaver head. The head was tilted, and rested on the headrest, enabling suitable access for performing drilling and vibrational measurements with the laser vibrometer.

5.2.2 Calibration of Sound Conducting Qualities

The sound transfer function of the middle ear of each specimen was determined at both stapes (METF-SS) and RW (METF-RW). The METF-SS is checked against middle ear transfer function standards to ensure the integrity of sound conduction of each specimen (J. J. Rosowski et al., 2007)(*ASTM F2504 - 05, Standard Practice for Describing System Output of Implantable Middle Ear Hearing Devices*, 2005). The METF-RW will be used in the computation of equivalent sound pressure levels (SPL_{eq}).

An illustration of the calibration experimental setup is provided below in Figure 5.2.2-1. A probe microphone ER-7C (Etymotic Research, Elk Grove Village, IL 60007, USA) and a wide band earphone ER-2 (Etymotic Research), both coupled to an ER1-14A disposable foam eartip (Etymotic Research), were inserted into the external ear canal. The end of the probe tube of the microphone was placed at 2mm lateral to the tympanic membrane. The earphone was driven by a frequency logarithmic sweep signal from 0.1 to 10 kHz at 1 Vrms from R&S UPV Audio Analyser (Rohde & Schwarz, 6821 Benjamin Franklin Drive, Columbia, MD 21046, USA). According to sensitivity of the ER-2 earphone, tones delivered were at 100 dB SPL. A standard calibration process of the probe microphone was implemented before measurement and a sensitivity value was checked against the range of 40 - 60 mV/Pa and recorded. The actual setup in the lab for the section covered in the green dashed circle is presented in 5.2.2-2.

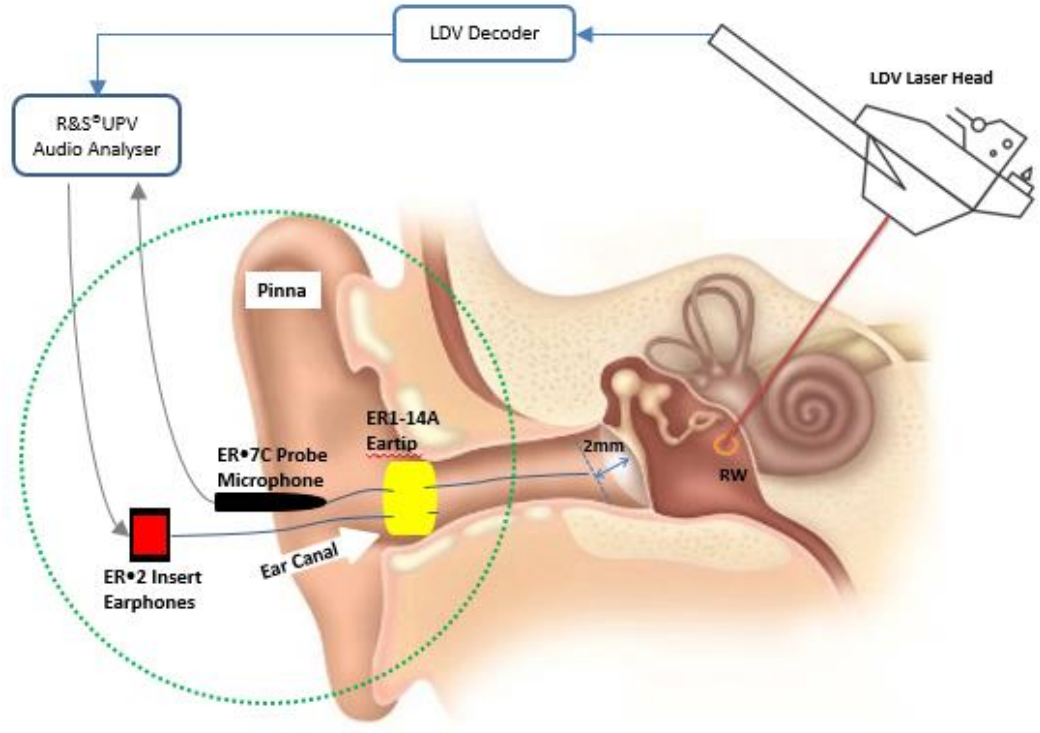

Figure 5.2.2 - 1 | Schematic illustration of the calibration setup

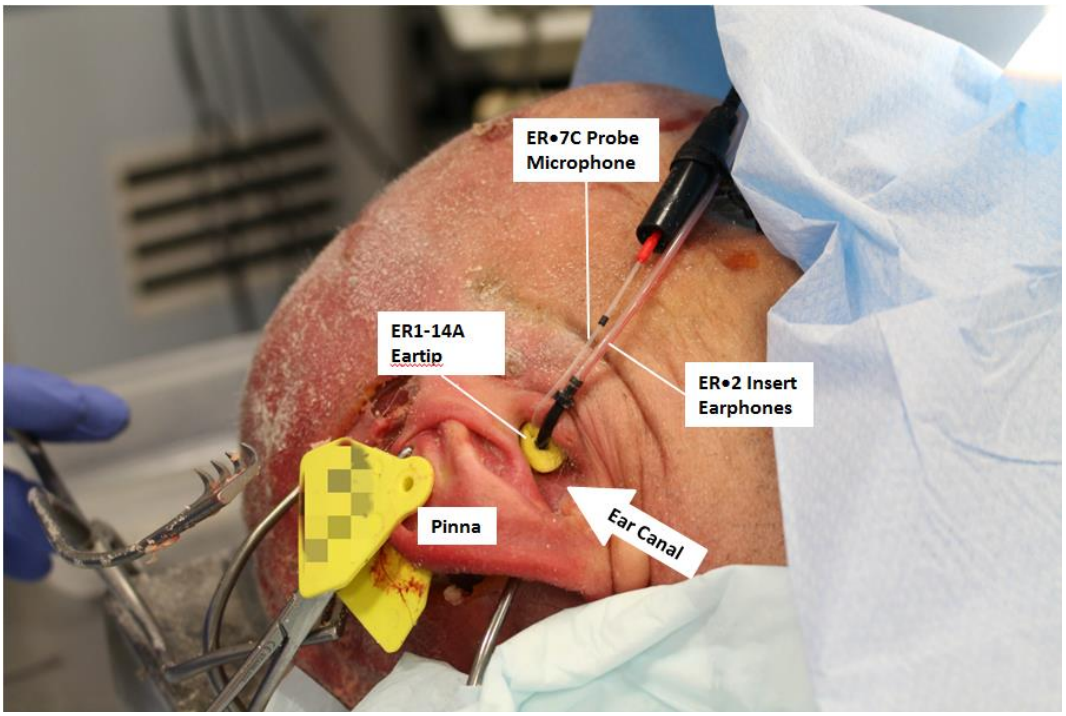

Figure 5.2.2 - 2 | Calibration setup in the lab on the human cadaver head (proximal)

Figure 5.2.2-2 shows the setup in the lab for calibration measurement. The corresponding schematic can be found in Figure 5.2.2-1. The cadaver head was rested on the anti-vibrational table, and tilted to facilitate observation and measurement of the inner ear. An incision was made behind the ear. The pinna was anteriorly raised and held in place by self-retaining retractors. The temporal bone was thus exposed. A wide cortical mastoidectomy and posterior tympanotomy was performed to provide an unblocked access of laser to the round window, as well as to enable drilling on the cochlea. Both probe tubes of the probe microphone and the ear phone were inserted into the ear canal via the ear tip.

A compact laser vibrometer system was used to measure both stapes and RW velocity. The laser head part of the compact sensor head system OFV-534 (Polytec, D-76337 Waldbronn, Germany) and micro-manipulator A-HLV-MM30 (Polytec) was mounted over the lens of a surgical microscope (Wild Heerbrugg, CH - 9056 Gais, Switzerland). Self-adhesive retroreflective tape ($<1mm^2$) was placed on the posterior crus of the stapes, and later at the centre of RW, to achieve a reasonably strong reflected signal and a signal to noise ratio within the acceptable range (>10dB). The reflected signal was captured and decoded by the OFV-5000 vibrometer controller (Polytec) to produce an output voltage proportional to the velocity detected. The voltage signal is fed into R&S UPV Audio Analyser for real-time monitoring and recording. The angle of the laser to vibration axis in both cases was kept less than 45° and compensated for in data analysis.

5.2.3 Measurement of Round Window Velocity during Drilling Procedure

The robotic surgical drill developed at Brunel University which auto-detects and stops drilling on contact with a membranous surface was used to create a cochleostomy, followed by another cochleostomy on the same ear (<1mm apart) with a conventional surgical drill. After each cochleostomy was made, METF-RW was measured and checked to make sure that no significant change has incurred in the dynamics of the cochlea and the wider hearing conducting system.

All drilling was performed without the surgeon touching or resting any of his body part on the specimen, microscope or anti-vibrational table to avoid transmission of energy. In both scenarios, drills were running before touching cochlea, in an attempt to avoid 'uncontrollable drill bit jumping', which can introduce discrepancies and may damage inner and middle ear structures. In the case of robotic drilling, a very shallow dip was created using conventional surgical drill before performing robotic cochleostomy. This avoided the drill tip drifting on the cochlear bony wall.

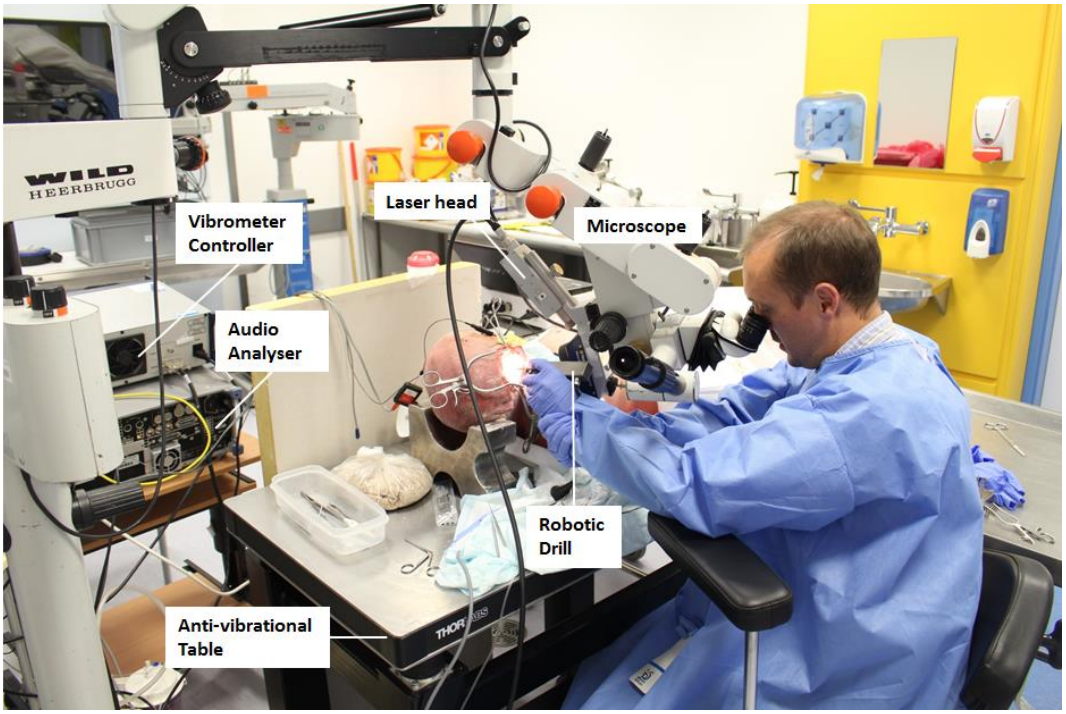

Figure 5.2.3 - 1 | Round window vibration measurement using laser vibrometer while the surgeon was performing cochleostomy drilling

Figure 5.2.3 - 1 is a comprehensive view of the laboratory setup of the measurement of RW response to cochleostomy drilling on human cadaver heads. The robotic drill was in use here. As illustrated in the figure, the surgeon's drilling arm was supported by the armrest of a surgery stool which was ensured to bear no contact with the anti-vibrational table. This removes the direct transmission of the energy from hand and arm movement to the workbench, i.e. the anti-vibrational table where the cadaver head was laid. Apart from that, the surgeon's drilling hand was aided by his other hand to ease the maintenance of a consistent posture throughout the whole drilling session. The supporting arm was refrained from touching the workbench for the same reason. All drilling processes were performed under the microscope, with the laser focused through the microscope on the retroreflective tape at the centre of RW. Great care was

made to ensure the laser beam remained on the retroreflective tape and that the beam was not interrupted by the surgeon's hand or instruments. Axial force exerted throughout the robotic drilling process was monitored and kept constant at approximately 1N – the surgeon was able to correct the force applied according to a real-time indication signal. The signal is available to the surgeon as a coloured light band where three bars of green light means the correct force, i.e. 1N, is applied. This ensures any adjustment of force can be instant, and the force applied stays reasonably consistent before the penetration of the cochlear wall, i.e. the completion stage, as evidenced in Figure 5.2.3 - 2.

During the conventional drilling measurements, standard cochleostomy drilling surgical procedure and approach was followed and no attempt was especially made to apply constant pressure or remain contact. No irrigation was used in either drilling case, as this would interrupt the vibrometry signal.

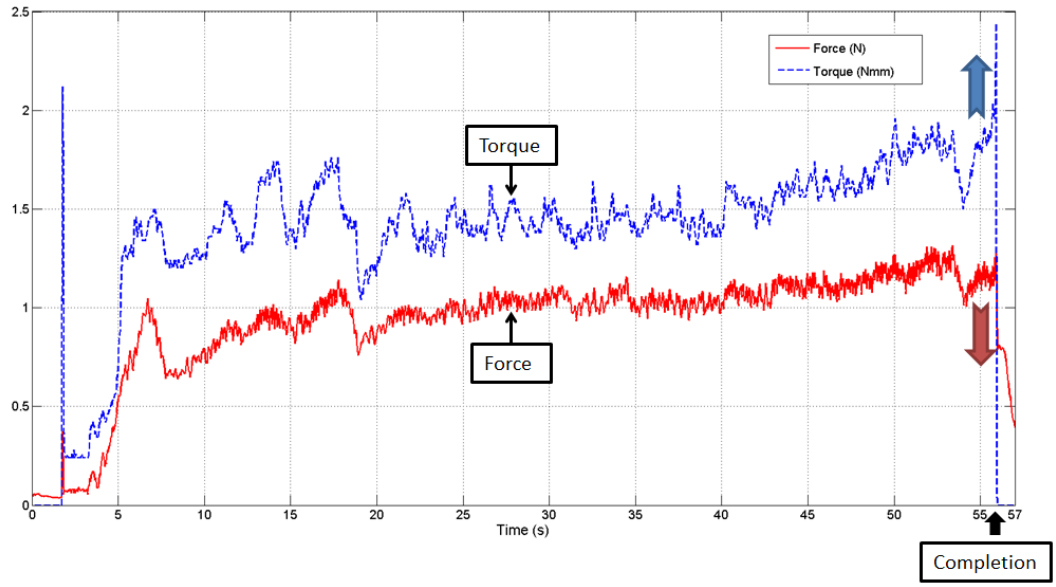

Figure 5.2.3 - 3 | Force and torque transients versus time during robotic drilling

Figure 5.2.3-2 shows the plot of the force and torque transients obtained real-time during the robotic drilling process. The force level during drilling was maintained at about 1N, with fluctuations within the range of 0.6N to 1.3N. The surgeon started the process by increasing feed force to ensure that the drill is cutting and is stable on the surface. This corresponds to an initial force building transient during the first 2 seconds. Following this period, the force amplitude is fluctuating primarily due to the unsteady motion imparted by the surgeon. At the end of the drilling process (between 55s and 57s), a surge of the torque and a drop of the force can be observed. This indicates the completion of the cochleostomy. A clear disturbance due to the hand movement of the surgeon can be seen just before completion. Such disturbance did not interrupt the drilling process and the robotic drilling of cochleostomy was successfully completed.

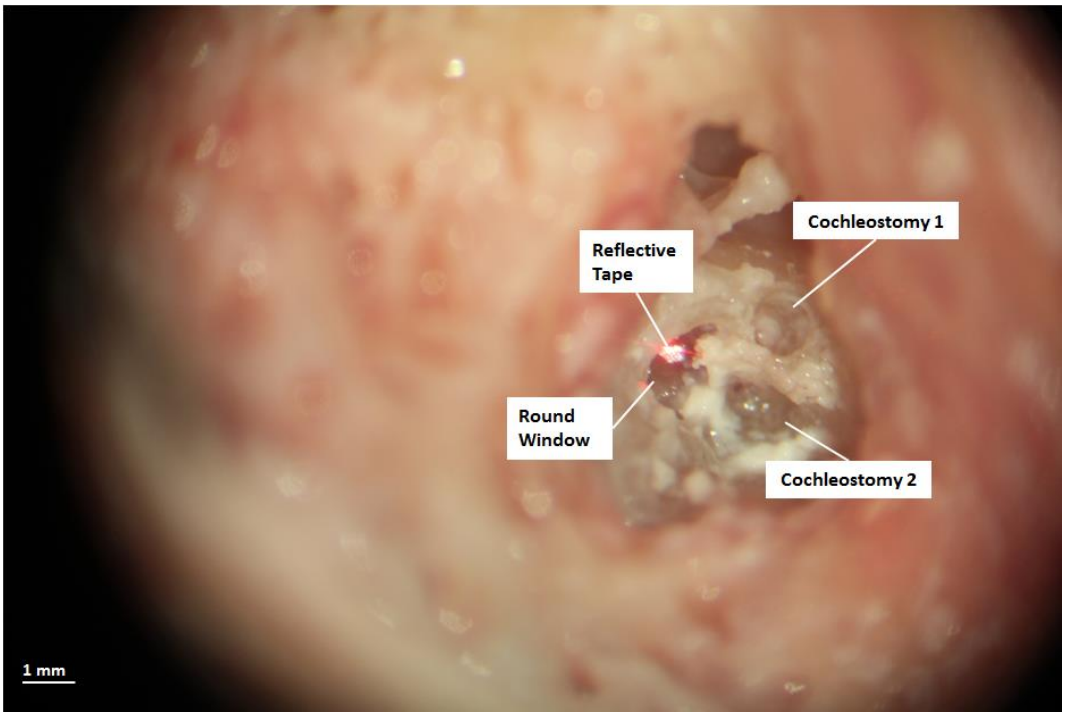

Figure 5.2.3 - 4 | Surgeon's microscopy view showing two complete cochleostomy formations and the round window with retroreflective tape

Two complete cochleostomy formations, i.e. two-off third windows can be seen in Figure 5.2.3-3. The endosteal membrane was left intact. Cochleostomy 1 was performed using robotic drill, while Cochleostomy 2 with standard otologic drill. The milling, lifting and pushing motion during the conventional drilling procedure can make the opening slightly enlarged and not perfectly circular as manifested by Cochleostomy 2.

The round window velocity during drilling was measured with the laser vibrometer. A retroreflective tape was applied at the visual-estimated centre of the round window, as shown in Figure 5.2.3-3, to aid the reflection of laser light. Sampling rate was set to 48 kHz to cover the whole hearing frequency range of interest. Due to limited on-chip memory of the analyser, only a period of 10s of

data is achievable at every saving. Best strategies have been applied to make sure the gap between each saving is less than 0.0001s while continuous drilling is not interrupted to best resemble surgical practice.

The sequence of drilling on each cochlea is summarised in Table 5.2.3-1. Two complete sessions of cochleostomy were conducted on each of Cochlea A, B and C. Cochlea O was primarily for the surgeon to practice the use of robotic drill on – mitigating the gap in surgeon's experience with the two tools used in comparison. On three out of the four cochlea specimens, robotic drilling was conducted first to take advantage of the integrity of an untouched cochlea, on consideration that an accurate quantification of robotic drilling disturbance is of priority due to the uniqueness of the tool and the robotic drilling technique. Conventional drilling was conducted first on one of the cochlea specimen, with the intention to discount the potential influence of drilling sequence, even though METF-RW measurement was taken before and after each cochleostomy - demonstrating that the existence of one TW has no effect on the RW response to stimuli. Another fact worth noticing is that the two cochleostomy has to occur at two different sites, one relatively superior than the other. The superior site has thicker bone therefore it takes longer to drill through. This may lead to lower noise transmitted into the cochlea at the start of the drilling due to damping of the thicker layer of bone. However the longer drilling session can expose the ear to more events of human intervention especially in the case of the conventional drilling, assuming the probability is equal if using the same drilling technique.

To avoid biasing the results, the choice of sites is kept statically random - two out of four robotic drillings were completed on the superior sites.

Table 5.2.3 - 1 | Experiment sequence: drilling methods used*, drilling sites and the corresponding drilling time

Cochlea #	First TW	Second TW	Drilling Time, sec	
			Conventional	Robotic
O (1L)	Robotic [superior]	N/A**	N/A	407
A (1R)	Robotic [superior]	Conventional	195	90
B (2R)	Robotic [superior]***	Conventional	125	513
C (2L)	Conventional [superior]	Robotic	220	50

**Rotation speed for the robotic drill in use was limited at 2000 rev/min, while that of conventional drill was set at 10,000 rev/min during experiment.*

***Underlying membrane was penetrated upon completion of the first cochleostomy.*

****A worn 1.2mm diamond burr (replaced by 1mm diamond burr during measurements on Cochlea B) was used with the robotic drill, while 1mm diamond burr was used in the case of the conventional drill.*

5.2.4 Calculation of Equivalent Sound Pressure Level

The equivalent sound pressure level (SPL_{eq}), in units of decibels, is a sensible measure of the disturbance caused in cochlea. It relates the disturbance to natural sound and is easily comprehensible to clinicians and health care providers. According to the IEC definition of sound pressure level, the equivalent sound

pressure level can be calculated from equivalent sound pressure ($P\,eq$) using Equation 5.2.4 -1 below:

$$SPL\,eq = 20 \cdot \log_{10} \frac{p_{eq}}{p_0}, \qquad (5.2.4\text{ -1})$$

where p_0 is the reference sound pressure corresponding to the threshold of hearing. It is a constant value equal to 20μPa, i.e. $2 \times 10^{-5} Pa$.

The equivalent sound pressure can be derived from the measured vibration velocity v_I of the cochlear membrane in response to machine or human interventions as shown in Equation 5.2.4 -2:

$$p_{eq} = \frac{v_I}{METF}, \qquad (5.2.4\text{ -2})$$

where v_I as mentioned above is the cochlear membrane's velocity of vibration in response to surgical intervention, measured in units of mm/s; and the middle ear transfer function METF is defined as

$$METF = \frac{v_A}{p_A}, \qquad (5.2.4\text{ -3})$$

where v_A is the velocity of membrane vibration in response to acoustic stimuli, specified in units of mm/s; p_A is the sound pressure of the stimulus acoustic signal, specified in units of pascals. In this study, METF is frequency dependent, and is assumed to be constant at a specific frequency for the same cochlea, i.e. there is a linear relationship between membrane velocity and the pressure at the

tympanic membrane (Voss, Rosowski, Merchant, & Peake, 2000). The use of the equations listed above are all frequency specific. Conversion is done at each specific frequency or frequency band before integration if a global view of the overall sound pressure level is needed.

Substituting Equations 5.2.4 -2 and 5.2.4 -3 into Equation 5.2.4 -1 yields

$$SPL\ eq = 20 \cdot \log_{10} \frac{v_I}{p_0 \cdot METF} = 20 \cdot \log_{10} \frac{v_I \cdot p_A}{p_0 \cdot v_A}, \qquad (5.2.4\text{ -4})$$

where v_I and v_A are velocity measured at the same spot on the same membrane.

Applying the above calculation at each specific selected frequency makes it possible to convert the mechanical disturbance that is induced in the cochlea to the equivalent sound pressure level. This enables us to answer the question: if it is a sound that is generating this amount of disturbance, how loud this sound must be. Compared to the mechanical energy measured in kinematic units, the equivalent sound pressure level in dB leads to a different angle of assessing the mechanical disturbance - one that is much more comprehensible to the wider audience including clinicians and healthcare providers who may not necessarily come from an engineering background.

5.3 Data Processing

Due to the analyser's limited on-chip memory, and the high fidelity measurements performed to cover the full spectrum of human hearing frequencies, only 10 seconds of recording can be taken at one time. To obtain a recording of the whole cochleostomy session, multiple continuously-taken 10-second recordings were attached in sequence in MATLAB. This recording of the full drilling session in the time domain was then processed through a set of algorithms to remove the unwanted off-target oscillation signals due to the unstable focus of the laser light. The 'off-target' events are typical to laser vibrometry measurement on a non-rigid moist biological membrane surface, and are artefacts introduced by the measurement procedure rather than the medical procedure under investigation. The limited size of the retroreflective tape ($<1mm^2$), in consideration of minimising mass load on the membrane, makes it more difficult to maintain laser reflection. A video footage of the drill and the hand movement coupled to the drilling signal, if taken in future studies, can assist interpretation of these sudden amplitude surges emerging randomly across different stages of drilling, and consolidate its relevance to incidental 'laser not-on-target' - an unintentional impact of human intervention, and its irrelevance to the surgical drilling procedure.

The procedure for processing the raw data is summarised in Figure 5.3-1. The multiple 10-second recordings are attached in a sequence to form a raw data trace. The signal-to-noise ratio (SNR) is calculated by comparing signal power to the power of the ambient noise captured before drilling.

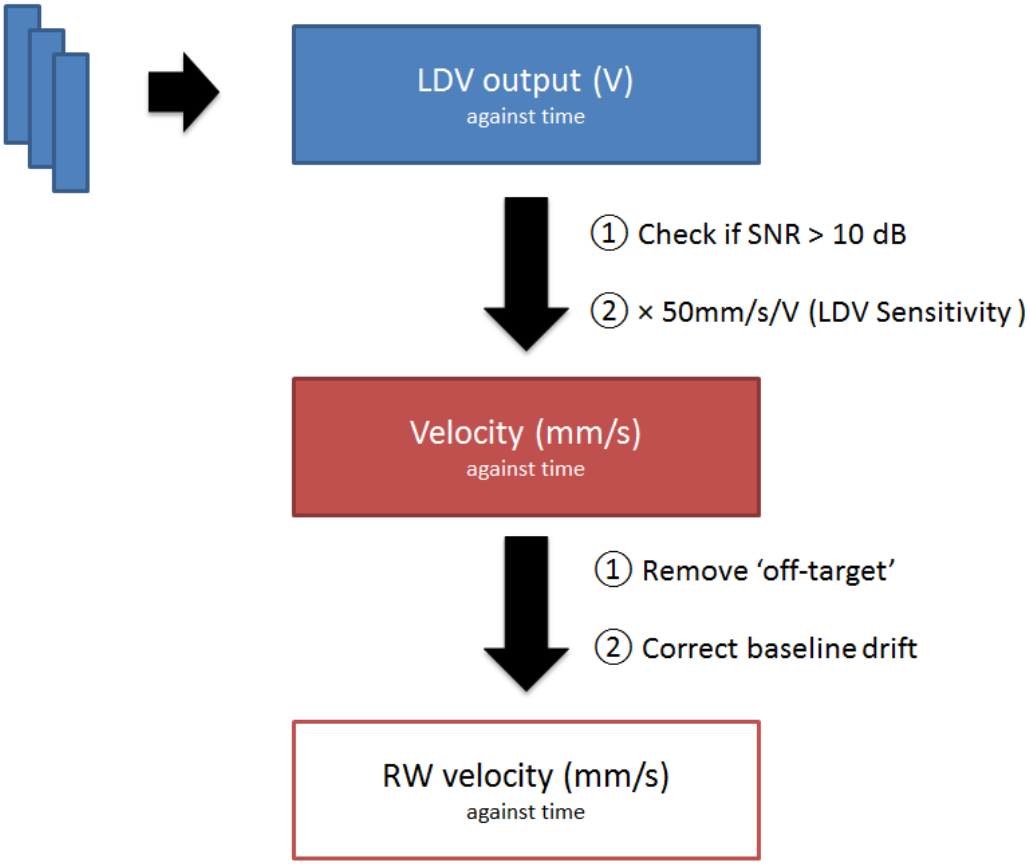

Figure 5.3 - 1 | Data processing flow chart: Time Series Analysis

5.3.1 Algorithm for Signal Drop-off Recognition

Stage A: Removal of 'Off-target' Events

As mentioned at the beginning of this section, the recordings of the drilling disturbance were contaminated by high-amplitude oscillation signals that correspond to periods when the reflected laser signal is too weak to be detected - laser appears to be 'off-target'. The reasons for weak or temporarily losing reflection in this cadaver drilling study can be, but not limited to, a combination of the followings: bone dust covering retroreflective target; drill or hand blocks

the laser; lifting and re-applying the drill and breaks the alignment between laser and target.

Based on the conversation with engineers at Polytec Ltd, if no laser signal is detected by the reflection sensor, the laser vibrometer recognises that the target is moving away from or towards the sensor, i.e. oscillating, at an infinite speed. The output signal, indicating the oscillating velocity of target surface, oscillates between top and bottom cut-off values until reflection regained.

To eliminate the interference of the high-amplitude off-target oscillations and extract the true disturbance level, a discrimination algorithm was developed, based on the distinctive features of the drilling signal. The drilling signal satisfies one of the following conditions.

Condition 1: Consistent low-variance;

Condition 2: Smooth curve with limited gradient between every two points, without prominent local maxima.

Please note that the raw recording is identified as a drilling signal in units of milliseconds, i.e. only data sequence continuously satisfying either of the above conditions for at least 2 milliseconds can be identified as a drilling signal. This is based on the assumption that the 'off-target' events are caused, directly and indirectly, by some form of human interventions. It is beyond human capability to carry out two interventions so rapidly that the gap between two actions is

smaller than two milliseconds - the shortest possible time that the neuron needs to respond to the next stimulus (Silverthorn & Johnson, 2010). Therefore, the gap between two 'off-target' events, i.e. the 'on-target' period, cannot be shorter than two milliseconds. Taking the above into consideration, the signal is assessed in units of two milliseconds, i.e. a two-millisecond sliding window is used in the analysis along the time axis.

A protocol is designed to carry out the signal processing according to the criteria defined above, in the following steps.

Step 1 – Calculate the 3-point moving variance of the original trace.

The output is an array of variance values, where each value corresponds to the variance of the current data sample and the two neighbouring data samples. Changing the size of the sliding window to 4 or 5 does not affect the functionality of the signal processing and does not substantially change the outcome.

Step 2 – Take a 1-millisecond equivalent sliding window, if all variance values within the window are below the variance threshold*, data samples within this window are identified as 'on-target'.

Step 3 – If not all variance values are below the variance threshold, within the same 1-millisecond window, find out if there are prominent* peaks or valleys, and if any gradient between each two data points are higher than gradient threshold* between two points along the whole trace. If not, all data samples within this window are identified as 'on-target'.

Step 4 – Keep the original values of 'on-target' data samples; discard other data samples that are not recognised as 'on-target' – by setting the values to zero so that they are easily distinguishable and removable in latter process.

**All parameter values have been selected to optimise the performance of removing 'off-target' oscillation – without sacrificing data that has unique medical meanings. Before being applied on all drilling traces, the combination of parameters and their values has been trialled and tested on at least 10 seconds of recordings at multiple stages of both conventional and robotic drillings and demonstrate consistent relevance.*

The MATLAB implementation of the Stage A algorithm is presented and discussed in Appendix A.1.

Examples of the outcomes of Processing Stage A are presented here in Figure 5.3.1 - 1 and Figure 5.3.1 - 2. Both are 10-millisecond clips. The original recording of velocity is plotted in blue against time in the upper half of the figure. Also plotted in the upper half of the figure is the trace after being processed by Processing Stage A. The corresponding variance is plotted against time in the lower half of the figure. As mentioned above in Step 1, the each data on the variance trace denotes the variance of the corresponding data sample at the same point in time and its neighbouring data samples. In Figure 5.3.1 – 1, consecutive data samples with variance lower than threshold for more than 1 millisecond, i.e. satisfying condition 1, are retained as drilling signal. The impulses at 100.783s, between 100.787s and 100.788s, and between 100.789s and 100.79s are

discarded because none of the one-millisecond windows that contain these data samples satisfy either condition 1 or condition 2. In Figure 5.3.1-2, data samples with high variance - right after 102.208s and after 102.214s - get retained because for each sample, there is at least one one-millisecond window containing it that satisfy condition 2.

Please note that although the oscillation in Figure 5.3.1-2, for instance between 102.208s and 102.2085s, can have an amplitude as high as that in Figure 5.3.1-1, the former has a much lower frequency content – takes 5 samples from equilibrium point to peak in contrast to 1-2 samples in Figure 5.3.1-1. This makes it distinctively different from an 'off-target' event. It is also worth noting that these high-amplitude 'slow' oscillations only appear in conventional drilling traces – a unique feature of conventional drilling that can bear symbolic medical meaning. It also eliminates the possibility that they are 'off-target' events which should be common to both recordings of conventional drilling and robotic drilling.

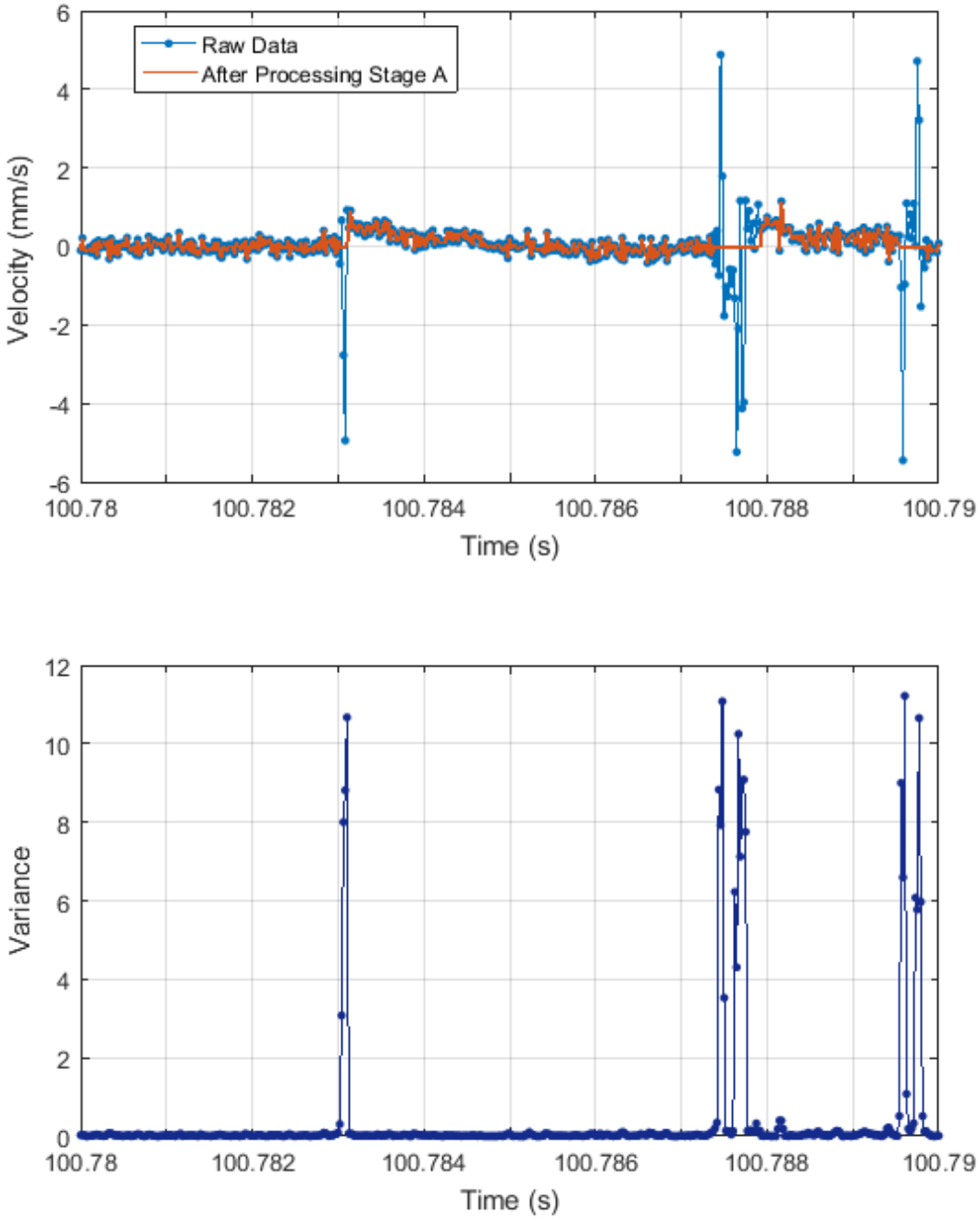

Figure 5.3.1 - 1 | After Processing Stage A, data samples satisfying condition 1 get recognised as drilling signal and kept their original values

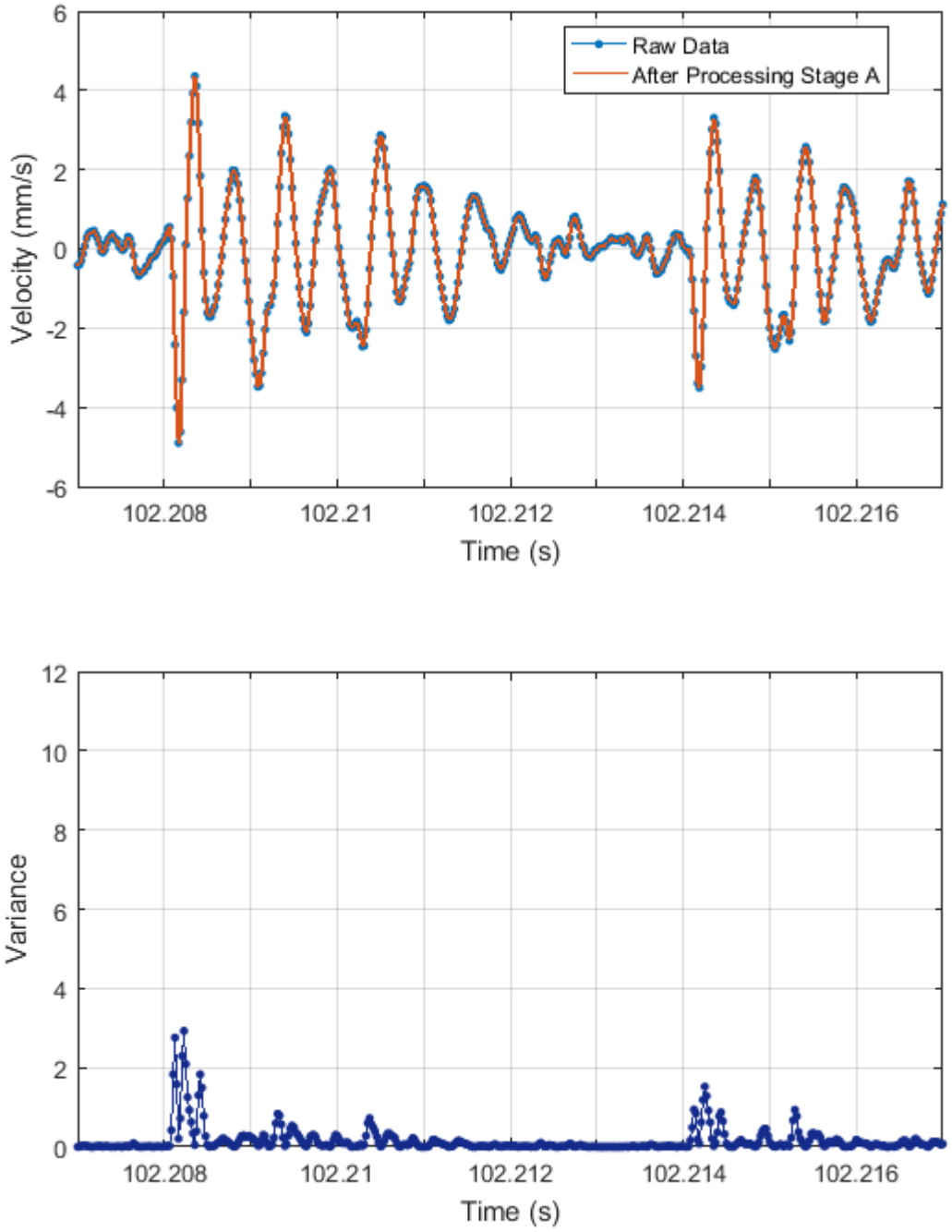

Figure 5.3.1 - 2 | After Processing Stage A, data samples satisfying either condition 1 or condition 2 get recognised as drilling signal and kept their original values

Stage B: Baseline Drift Correction

As shown in Figure 5.3.1-3, for approximately 2 milliseconds after the 'off-target' event, the baseline appears to be drifted away from zero. This phenomenon only appears after an 'off-target' event. It is physically possible for the whole cochlea to have a movement in one direction hence the continuously negative or positive velocity. However, it is inappropriate to count this absolute movement of the whole cochlea towards the membrane oscillation that is being measured. It is the relative motion of the cochlear membrane with respect to the cochlea bone that correlates to the level of mechanical disturbance and is of medical meaning in this study.

To correct the baseline drift within data retrieved after Processing Stage A, data samples following 'off-target' events are targeted. By applying local mean subtraction to the targeted data, the baseline can shifted back to zero as evidenced in Figure 5.3.1 – 3.

The algorithm works in a four-step process which is described as followings:

Step 1 – On the trace obtained after Processing Stage A, locate the end of an 'off-target' event;

Step 2 – Recognise the group of data that need to be corrected – within 2 milliseconds after 'off-target' before meeting the next 'off-target' even – an average length of 'after off-target' drifting time observed in this study;

Step 3 – Calculate an array of local mean values within the group selected - each mean is calculated over a sliding window of length 24 (0.5 millisecond) across neighbouring elements;

Step 4 – Subtract the local mean array from the group of data selected to be corrected.

The MATLAB code to implement the algorithms above is provided in Appendix A.2. The value is selected in a trial and error approach. As a general principle, to have the desired effect, the size of the sliding window needs to be larger than the period of the oscillation being studied; while smaller than approximately 1/8 period of the underlying fluctuation that needs to be suppressed.

Figure 5.3.1-3 illustrates the performance of this data processing strategy. The baseline drift between 16.3222s and 16.3242s is successfully suppressed while the higher frequency oscillation within this time frame is retained. Though the approximate underlying frequency of the drifting curve can be within the frequency range of interest, the fact that it is not periodic along the rest of the trace and only appears following an ‘off-target’ suggests that it is more related to an instantaneous event in measurement system, most probably cochlea or laser movement, not a medical event that needs to be captured in this study.

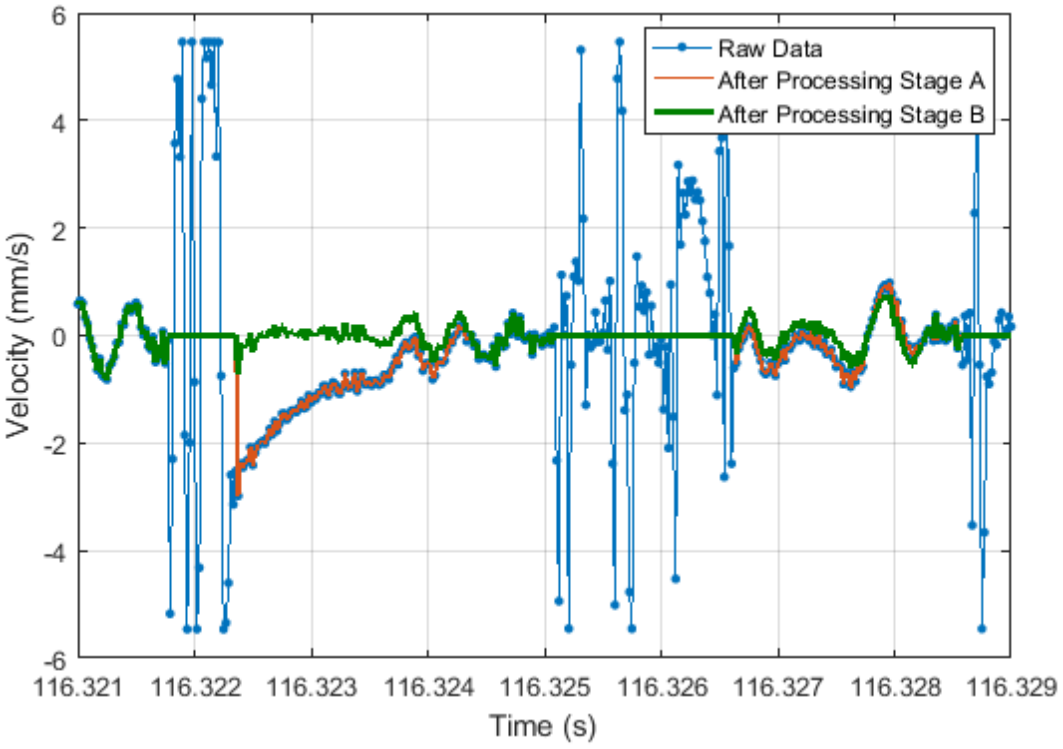

Figure 5.3.1 - 4 | A 3-millisecond recording before and after being processed

Chapter 6

Noise Exposure of the Cochlea during Cochleostomy Formation

In this chapter, the results of experiments described in Chapter 5 is analysed, presented and discussed. The measurements of disturbance induced in cochlea during drilling is converted into equivalent sound pressure level to help assess the mechanical energy in terms of the level of damage caused. There is also contrast between the manual and robotic approaches and discussion about the implications.

6.1 Analysis and Results

6.1.1 Time Series Analysis

Using the algorithm introduced in Section 5.3, the contamination in original recording is removed. The resultant clean data - three pairs of conventional and robotic drilling signal obtained on three specimens, is shown in Figure 6.1.1-1, Figure 6.1.1-2 and Figure 6.1.1-3. For all three cadaver cochleae, the disturbance induced by robotic drilling is more consistent and on average at a lower level throughout the full surgical procedure. Moving root-mean-square (RMS) value is plotted over the drilling signal to aid the visual perception. For each specimen, robotic drilling has a smaller amplitude and lower variance in terms of the amplitude of drilling-evoked round window vibration velocity.

This difference between robotic and conventional is expected as robotic drilling is intrinsically a more consistent surgical procedure compared with conventional drilling. It reduces the amount of human intervention by providing real-time axial force feedback and enabling anti-penetration – the drill stops automatically upon touching the membrane. This effectively eliminates the need to constantly manipulate the drill in order to, for instance, monitor and control the progression of cochleostomy.

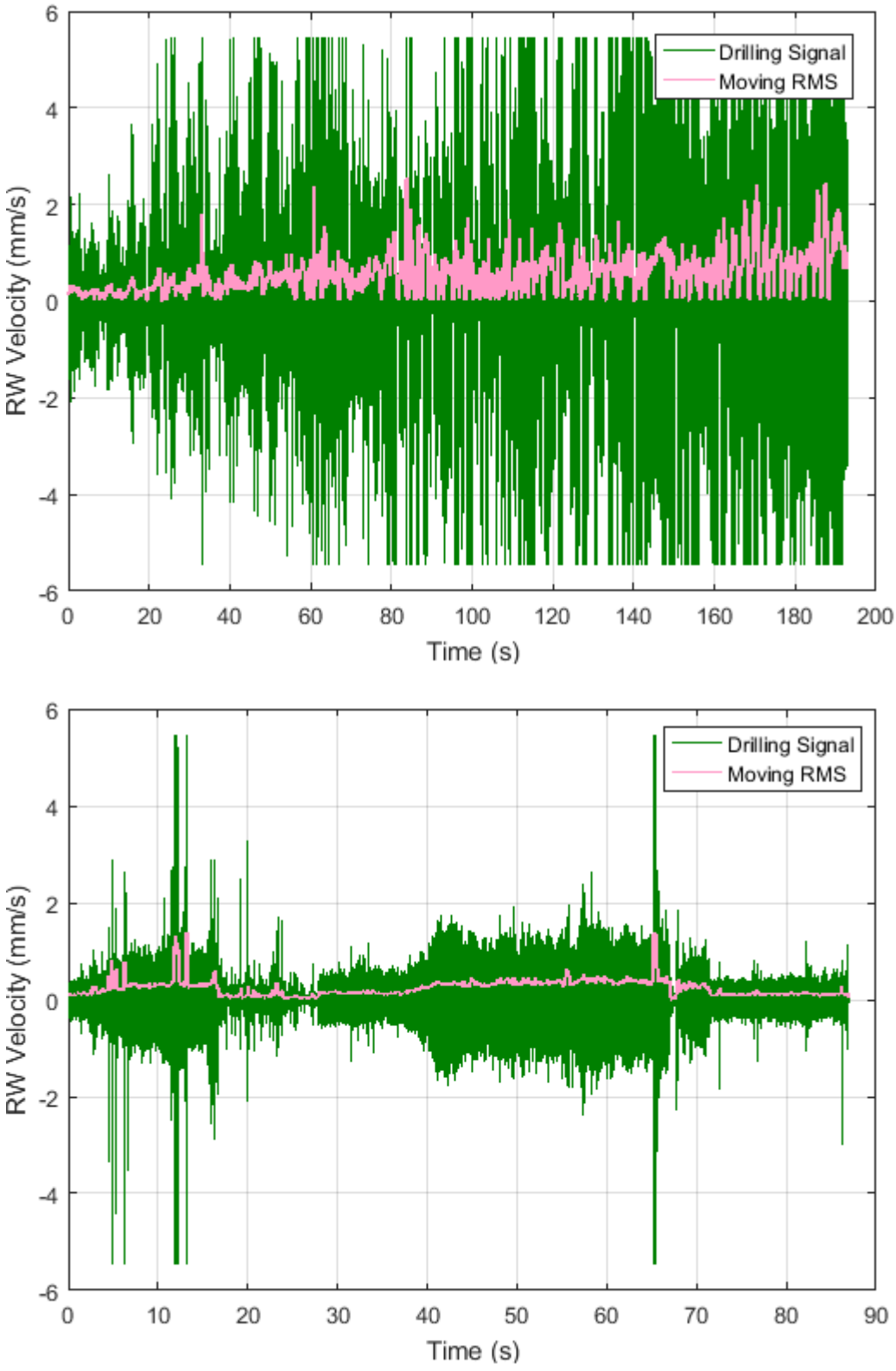

Figure 6.1.1 - 1 | Round window vibration velocity throughout the whole cochleostomy drilling procedure – Cochlea A. Top: conventional. Bottom: robotic.

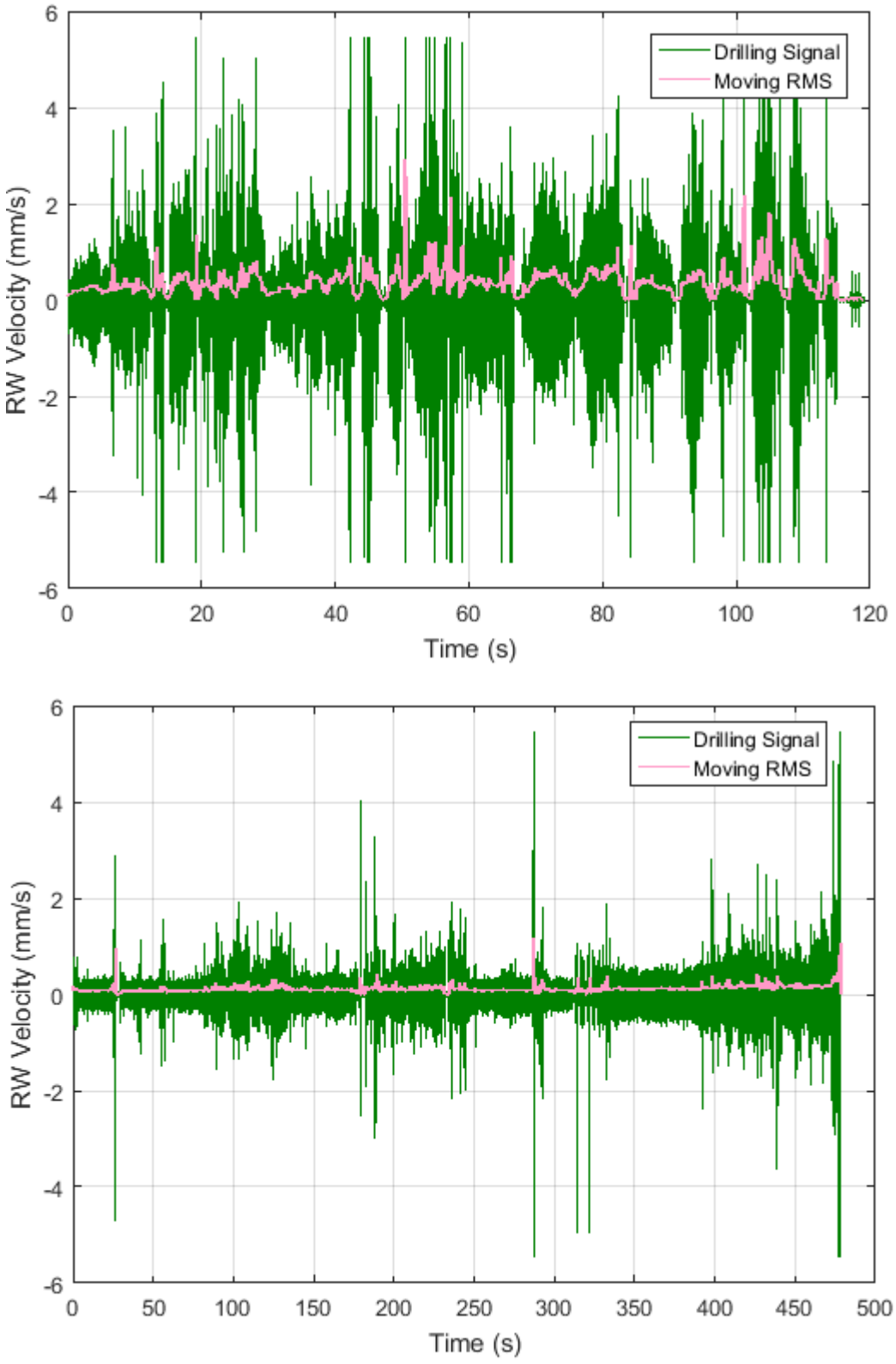

Figure 6.1.1 - 2 | Round window vibration velocity throughout the whole cochleostomy drilling procedure – Cochlea B. Top: conventional. Bottom: robotic.

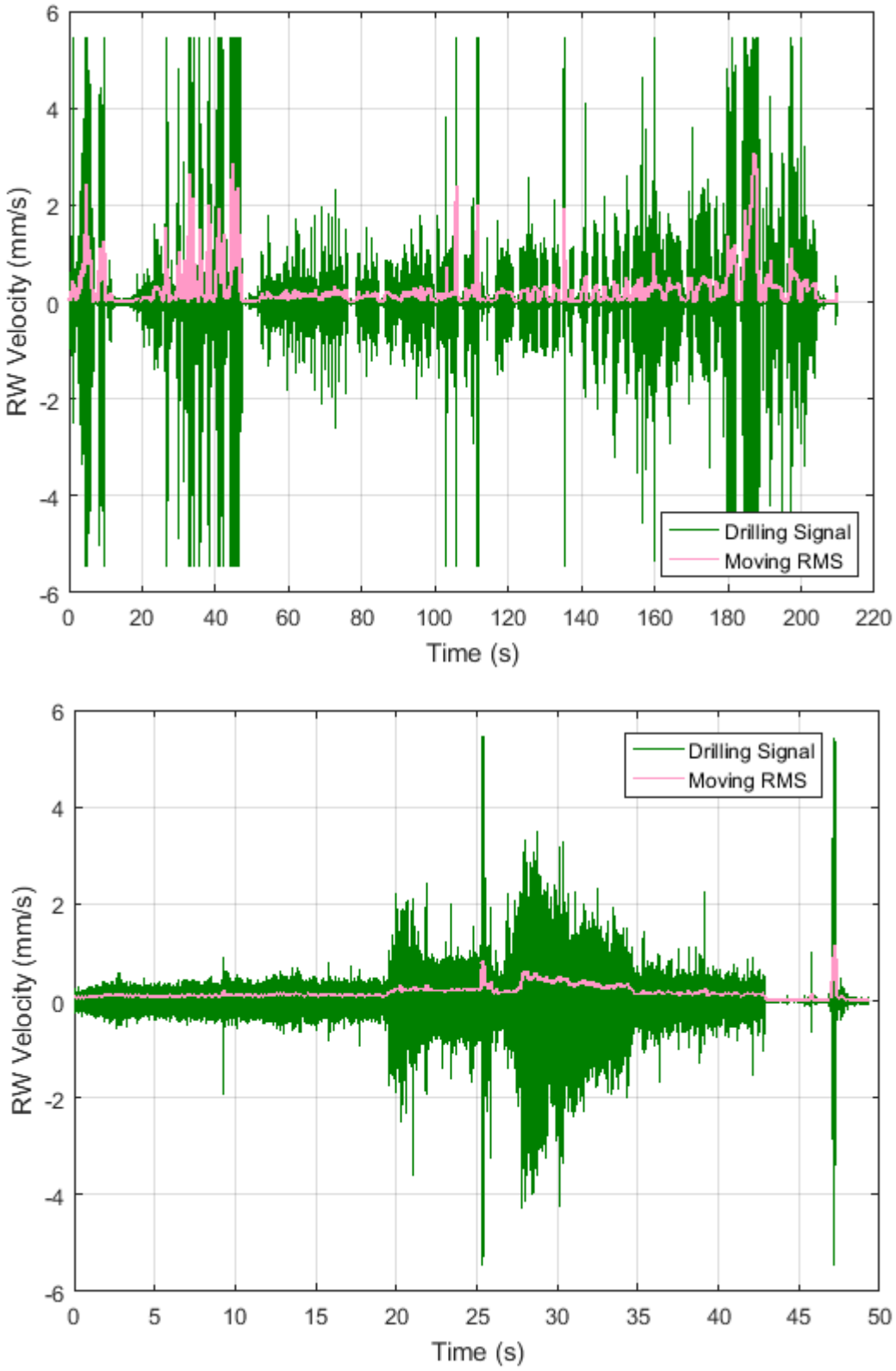

Figure 6.1.1 - 3 | Round window vibration velocity throughout the whole cochleostomy drilling procedure – Cochlea C. Top: conventional. Bottom: robotic.

The statistics of the time series drilling signal confirms the above observation. A direct comparison between conventional and robotic drilling on Cochlea A, B and C, is presented in Figure 6.1.1-4. Each bar value is the RMS velocity of round window vibration over the whole procedure of cochleostomy drilling. In all three cases, robotic drilling delivers a RMS velocity that is approximately 1/3 of that of conventional drilling.

It is worth noting that RMS velocity values for Cochlea B and Cochlea C are closer to the values obtained on Cochlea A, especially for conventional drilling. Considering the fact that Cochlea A is from a different cadaver body than Cochlea B and C, this difference can be caused by the difference in specimen condition. Cochlea A was also defrost earlier than Cochlea B and C, though best measures have been taken to maintain the condition of the specimen. It is possible that the difference is simply due to the physiology difference between individuals, as shown in Figure 6.1.1-4, no two specimens has the same average amplitude for either conventional or robotic. However, even though there is quantitative difference in the measurements on different specimens, the claim that robotic generates lower level of disturbance is supported by each of the three cases.

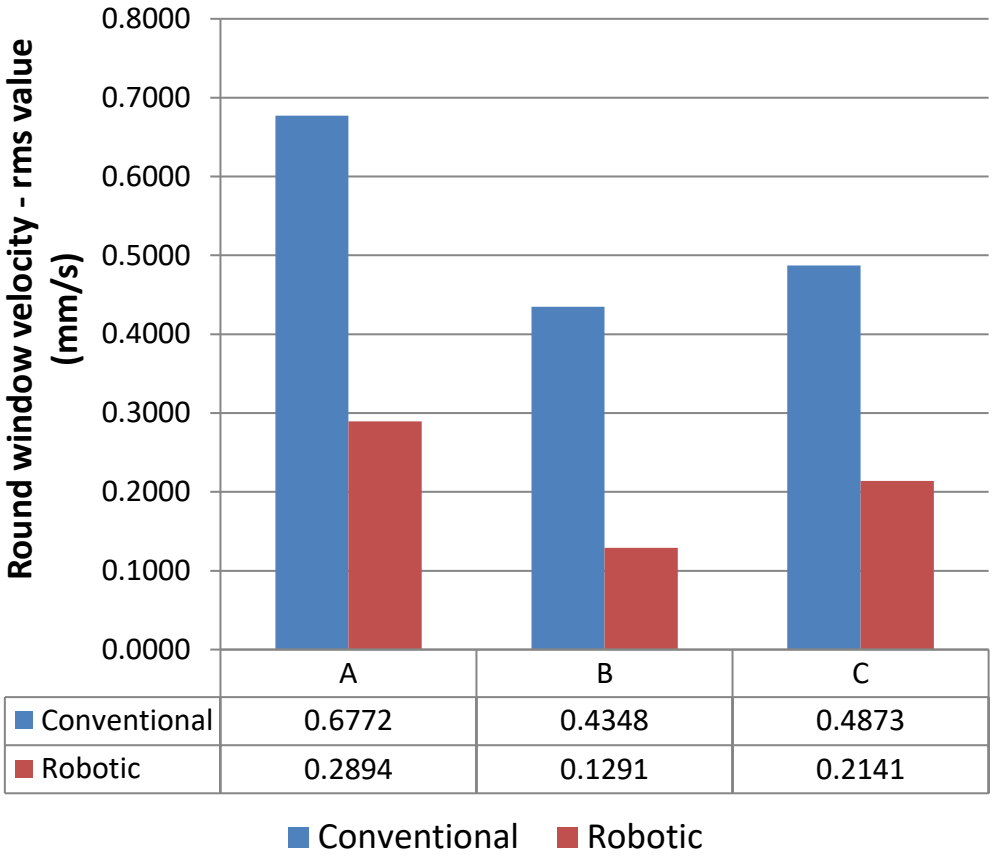

Figure 6.1.1 - 4 | Comparison between conventional and robotic drilling methods - round window velocity, rms-averaged over the whole cochleostomy procedure

6.1.2 Determination of the Middle Ear Transfer Function

The Middle Ear Transfer Functions (METFs) for all three ears before cochleostomy drilling is plotted here in Figure 6.1.2-1. As discussed in Section 5.2.4, an important step in determining the equivalent sound pressure level (SPL_{eq}) in human ear is to measure and calculate the METF. As the drilling disturbance was measured on the round window (RW), METF-RW would be used to calculate SPL_{eq} in this study. METF-Stapes was measured to determine

if the specimen possess normal middle ear mechanical properties. In each plot, Rosowski Mean with its estimated ± 95% confidence interval (CI) (J. J. Rosowski et al., 2007)(*ASTM F2504 - 05, Standard Practice for Describing System Output of Implantable Middle Ear Hearing Devices*, 2005) is plotted in the background as a reference – representing a criteria range for a normal functional middle ear. Rosowski Mean is the average of the ten means from ten published studies; each quantifies the average stapes velocity of measurements on normal temporal bone sample. The estimated ±95% confidence interval is indicated by the dashed lines, assuming that the Rosowski Mean represents the population mean and that each of the ten means was independently taken on samples of identical sample size of the same population. In all three plots, both METF-Stapes and METF-RW correlates well with the reference trace. Therefore it is safe to conclude that all three ears fulfil the prerequisites that the middle and inner ear structures are perfectly normal and suitable for investigation.

The persistent peak between 4000 and 6000 Hz obtained from all three cochleae, on both stapes and RW, is not shown on the curve from the reference trace. Looking at the LDV velocity measurement and probe microphone pressure measurement separately, it is clear that the former has a smooth curve while the latter has a dip between 4000 and 6000 Hz, thus the peak in METF. According to the acoustic setup in ear canal, it is possible that this dip in probe microphone pickup is due to standing waves in the external ear canal. In short, this is more likely to be an error introduced in the measurement procedure rather than the true mechanical characteristics of the ear. The fact that this peak appears consistently

at the same frequency in measurements on three different cochlea further proves the point. The three ears can therefore be considered suitable for experimental investigation of cochlea mechanics. The fact that the overall trend of METF trace follows the reference trace closely and the fact that the purpose of this study is a comparison between two drilling methods which will be impacted equally by this 'METF-anomaly' in the calculation later on indicates that the ultimate impact on our conclusion will be trivial.

The difference between Cochlea A and Cochlea B, C is evident in the form of METF trace as well. The METF traces for Sample C follows a trajectory that is much more similar to that of Sample B than that of Sample A. It demonstrates that every cochlea acts as its own control. In this study, higher round window velocity does not necessarily guarantee that higher energy is induced in the cochlea. It can also be the same amount of energy or level of disturbance in the cochlea however within an ear that has a much more rigid oval window or ossicular chain. To accommodate this anatomical difference and the consequent mechanical difference between specimens, the round window velocity is converted to equivalent sound pressure level using the ear's acoustic response as reference. It also enables presenting the results in a more intuitive way.

It is also interesting to see that for all three cochleae, for a considerable width on the frequency domain, RW vibrates at a much higher velocity magnitude compared to stapes if subject to the same amount of acoustic stimulus in Pa. The difference is quite significant and consistent over the entire frequency range from 100 Hz up to around 4k Hz for Cochlea B and Cochlea C. It is possible that

because the measurement was taken on the centre of the RW, the magnitude of the velocity is higher than that measured on stapes footplate though the total volume displacement across RW membrane should be close to that of the stapes footplate (Stenfelt et al., 2004a) . Measurements on more specimens are required to generate a firm conclusion on this trend.

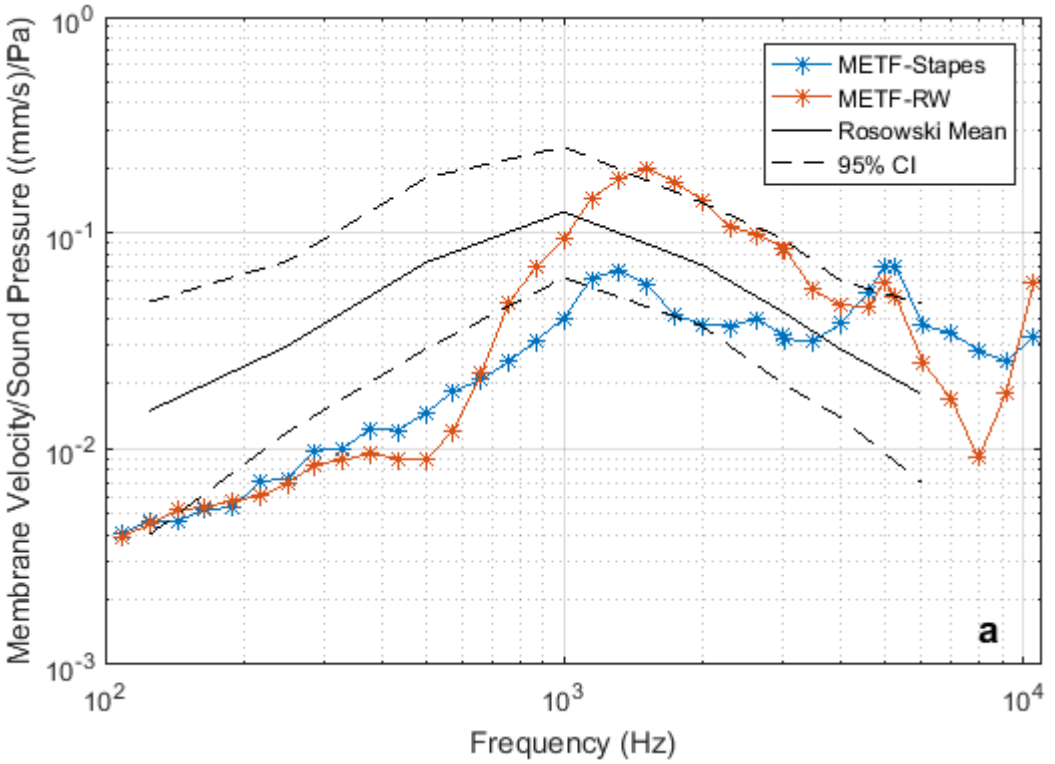
METF-Stapes
METF-RW
Rosowski Mean
95% CI
Membrane Velocity/Sound Pressure ((mm/s)/Pa)
Frequency (Hz)
a

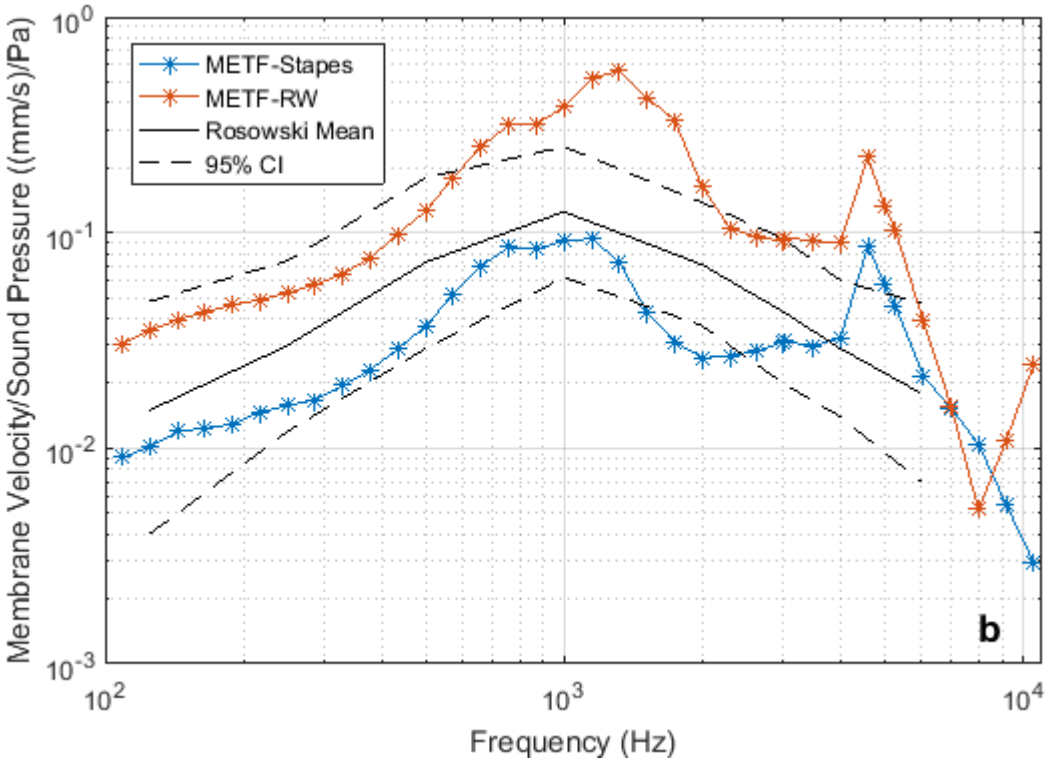
METF-Stapes
METF-RW
Rosowski Mean
95% CI
Membrane Velocity/Sound Pressure ((mm/s)/Pa)
Frequency (Hz)
b

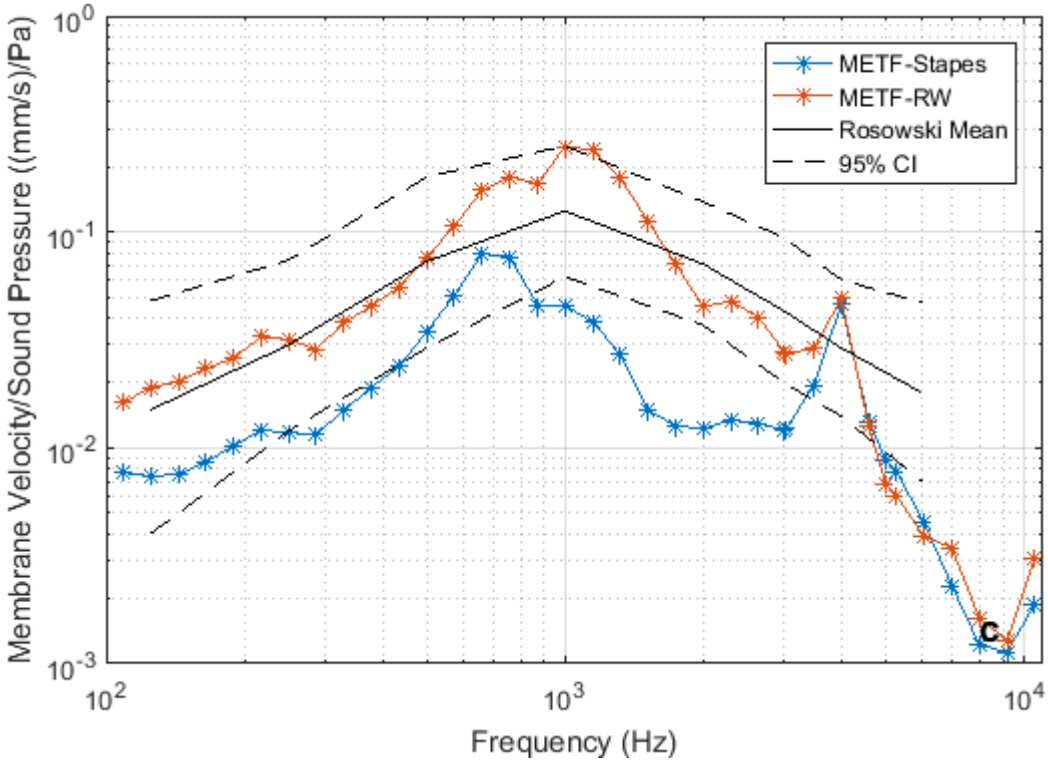

Figure 6.1.2 - 1 | Middle ear transfer function(s) of Cochlea A, B and C, plotted against frequency, in comparison with Rosowski Mean and the estimated ±95% confidence interval indicated by the dashed lines.

6.1.3 Frequency Spectrum of Round Window Velocity

Before calculating the equivalent sound pressure level using METF-RW in frequency domain, the frequency spectrum of the drilling signal is obtained from the post-processing time series data, via a fast Fourier transform (FFT) algorithm. The MATLAB code to implement the FFT algorithm is included in Appendix B.

The frequency spectra for Cochlea A, B, C are plotted here in Figure 6.1.3-1, Figure 6.1.3-2, Figure 6.1.3-3 respectively. Also plotted are the traces indicating the equivalent round window velocity if 100 dB and 85 dB sound is introduced

into the ear, calculated from the METF-RW presented in Section 6.1.2. The two traces are introduced because they denote critical thresholds for hearing protection. According to NIOSH, the National Institute for Occupational Safety and Health, long or repeated exposure to sounds at or above 85 dB can cause hearing loss. The maximum time recommended that a healthy individual can be exposed to 100 dB sound is limited at a maximum of 15 min. The threshold time is halved for every 3 dB increase. Above all, the reference traces provide a snapshot of the level of disturbance in the context of hearing and bring home the reality of acoustic trauma.

For all three conventional drilling traces, there is a peak at 167 Hz which corresponds to the 10,000 rev/min rotation speed of the drill. The second and third harmonics are present in the spectra as well. Higher harmonics have considerably high amplitude however are lower than or further distant from the 85 dB sound reference trace therefore are less likely to be traumatic. In contrast, there is no resonance corresponding to robotic drilling speed on robotic spectra. The more controlled axial force applied on cochlea during robotic drilling can be relevant to this reduced impact of the rotation of the drill bit. The 83 Hz peak on the Conventional A spectrum is not seen on Conventional B and Conventional C therefore is more likely to be due to sample condition or defects in the experimental process rather than the drilling itself.

The robotic trace has a much smoother and flatter spectra in general. On all three specimens, robotic drilling generated disturbance close to or lower than 85 dB SPL equivalent over the frequency range of interest. Robotic drilling disturbance

is especially low on Cochlea B – well below the 85 dB reference and lower than the other five measurements. Assuming that LDV measurement has the same accuracy in this case compared to the other five measurements, this moderate amplitude could be related to considerably longer drilling time – indicating thicker cochlea bone at the drilling site at the beginning of cochleostomy.

Apart from on Cochlea A, both conventional drilling and robotic drilling generate disturbance that causes round window to oscillate at a lower velocity than 100 dB SPL sound can cause. Considering the actual drilling on cochlea normally takes less than 15 minutes, it is sensible to conclude that both conventional and robotic method can be considered safe to patients' hearing if standard cochleostomy procedure applies.

However, compared to robotic drilling, the disturbance induced during conventional drilling procedure is more influenced by drilling speed, with the possibility for response to surpass 100 dB SPL equivalent thresholds. On the other hand, robotic drilling generates consistently low disturbance over the hearing frequency range hence having lower possibility to distress patients' hearing.

Apart from conducting spectral analysis over the whole drilling procedure, spectral analysis for the time point of highest round window velocity is worth investigating. Those instantaneous peaks have been smoothed out hence the associating message suppressed when the spectrum is generated over the whole measurement time.

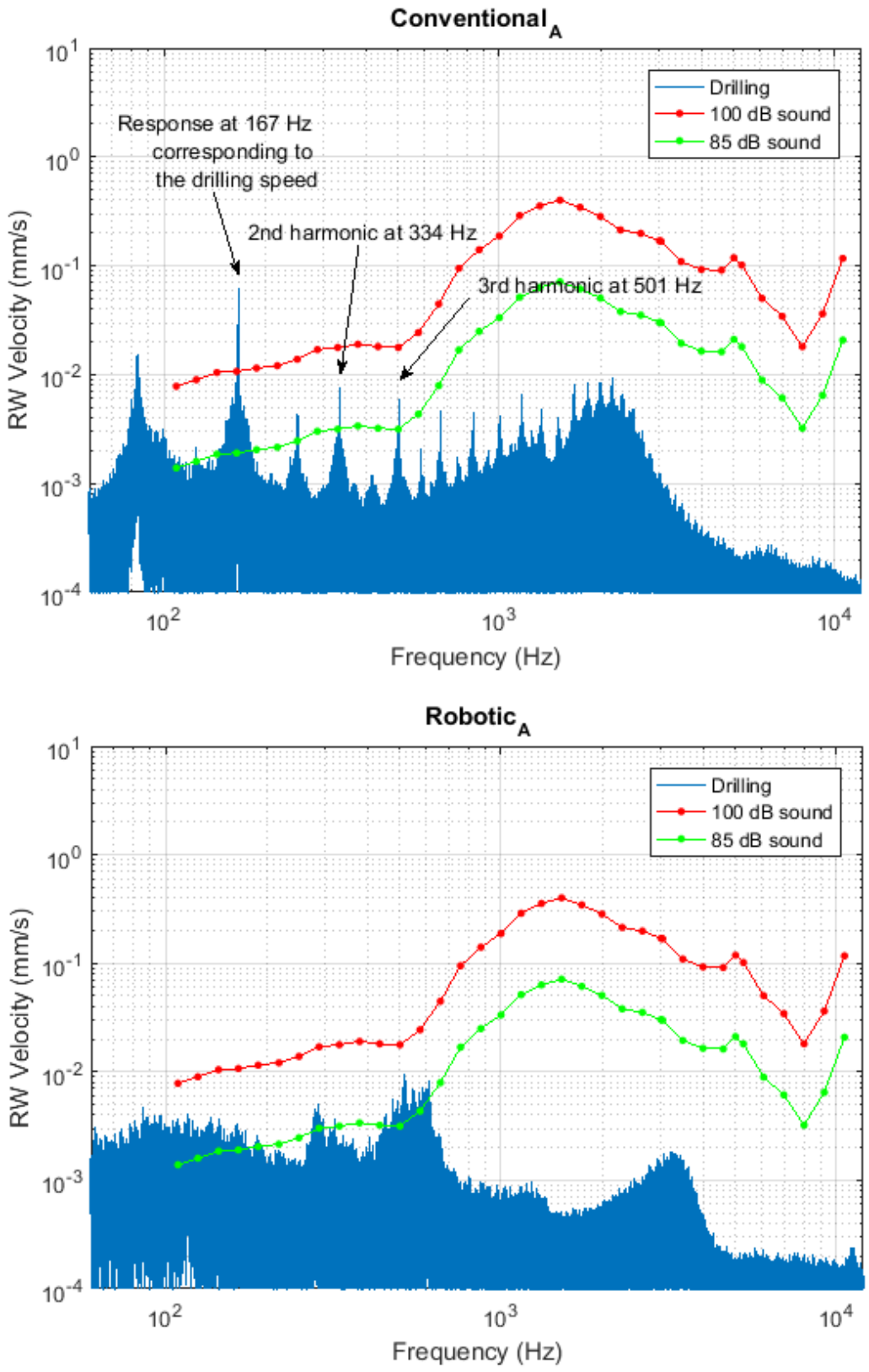

Figure 6.1.3 - 1 | Frequency spectrum of the drilling signal covering the whole cochleostomy procedure – Cochlea A. Top: conventional. Bottom: robotic.

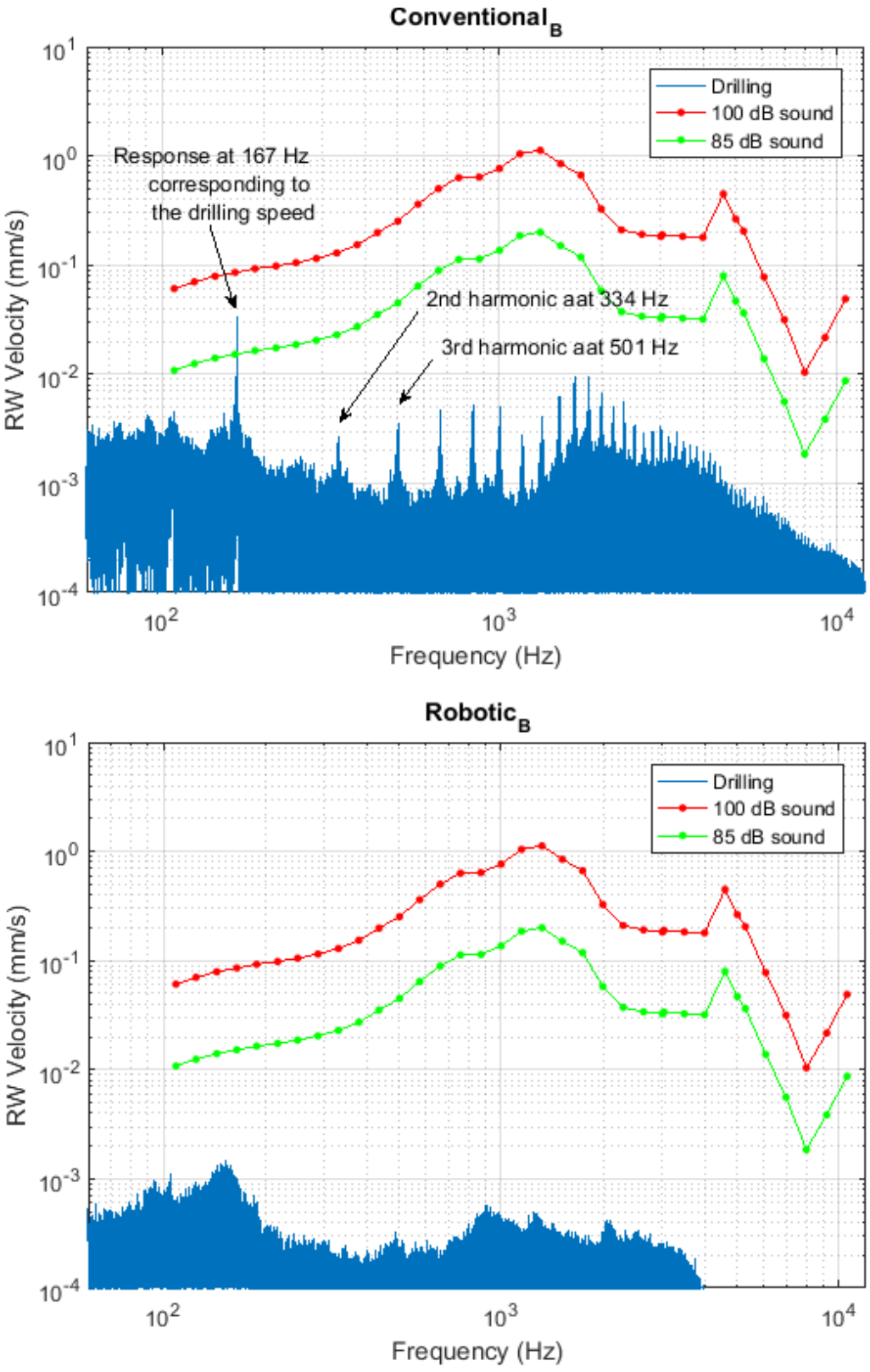

Figure 6.1.3 - 2 | Frequency spectrum of the drilling signal covering the whole cochleostomy procedure – Cochlea B. Top: conventional. Bottom: robotic.

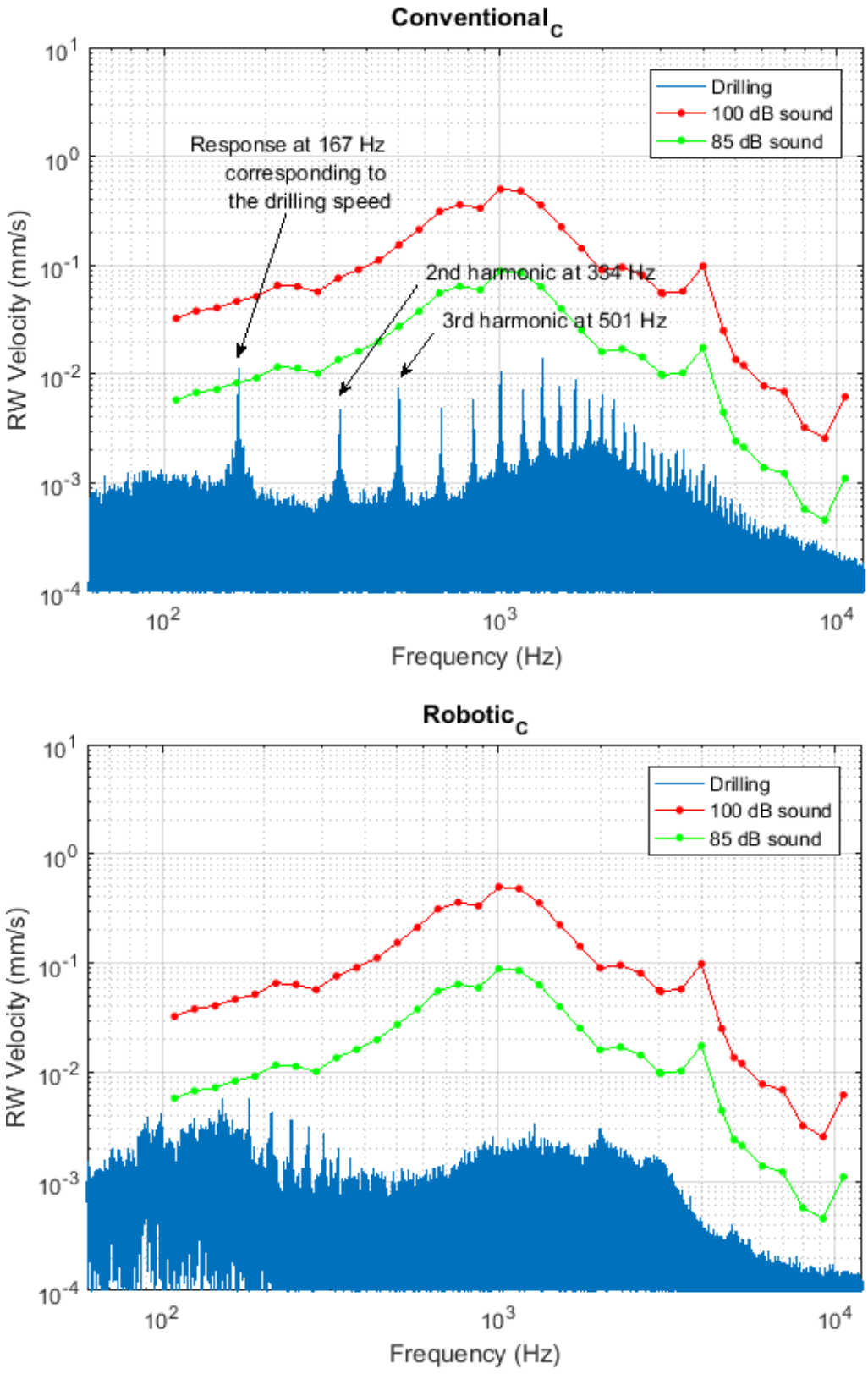

Figure 6.1.3 - 3 | Frequency spectrum of the drilling signal covering the whole cochleostomy procedure – Cochlea C. Top: conventional. Bottom: robotic.

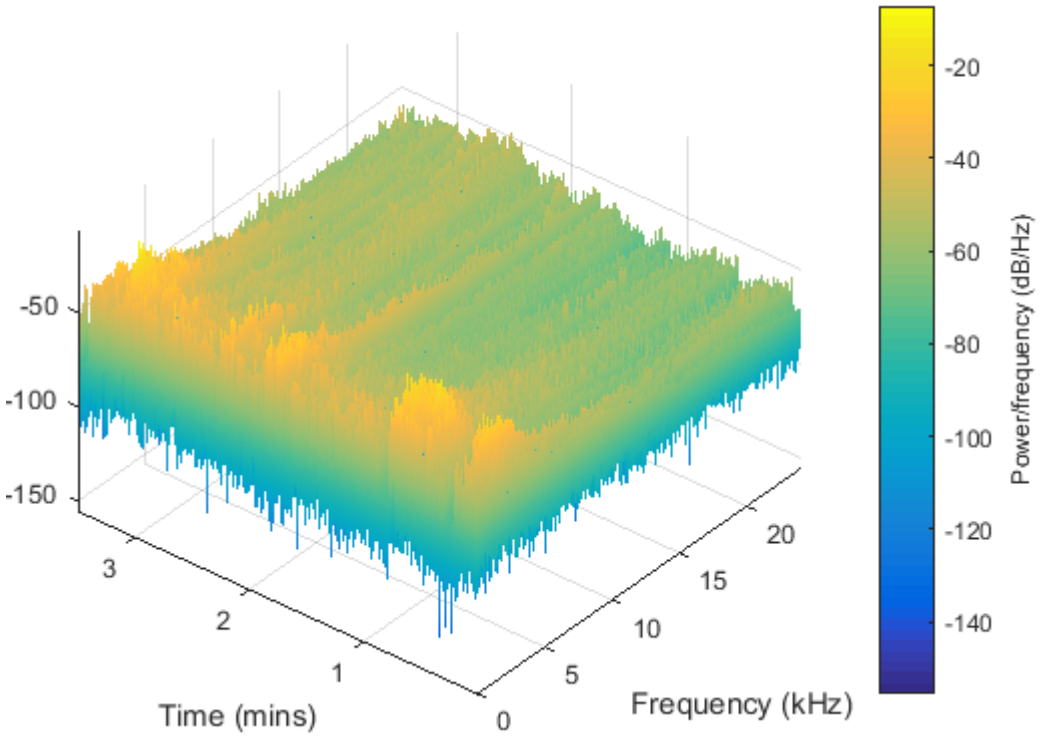

Figure 6.1.3 - 4 | 3-D Spectrogram of drilling-evoked round window vibration velocity. Data obtained from Cochlea C using conventional drill is presented to illustrate a trend observed in all cases – concentration of energy at low frequency band (<5kHz).

To disclose the trend of the change of frequency content over time, spectrogram of drilling signals were generated computationally using short-time Fourier transform. Figure 6.1.3-4 is a 3D view of the spectrogram of the drilling signal obtained when conventional technique was used. While time and frequency is displayed on two axes on the horizontal surface, the intensity in units of dB/Hz is rendered with both colour and height along the vertical axis. In this example, each frequency spectrum is generated over a 0.1s window with 50% overlap. The plot presented is a typical representation of the spectrogram of drilling signal, in terms of its consistent emphasis on low frequency content, i.e. an accumulation of energy at frequencies lower than 5kHz throughout the drilling procedure. This

accumulation of energy at lower half of the frequency band of the hearing range matches the trend that can be observed in Figure 6.1.3-1, Figure 6.1.3-2 and Figure 6.1.3-3.

6.1.4 Equivalent Sound Pressure Level Induced during Cochleostomy Formation

To facilitate discussion and provide a more comprehensible comparison between the two drilling methods, the round window velocity during drilling is converted into equivalent sound pressure level, expressed in units of decibels. The mathematical relationship is introduced in Section 5.2.4.

To obtain the round window velocity induced by drilling at the corresponding METF frequency, the value at the first frequency, in ascending order, that is equal to or larger than the corresponding frequency on the METF is selected. This round window velocity amplitude is then converted into decibels using Equation 5.2.4-4. The resultant equivalent sound pressure levels on each specimen can be found in Appendix B. The mean equivalent sound pressure levels for conventional drilling and robotic drilling are plotted respectively in Figure 6.1.4-1.

An alternative approach to obtain the corresponding round window velocity is to calculate the RMS value over the 1/3 octave band centred around each frequency on METF, in order to reflect the more general picture. As illustrate in Figure

6.1.4-2, the resultant trend lines are smoother and in a sense more realistic compared to that shown in Figure 6.1.4-1.

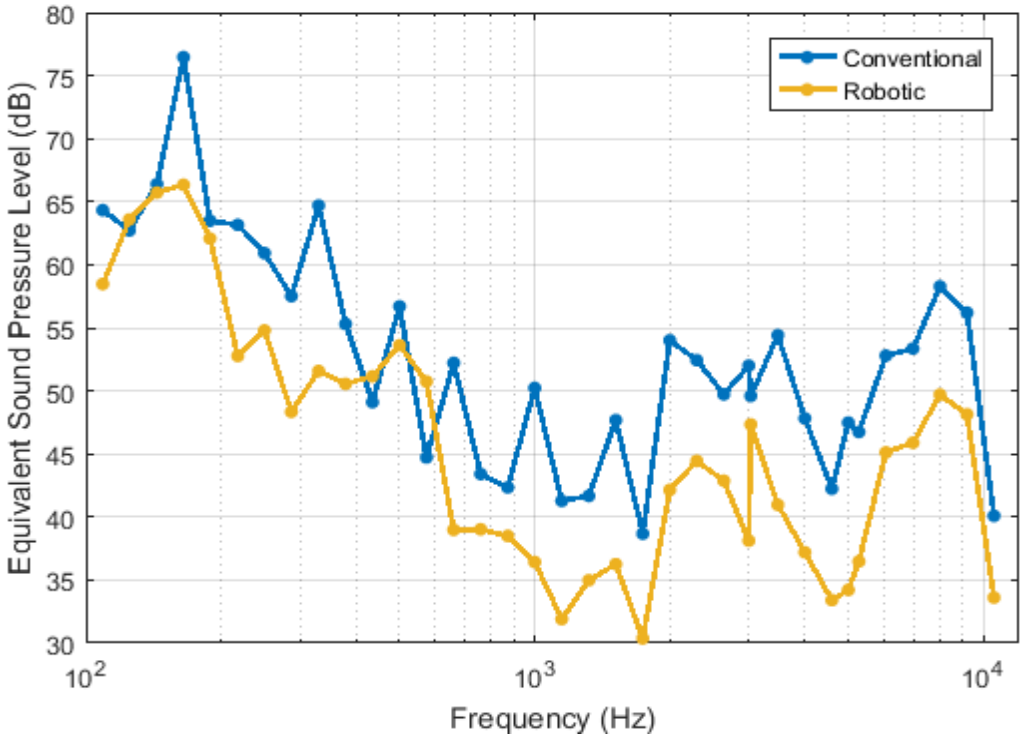

Figure 6.1.4 - 1 | Mean equivalent sound pressure level. Each value is an average of three trials at the corresponding METF-specified frequency.

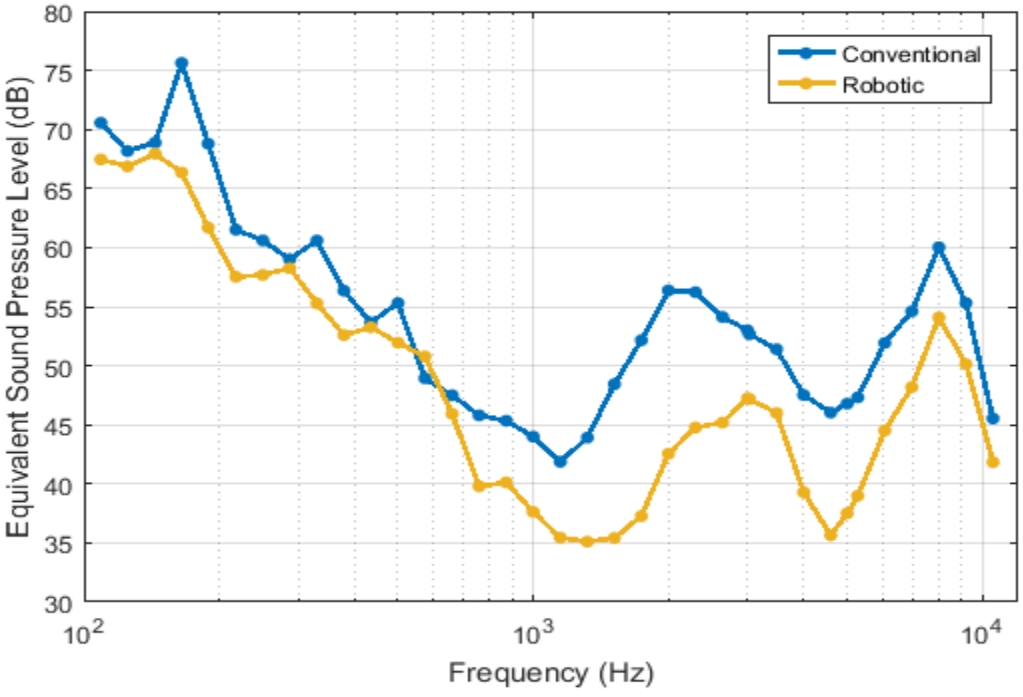

Figure 6.1.4 - 2 | Mean equivalent sound pressure level. Each value is an average of three trials over 1/3 octave band of the corresponding METF-specified frequency.

Both Figure 6.1.4-1 and Figure 6.1.4-2 show that on average, both conventional and robotic drilling methods produce acceptable levels of disturbance in terms of equivalent sound pressure levels. However, robotic drilling induces a lower level of disturbance across the majority of the hearing frequency band, especially at higher frequencies where the natural loss of hearing is more common.

However, some peaks are not presented in the equivalent sound pressure level plots because there is no corresponding frequency on METF, for instance the 167Hz peak response on conventional drilling spectra. If estimating the corresponding METF value by interpolation using the existing METF values, the peak equivalent sound pressure levels can be evaluated.

One approach of achieving this is to interpolate METF to a finer mesh – using the corresponding array of frequencies on round window velocity spectra as query points. The resultant METF-RW after spline interpolation for Cochlea A, corresponding to conventional drilling, is presented in Figure 6.1.4-3 as an example. The robotic counterparts follow the same shape except the resolution can be different. According to the interpolation details given above, for a given measurement, the frequency resolution of the interpolated METF is the same as that of the corresponding drilling-induced round window velocity spectrum. The frequency resolution of an FFT-resolved spectrum depends on the sampling frequency and the number of samples acquired. The latter is different among the six measurements that are being analysed here.

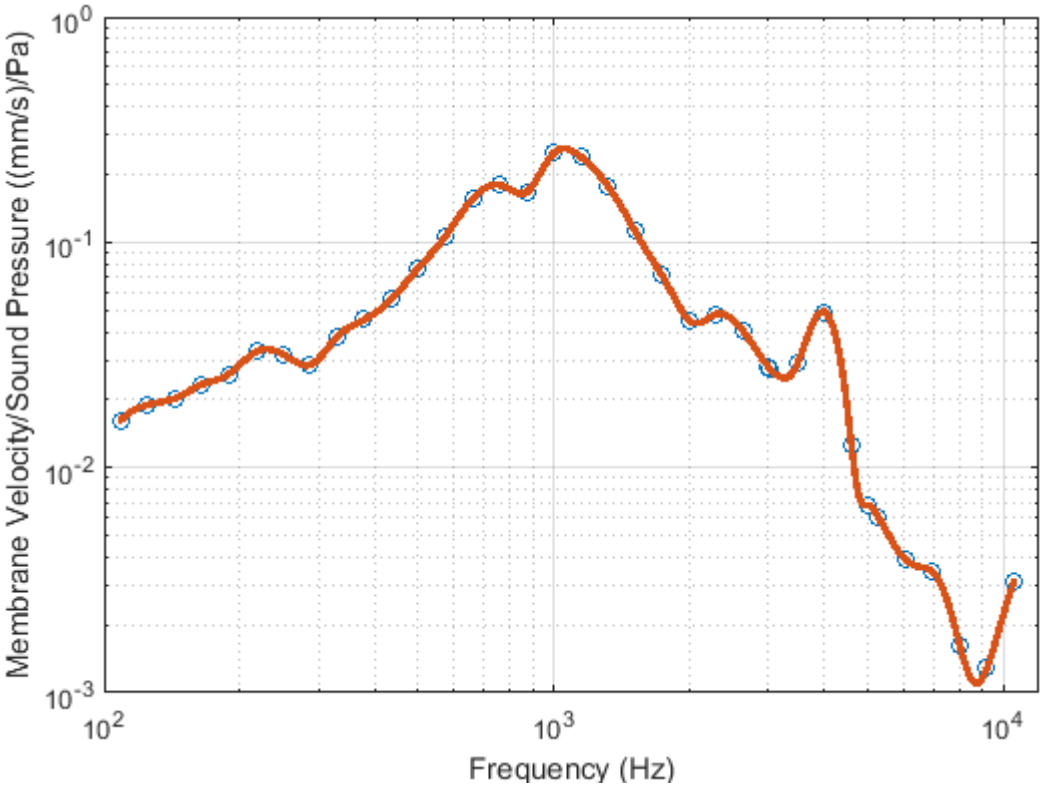

Figure 6.1.4 - 3 | METF-RW after spline interpolation. METF-RW is the round window velocity normalised by the corresponding sound pressure in the external ear canal. The blue circles are the samples of the normalised round window velocity measured at selected frequencies. The red line is the spline interpolation of the acquired data.

The METF-RW after interpolation can be used to calculate the equivalent sound pressure level at a finer resolution, at the resolution of the round window velocity spectra obtained during drilling on the same cochlea. The results are plotted in blue in Figure 6.1.4 – 4, Figure 6.1.4 – 5 and Figure 6.1.4 – 6. As anticipated, prominent peaks are retained in this manner. From the perspective of equivalent sound pressure level, 167 Hz is still the most significant component in the case of conventional drilling – peaking sound pressure level spectra on all three samples. As aforementioned, 167 Hz corresponds to the frequency-

equivalent of drill rotation speed at 10,000 rev/min. On the contrary, there is no consistent prominent peak during robotic drilling. Neither is there peak corresponding to drill rotation speed 2000 rev/min or its harmonics.

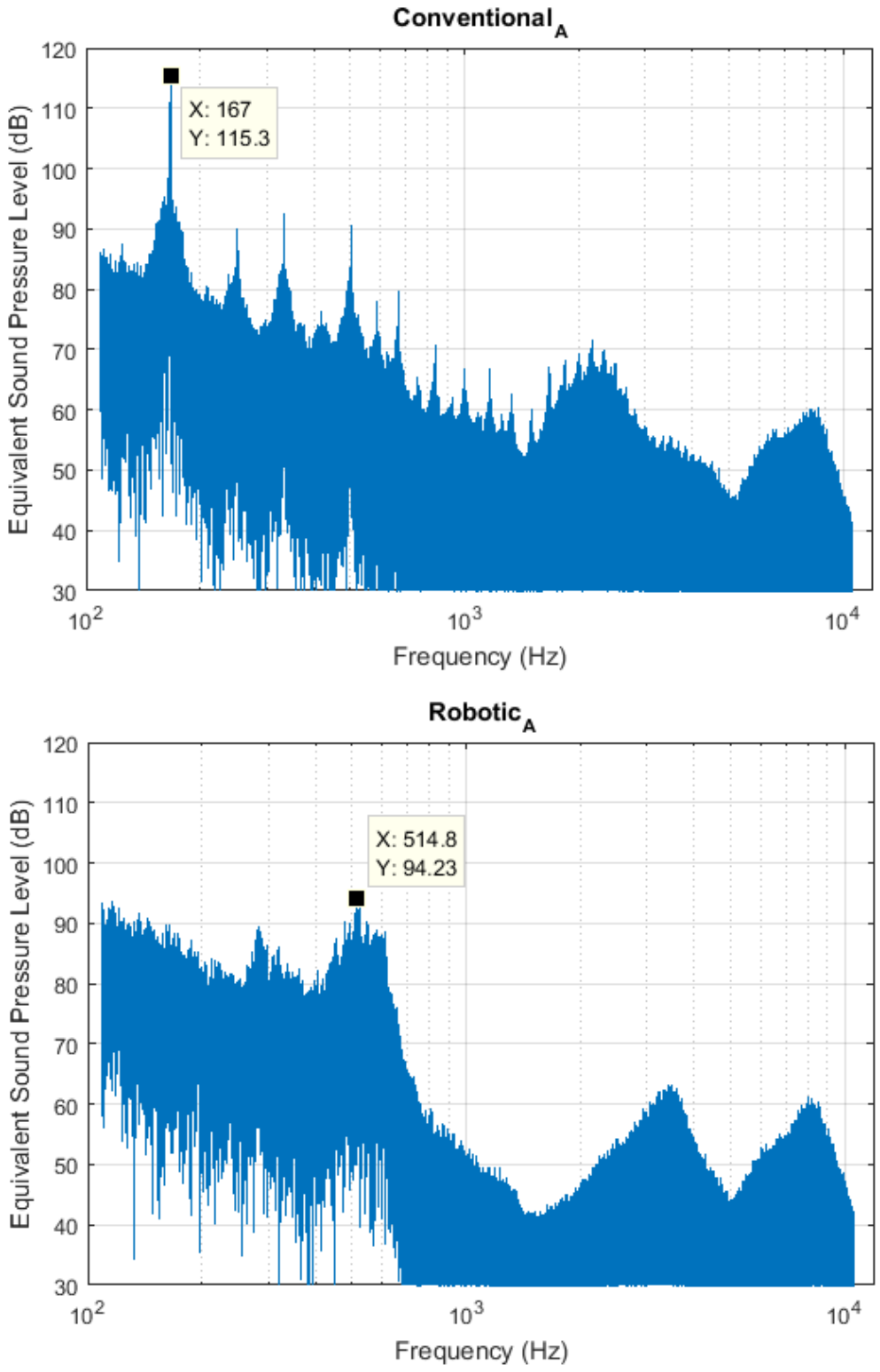

Figure 6.1.4 - 4 | Equivalent Sound Pressure Level generated during conventional and robotic drilling - on Cochlea A.

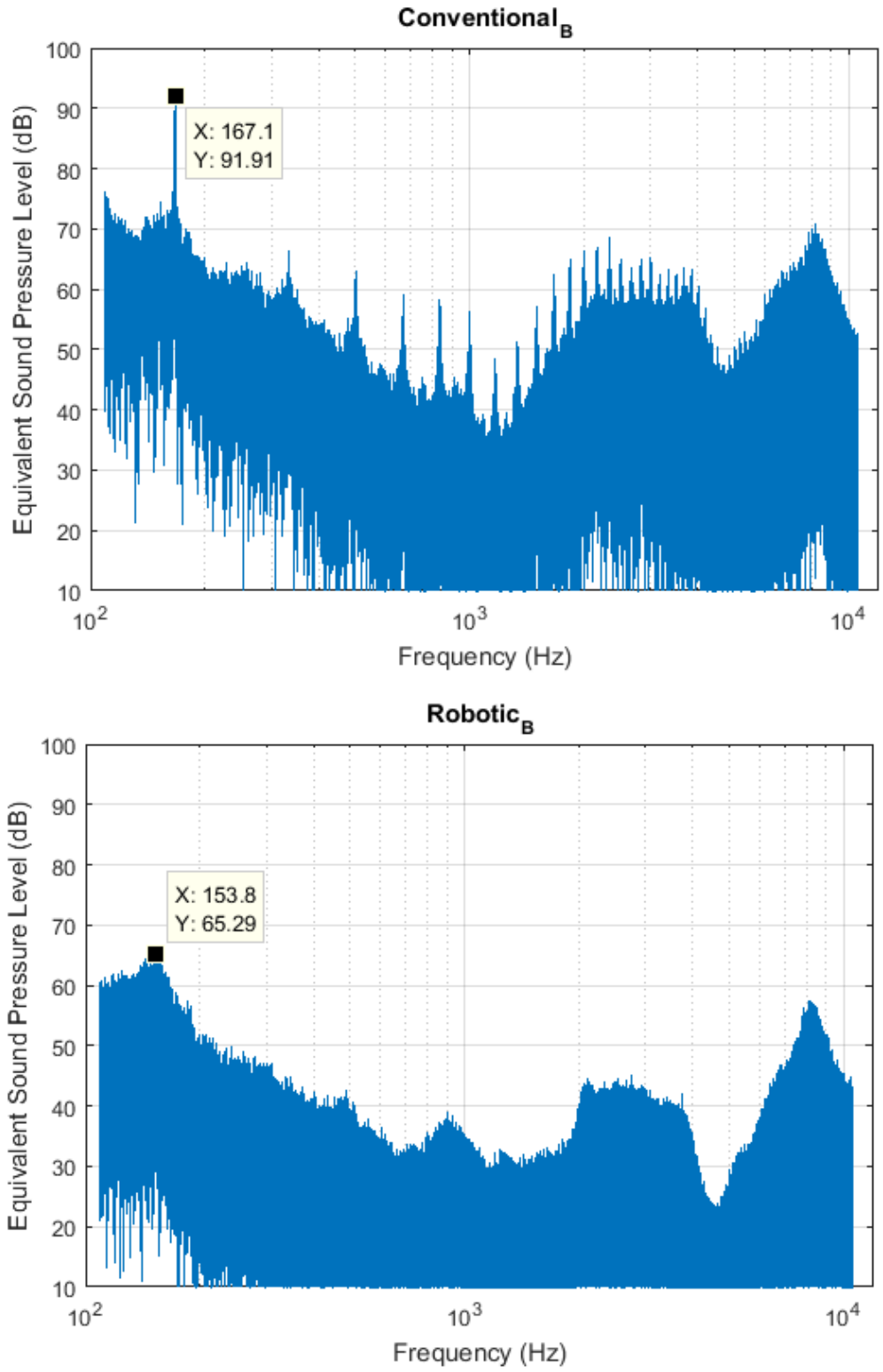

Figure 6.1.4 - 5 | Equivalent Sound Pressure Level generated during conventional and robotic drilling - on Cochlea B.

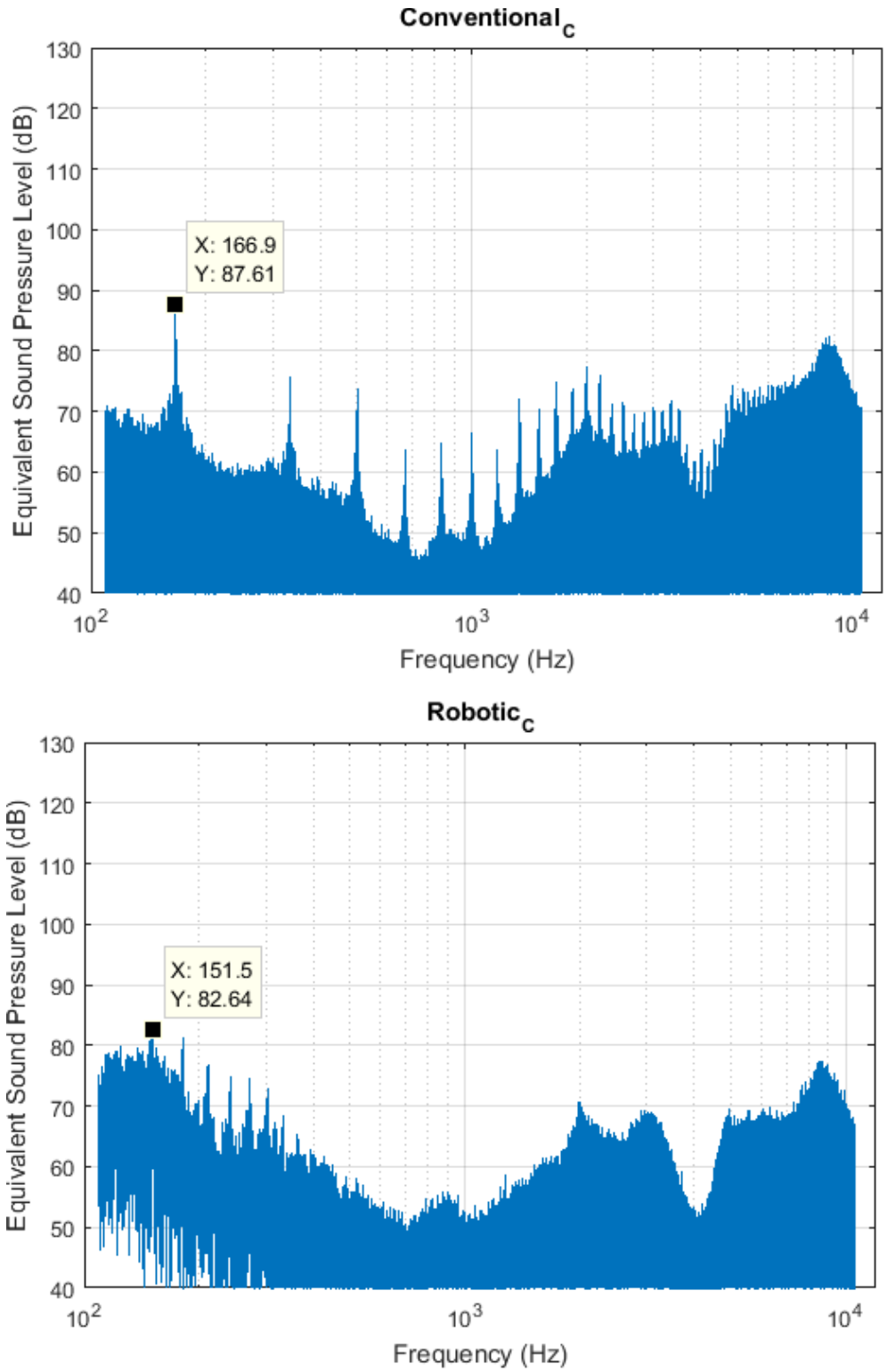

Figure 6.14 - 6 | Equivalent Sound Pressure Level generated during conventional and robotic drilling - on Cochlea C.

The peak amplitudes of equivalent sound pressure level, as marked in Figure 6.1.4-4, Figure 6.1.4-5, Figure 6.1.4-6, are summarised in the table at the bottom of Figure 6.1.4-7. A comparison between conventional and robotic, in respect of the peak amplitude of the frequency-specific equivalent sound pressure level is presented on top of the table. On all three cochlea specimens, robotic delivers a decrease in peak equivalent sound pressure level compared to conventional, ranging from 6% on Cochlea C to 29% on Cochlea B.

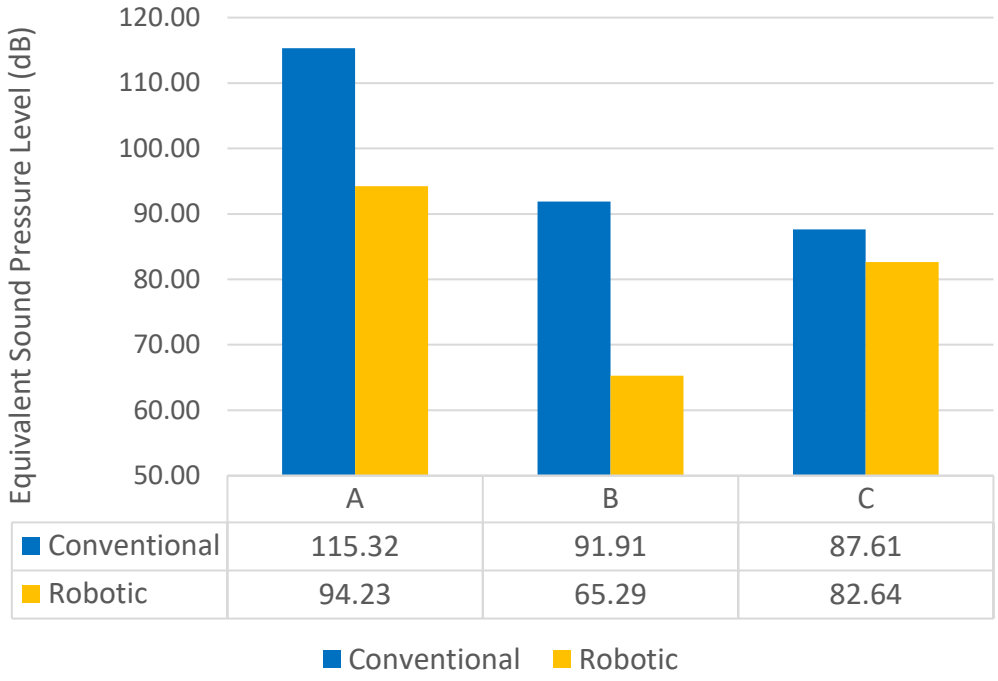

Figure 6.1.4 - 7 | A comparison of the peak amplitude of the induced mechanical disturbance in terms of equivalent sound pressure level - between conventional and robotic drillings. Estimated using interpolation based on existing values of METF.

6.1.5 Instantaneous Total Sound Pressure Level Induced during Cochleostomy Formation

Through analysing the data obtained from human cochlea in cadaver heads, the level of disturbance induced in cochlea during the complete cochleostomy procedure is assessed. The average level of disturbance is acceptable in terms of the equivalent sound pressure level, if the whole drilling procedure is taken into calculation.

It is also possible to obtain the instantaneous equivalent sound pressure level from the data collected on cadaver heads, by accounting energy of all frequency components within the frequency range of interest. According to IEC standard (International Electrotechnical Commission, 2002), the sound pressure level is defined as:

$$SPL = 20 \cdot \log_{10} \frac{p}{p_0} = 10 \cdot \log_{10} \frac{p^2}{{p_0}^2} \qquad (6.1.5 - 1)$$

For any particular time internal, the total sound pressure level can be calculated by substituting p^2 in Equation 6.1.5-1 with the summation of the squares of the equivalent sound pressure at all frequencies (Guyer, 2009). Since the sound energy is proportional to the square of the sound pressure (Schnupp, Nelken, & King, 2011), this is equivalent to taking each frequency component as an independent source of energy and calculated the total impact of energy in units of dB SPL.

Using short-time Fourier transform and the METF-RW curve after interpolation, the time-resolved equivalent sound pressure levels can be determined. Instead of peak amplitude obtained straight from Fourier transform, root-mean-square amplitude of the sinusoidal component at each specific frequency is used here, to properly reflect the corresponding energy content (González-Prida, 2015) (Scheffer & Girdhar, 2004).

The MATLAB code to implement the aforementioned calculation is included in Appendix B. The equivalent total sound pressure level is plotted against time in Figure 6.1.5-1, Figure 6.1.5-2 and Figure 6.1.5-3. The relevant statistics are summarised in Table 6.1.5-1. To facilitate the direct comparison between results that are of different recording lengths, the time is normalised by total cochleostomy time of each particular measurement. Accordingly, the calculation of sound pressure level is done in sliding sections of 1% of drilling time. The pain threshold of 120-140 dB SPL (Ahlbom et al., n.d.) is denoted by the red-shaded area in the figure. Frequency weighting is considered however not reported here since the threshold referred to (120-140 dB SPL) is an unweighted value.

Both Figure 6.1.5-1 and Figure 6.1.5-2 show that the disturbance induced in cochlea during drilling can be over the 120 dB threshold of pain. This applies to both of the two drilling techniques under study. However, the percentage of time that the disturbance is over 120 dB SPL is 15% higher during conventional drilling than during robotic drilling on Cochlea A. On Cochlea C, the disturbance is over 120 dB SPL equivalent for 37% of the time during

conventional drilling. Using robotic drill, only for 2% of the time there is a disturbance level higher than 120 dB SPL.

As for B, the equivalent sound pressure levels for both drilling techniques are significantly lower. The actual disturbance level measured may vary due to the difference in the conditions of the individual cochlea. However, the disturbance evoked by conventional drilling is still higher - for over 86% of the duration of cochleostomy. The peak sound pressure level during conventional drilling is approximately 9.7 dB higher than the robotic peak.

For the same point on time axis, the biggest difference between conventional and robotic values is 39 dB SPL during the first tertile of the cochleostomy on Cochlea A, 23 dB during the middle 1/3 of the procedure on Cochlea B and 38 dB during the latter 1/3 of the cochleostomy. In all three cases, the disturbance induced by conventional drilling is higher than robotic drilling. However there is no tendency in terms of during which part of the cochleostomy procedure the biggest difference is more likely to occur.

There is also no indication from the measurements in terms of when the peak values of drilling disturbance are more likely to appear during the procedure of drilling, for either drilling technique. Even though it seems that there is higher time-average for either second or third tertile of the cochleostomy process, the difference between tertiles with the highest value and the lowest value is within 6 dB among all six measurements. Furthermore, the first 1/3 period of drilling does not always has the lowest average value as evident in Column 5-7 in the

same table. Above all, it is difficult to determine if thickness of remaining bone has any effect on the disturbance level.

As shown in the rightmost column in Table 6.1.5-1, robotic drilling on average generates 5-8 dB SPL lower than conventional during cochleostomy. The peak sound pressure level associated with robotic drilling is also consistently lower than that of conventional drilling, by as much as approximately 10 dB as shown by results on Cochlear B and Cochlea C.

Table 6.1.5 - 1 | Statistics for the equivalent sound pressure level over time

Cochlea #	Drilling Technique	Max SPL (dB)	% of time that generates a higher disturbance	Average SPL (dB)
A	Conventional	136.25	62.29%	121.29
A	Robotic	134.87	37.71%	116.11
B	Conventional	117.04	86.20%	104.94
B	Robotic	107.35	13.80%	97.46
C	Conventional	134.17	82.15%	117.63
C	Robotic	124.62	17.85%	109.71

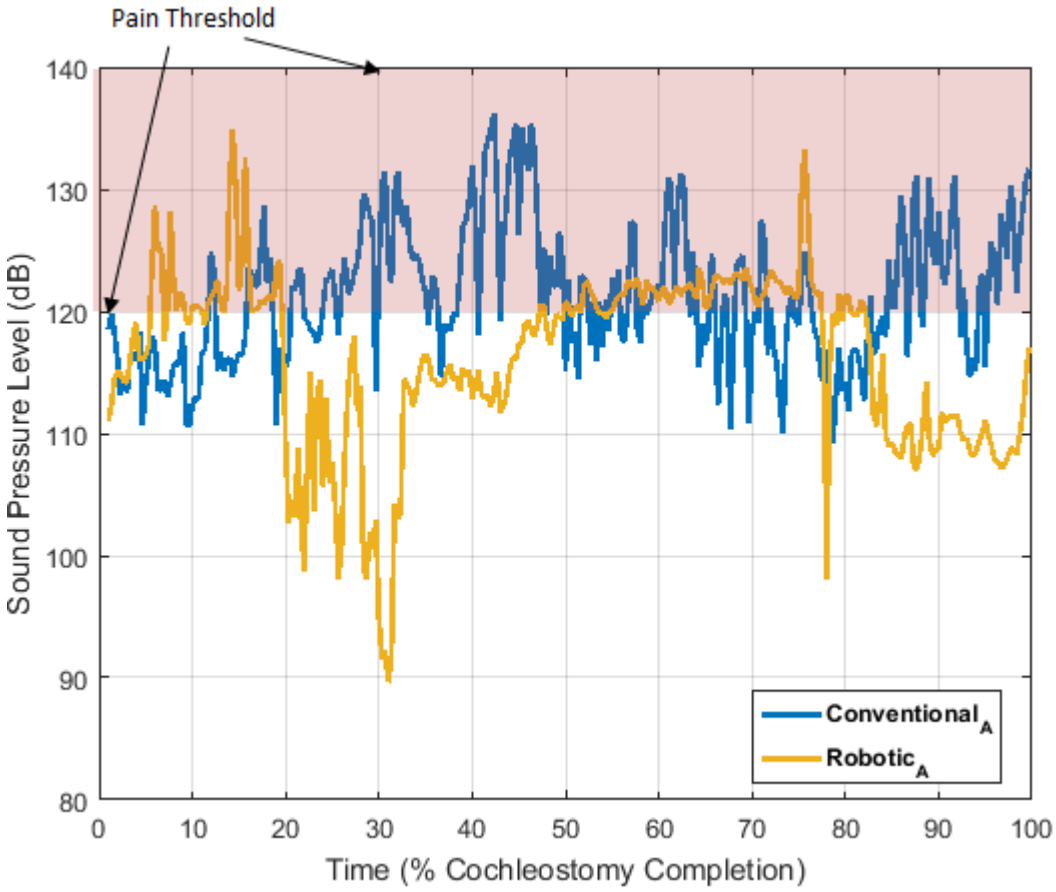

Figure 6.1.5 - 1 | Sound Pressure Level plotted against time that is normalised by total recorded cochleostomy drilling time, representing measurement on Cochlea A. Shaded in red is the pain threshold of 120-140 dB SPL.

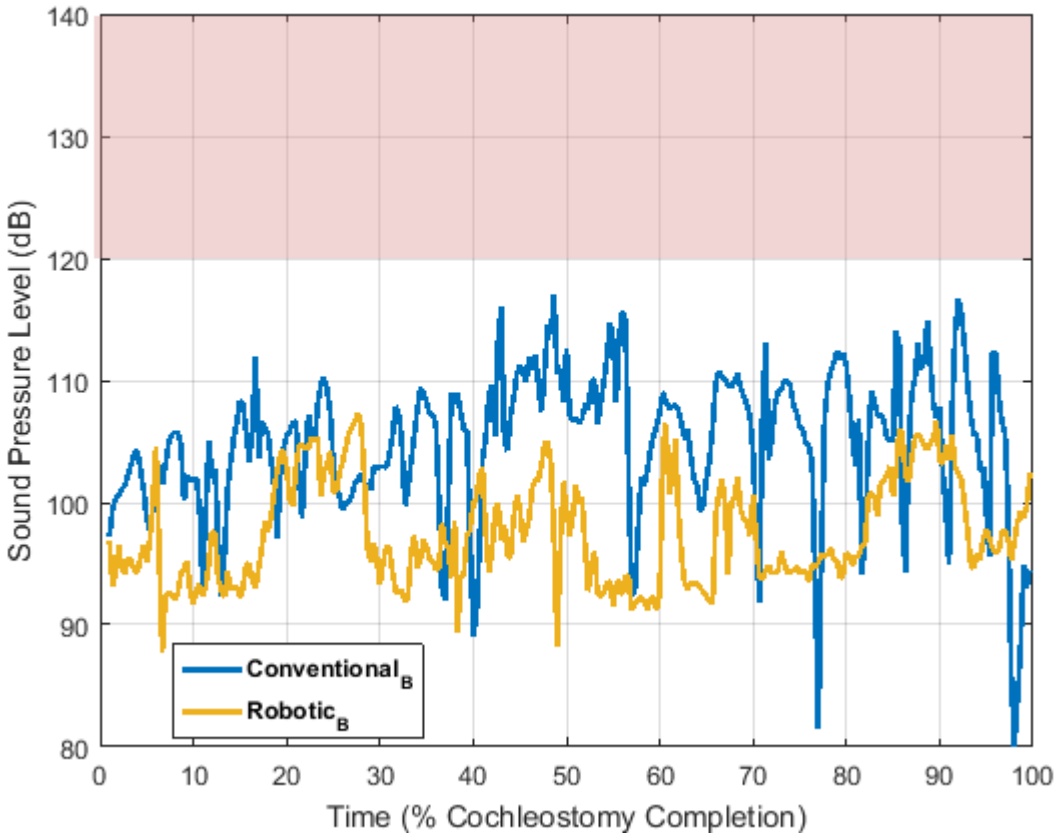

Figure 6.1.5 - 2 | Sound Pressure Level plotted against time that is normalised by total recorded cochleostomy drilling time, representing measurement on Cochlea B. Shaded in red is the pain threshold of 120-140 dB SPL.

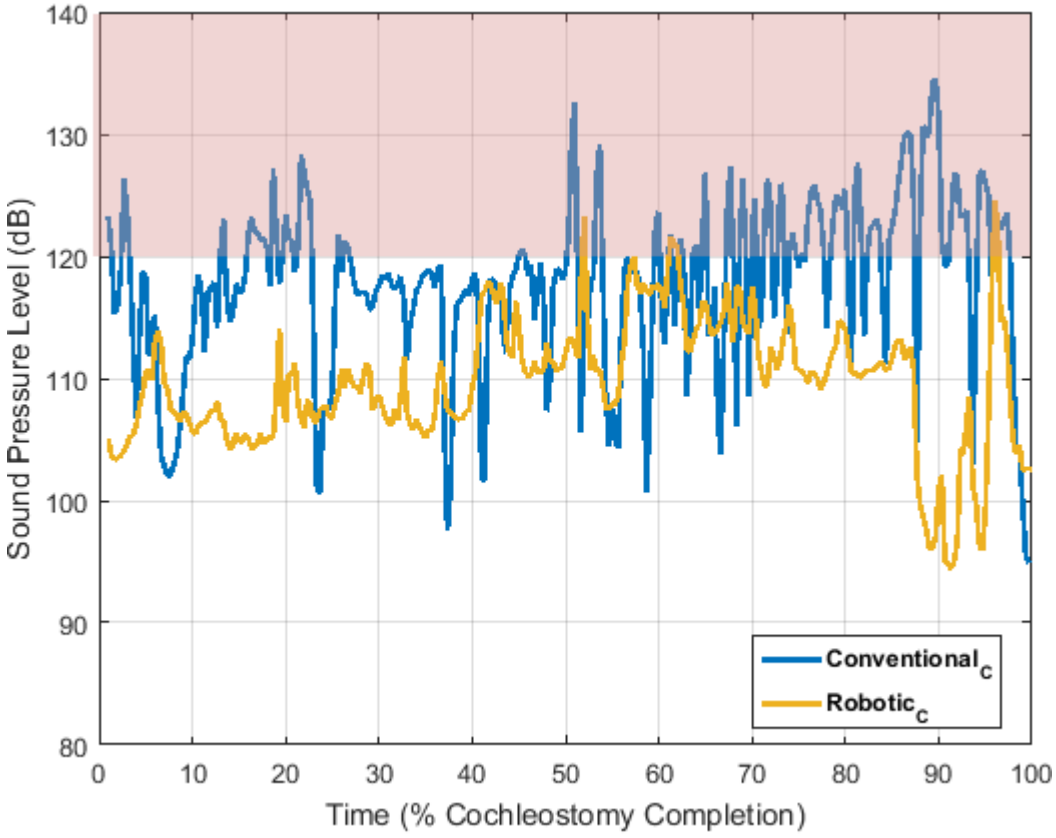

Figure 6.1.5 - 3 | Sound Pressure Level plotted against time which is normalised by total recorded cochleostomy drilling time, representing measurement on Cochlea C. Shaded in red is the pain threshold of 120-140 dB SPL.

6.2 Discussion

Results from Section 6.1.4 and Section 6.1.5 show that the level of disturbance induced by robotic drilling is consistently lower, and below the pain threshold for much longer, compared to that of conventional drilling. The peak disturbance amplitude during conventional drilling can be 10 dB SPL larger than that during robotic drilling, as per the trace of drilling-evoked equivalent sound pressure level over time. This, if converted to field quantity in units of pascal, indicates that conventional drilling evokes a peak pressure value that is more than 3.16 times that of robotic drilling. Throughout the duration of cochleostomy, robotic drilling can reduce as much as 30% of the equivalent tympanic membrane pressure generated by conventional drilling, based on data collected on Cochlea A as shown in Figure 6.1.5-1.

There is no obvious surge of disturbance level at the end of cochleostomy drilling which has been reported by other groups (Pau et al., 2007) (Eze et al., 2014). It is probably because in this study, both the drilling and the recording were stopped as soon as fenestration was complete. Therefore, the running drill burr has little direct contact with the exposed endosteum. This also confirms the observation by other groups (Pau et al., 2007) (Eze et al., 2014) that the level of drilling-induced disturbance is relatively consistent as long as the running burr is not in direct contact with endosteal membrane, despite the thinning of the bone layer between drill burr and the endosteal throughout the progress of cochleostomy.

Figure 6.1.5 and previous plots show quite significant differences in amplitude between conventional and robotic. This is important as much of the difference is caused by the conventional drill re-contacting following inspection of the progress of the cochleostomy, simply because the human operator cannot obtain feedback otherwise. It is completely avoidable with the robotic system.

Further, with the conventional system it would be more by luck than judgement to drill close to the endosteum without perforation. The puncture needed to bust through the remaining bone tissue and endosteum by the conventional approach would also be more traumatic as a result of the greater impulse needed due to the thicker remaining tissue. Further work would be needed to prove this in the future.

It is by far almost impossible to assess trauma before the completion of the entire cochlear implantation surgery. With the lack of appropriate immediate knowledge of the degree of trauma, it would be beneficial to minimise any type of disturbance in both time and amplitude - including some compromise between these factors, in which case the robotic approach should be favoured.

6.3 Concluding Section

Robotic drilling, in comparison to the conventional drilling method, creates a consistently lower level of disturbance in cochlea both in time domain and across the hearing frequency range. It is therefore reasonable to conclude that robotic drilling has a lower possibility of creating acoustic trauma in cochlea that endangers the residual hearing of patients.

The results presented in study are early results which indicate the possibility of lowering disturbance to hearing organ by utilising the robotic-assisted approach. To consolidate and further establish the trend observed in this study, data from more subjects are needed. This will enable, to the best possible extent, removing variance in specimen condition, for instance specimen freshness, anatomy, age, gender and intrinsic hearing ability. To facilitate accessibility to specimens, porcine cochlea is a considerably cheaper alternative, in terms of both time and monetary cost, to construct the set up and test hypothesis at an early stage. Though at the present stage, it is considerably challenging to gain access to the cochlea with the hearing chain intact, especially with limited surgical expertise and facility in lab.

Regarding the contamination in signal discussed in Section 5.3, a perfectly synchronised video recording taken in parallel to drilling can assist the identification of abnormal events. Both surgeon's hand and microscopic view of the retroreflective target on membrane should be filmed during recording. Though avoiding the abnormal non-drilling events may be a better solution, it is

highly unlikely that the signal contamination can be totally avoided if the whole uninterrupted continuous procedure is to be captured. Although great effort has been made into signal processing especially the discrimination between effective and contaminated data, there might still be discrepancies due to inefficiency in the processing algorithm. For instance, additional data points that are not related to drilling procedure can be included in the processed data. To tackle this issue, apart from fundamentally enhance the data collection setup in lab, a better understanding of the events that lead to contamination should be formulated through techniques like video tracking. A more precise definition of the mathematical features of the contaminated data as well as a more efficient processing algorithm will undoubtedly enhance the analysing performance and the results.

Laser Doppler vibrometry enables the non-invasive measurement of characteristics of vibration. It is widely accepted as the standard instrumentation to study cochlear mechanics due to its ability to capture vibration at ultra-high resolution and precision without the need to contact or mass-loading the object. This non-contact feature makes it particularly useful in characterising the mechanical properties of extremely small and extremely lightweight structures. It also enables the measurement on target that is too difficult to reach or be attached to by other sensors. Similar signal contamination problem is also experienced by other researchers using Laser Doppler vibrometry for continuous measurement - described as ‘signal drop-out’ (Hosek, 2012). The issue was overcome by developing a post-processing algorithm custom to the target motion

under investigation, similar to the data processing procedure covered in Section 5.3 of this thesis.

Chapter 7

Conclusions and Suggestions for Future Work

7.1 Summary and Conclusions

This thesis investigated the level of disturbance induced in cochlea during surgical drilling on cochlea, i.e. cochleostomy. An assessment was made by making a contrast between a manually guided conventional technique and a manually supported tissue guided robotic drilling technique, in terms of the equivalent noise level of the mechanical energy transmitted into the cochlea during drilling a cochleostomy. Vibration induced was measured at the round

window – a natural, non-invasive approach to assess mechanical movement of the fluid inside the cochlea. To overcome the contamination in the measurements due to vibrometer signal drop-offs, an algorithm tailored for cochlea tissue vibration was developed and implemented to derive the true vibration signal. A mathematical model of cochlea was produced to provide a fundamental understanding of the cochlear dynamics, as well as assessing if an unavoidable structure modification made to the cochlea can leave an impact at an acceptable level. The claim asserted by the model was tested experimentally on porcine cochlea, before being implemented during the disturbance measurement on cadaver heads.

Hearing loss is a common impairment for human beings - affecting 55% of the UK population over 60. As suggested in Chapter 2, cochlear implant is one of the most effective treatment to hearing loss – with no prerequisite for any residual hearing. However, to enable more people to benefit from this treatment, hearing conservation rises in importance as an issue that does not exist to the original target recipient of cochlear implantation since they are profoundly deaf. Chapter 2 also demonstrates that as a tool to accurately assess the mechanical disturbance, laser vibrometer is the most compelling choice, due to its accuracy and non-intrusiveness.

In cochlea, the BM displacement increases along the length of BM, until reaching its peak value and quickly decreases beyond this point. This describes the physical event underlying the frequency demodulation functionality of the cochlea. The higher the input frequency, the closer to base that the BM vibration

peaks. It was shown in Chapter 3 that these qualities do not change with the creation of TW on cochlea wall. However, there is limited but noticeable level of change to cochlear dynamics especially when the third window is created towards the basal end. The third window therefore should only be created when necessary and no alternative approach is possible.

It was validated in Chapter 4 that creating a TW on the cochlea does not bring significant change to RW velocity – a non-intrusive indication of cochlear dynamics. This, along with the considerations made in the experimental setup for vibrational measurement on cochlea, lays a good foundation for the vibrational study on a human cadaver in Chapter 5.

As part of the endeavour to bring the benefits of cochlear implant to people with residual hearing, the surgical drilling procedure during cochlear implantation was studied in Chapter 5, with an aim to quantitatively assess the potential benefits of atraumatic surgery and hearing preservation during cochlear implantation. Utilising the original auditory chain, the tissue response to acoustic signal with known loudness can be measured and compared to that in response to the mechanical disturbance of surgical drilling. The comparison was conducted mathematically and across multiple frequency bands within the range of hearing.

This comparison enables the assessment of mechanical disturbance induced by the cochleostomy drilling in units of dB sound pressure level. It is the first time such assessment successfully covers the entire cochleostomy procedure from start to completion. More specifically, activities that are part of the standard

cochleostomy drilling that usually fail to be caught if measured short-term, such as lifting and repointing the drill in order for the surgeon to observe drilling progress, was captured in this study where the implication was studied.

The continuous recording of the entire cochleostomy procedure imposes challenges on post processing of the measured signal. This is mainly due to the limitation in the practical use of laser vibrometer. There is constant signal 'drop-off', or 'off-target' as described in Chapter 5, if the measurement time is longer than 10s. An algorithm was developed and successfully removed the signal contaminination due to laser 'off-target'. This algorithm is tailored to the characteristics of the target signal to be retained, i.e. RW vibrational response to cochleostomy drilling disturbance, in terms of the scale of amplitude and frequency.

It is the first time that a surgical robotic drill was trialled on a human cadaver head, and more importantly, with its intracochlear disturbance level measured and correlated to equivalent loudness in dB SPL. The assessment in dB SPL offers a much more tangible set of results – much easier to be communicated to audiologists, clinicians, health care providers and its governing authorities.

It was concluded in Chapter 6 that robotic drilling is a less traumatic approach to cochleostomy compared to conventional drilling - induced lower level of equivalent SPL for up to 86% of the time. The peak disturbance can be reduced up to 10 dB using robotic drilling. Over the progress of cochleostomy, the disturbance induced by robotic drilling can be as much as 39 dB lower than that

generated by conventional drilling. This delivers a positive indication as an early stage investigation. Due to the limited number of trials that was possible to be obtained in this study, further investigation on a bigger population would be sensible to make further and more conclusive claims.

Regarding removal of sources of trauma from the cochlear implantation surgery procedure, cochleostomy drilling, which is discussed in this thesis, represents only one aspect of the consideration. Another area that remain unaccountable, have limited level of control other than the experience of the surgeon, and on the other hand directly interfere with the sensing organ inside the cochlea and therefore potentially more likely to lead to trauma is the insertion of electrode array during cochlear implant surgery. Robotics can be helpful in several ways in this regard. Apart from measuring, monitoring and limiting the force at the tip of the electrode array during insertion, robotics can potentially also proactively guide the electrodes to follow the best trajectory – to avoid penetrating or damaging the basilar membrane, based on the judgement of the location and shape of the electrode array relatively to the sensitive tissue in cochlea. Experimental studies are required to find out both the relevant attributes and the model of how these attributes can cohesively determine the position and best trajectory during insertion. Nevertheless, it takes time and resources to research and develop this robotic insertion model - not enough evidence to support that the development of fully automated robotic electrode insertion would be accomplished in the near future. It is also unclear if its benefits can outweigh the complexity involved in developing the robotic insertion solution, given there are

already noticeable progress in alternative designs of cochlear implant electrode array in order to reduce trauma during insertion.

Reducing the potential trauma caused during the cochleostomy drilling is therefore still relevant. It is especially applicable with the increasing popularity of electric-acoustic stimulation cochlear implant which relies on the residual hearing at apical end of the cochlea. With the chances of damage during insertion reduced by its shorter electrode array by design, it is especially important for the damage that induced via cochleostomy drilling to be contained. In this thesis, it has been demonstrated that robotics can be helpful in the drilling stage of the cochlear implantation surgery. More sets of data, collected in an even more rigorous approach, would of course be ideal before obtaining the opportunity to trial in vivo to demonstrate there're sufficiently significant benefits over the manually guided conventional technique.

7.2 Future Work

Atraumatic drilling and hearing preservation during cochlear implantation is an active research area at the present time. It not only reduces the risk of compromising existing hearing and potentially allows people with mild hearing loss to benefit from cochlear implant, but also improves the performance of current cochlear implant by enabling both electrical and acoustic stimulation.

Moving forward from this study, continuous disturbance capturing during the entire procedure of cochleostomy drilling has been proved feasible. This experimental setup and signal processing methodology can be applied to similar

surgeries or research areas where mechanical disturbance is of interest. The algorithm can be refined by validating with an independent system monitoring in parallel such as a synchronised video capturing of hand movements and laser spot. With adequate level of accuracy and sophistication, this algorithm has the potential to benefit the wider community of laser vibrometer users in both academia and industry.

Appendix A

MATLAB Code for Time Series Data Processing

As described in Chapter 5, algorithms have been developed in order to computationally decontaminate the raw data and extract the true disturbance level. The implementation includes two steps. First, based on the distinctive statistical feature of drilling signal compared to ‘off-target’, identify and remove ‘off-target’ events which is covered in Section A.1. Second, further eliminate the influence of ‘off-target’ events on the rest of trace by correcting baseline drifts near ‘off-target’ events, covered in Section A.2.

A.1 Removal of 'Off-target' Events

Close observation of the raw data, coupled with the knowledge of the functionality of the laser vibrometer leads to an understanding of the characteristics of the drilling signal. This is summarised as two conditions. For each one-millisecond equivalent data samples to be recognised as the real drilling signal, it needs to satisfy one of two conditions, listed as follows.

Condition 1: Consistent low-variance;

Condition 2: Smooth curve with limited gradient, without prominent local maxima.

The MATLAB code to implement the above rules has been presented below. All static value parameters are fine tuned to deliver consistent, stable and satisfactory discrimination performance, as far as visual distinction is concerned, when applied on both manual and robotic drilling recordings.

Calculate moving variance:

```
load('trace.mat');
samplingRate = 48000; % unit: Hz or sample per second
ldvSensitivity = 50; % unit: mm/s/V
trace_test = trace.*ldvSensitivity;
variance_array = movvar(trace_test,3);
save ('variance_array_test.mat', 'variance_array');
```

Find and kill 'off-target' events:

```
load('trace.mat'); % unit:V
```

```
load('variance_array_test.mat');
samplingRate = 48000; % unit: Hz or sample per second
ldvSensitivity = 50; % unit: mm/s/V
min_onTarget_time = 0.002; % unit:s

trace_test = trace.*ldvSensitivity;
trace_length = length(trace_test);
time                                                    =
0+1/samplingRate:1/samplingRate:trace_length/samplingR
ate;
min_onTarget_sampleCount                                =
min_onTarget_time*samplingRate;
max_onTarget_diff          =          (max(trace_test)-
min(trace_test))/3;
% 3 is an estimate based on observation of the trace

trace_test2 = zeros(trace_length,1);
for i =3:trace_length-(min_onTarget_sampleCount+1)
    % Condition 1: continuous low-variance
    if    variance_array(i:i+(min_onTarget_sampleCount-
1))<0.1
        trace_test2(i:i+(min_onTarget_sampleCount-1))=
trace_test(i:i+(min_onTarget_sampleCount-1));
    else
        %  Condition  2:  if  high-variance,  drilling
trace is smooth and
        % relatively flat
        pks          =          findpeaks(trace_test(i-
2:i+(min_onTarget_sampleCount+1)),'MinPeakProminence',
2.5,'MaxPeakWidth',4);
        pks2         =         findpeaks(-trace_test(i-
2:i+(min_onTarget_sampleCount+1)),'MinPeakProminence',
2.5,'MaxPeakWidth',4);
        if isempty(pks) && isempty(pks2)
            if                    abs(diff(trace_test(i-
2:i+(min_onTarget_sampleCount+1))))< max_onTarget_diff;

trace_test2(i:i+(min_onTarget_sampleCount-1))=
trace_test(i:i+(min_onTarget_sampleCount-1));
            end
        end
    end
end
save ('trace_var_filtered.mat', 'time','trace_test2');
```

A.2 Baseline Drift Correction

After removing the 'off-target' events from the contaminated signal, Logics are applied to locate the start and end of each piece of signal that needs to be corrected. De-trending logics are then applied to remove the baseline drift in the signal. The full implementation in MATLAB is shown below.

```
clear; clc;
load('trace.mat'); % unit:V
load('trace_var_filtered.mat'); % unit: mm/s
samplingRate = 48000; % unit: Hz or sample per second
ldvSensitivity = 50; % unit: mm/s/V
%corrected trace legnth <=2ms
max_toCorrect_time = 0.002; % unit:s

trace_test = trace.*ldvSensitivity;
trace_test3 = trace_test2;
trace2_length = length(trace_test2);
trace_max = max(abs(trace)*ldvSensitivity);

i=1;
while i < trace2_length-1
    %Define the start of the piece of drifiting trace
to be corrected
    %by identifying where the orgininal 'off-target'
ends
    if trace_test2(i)==0 && trace_test2(i+1)~= 0
        n=2;
        % Define the end of the piece of drifting
trace to be corrected
        % by identifying: the next 'off-target' or the
maximum length of
        % correction whichever encountered first
        while trace_test2(i+n) ~= 0 && n<
max_toCorrect_time*samplingRate+1
            if i+n > trace2_length
                break;
            end
            n=n+1;
        end
        noisyDrilling_withTrend = trace_test2(i+1:i+n-
1);
        f_y = movmean(noisyDrilling_withTrend,24);
```

```
        Drilling_data = noisyDrilling_withTrend - f_y;
        for m = 1:length(Drilling_data)
            if abs(Drilling_data(m))> trace_max
                Drilling_data(m) =
noisyDrilling_withTrend(m);
                i+1
            end
        end
        trace_test3(i+1:i+n-1)= Drilling_data;
        i=i+n;
    else
        i=i+1;
    end
end
figure;
p1 = plot(time,trace_test);hold on; p1.LineWidth = 0.5;
p1.Marker = '.'; p1.MarkerSize=10;
p2 = plot(time,trace_test2);p2.LineWidth = 1.2;
p2.Color = [0.85,0.33,0.1];
p3 = plot(time,trace_test3);p3.LineWidth = 0.8;
p3.Color = [0,0.5,0];
xlabel('Time (s)');
ylabel('RW Velocity (mm/s)');
ylim([-6, 6]); grid on;
```

Appendix B

Sound Pressure Level Calculation

The decontaminated time series signal is converted and analysed in frequency domain – where sound pressure level is evaluated. It is then converted to equivalent sound pressure level using the middle ear transfer function as show in Section B2. Section B3 shows using the same methodology, the equivalent sound pressure level can be obtained for every 1% of drilling process, which is potentially provide more information than an overall equivalent sound pressure level for the entire procedure.

B.1 Spectral Analysis

The MATLAB code for converting the time series signal into frequency domain is shown as below.

```
%% Load clean trace
load('C_METFRW2L.mat');
load('trace_var_filtered_driftCorrected.mat');

trace_test = trace_test3; % mm/s
Fs = 48000; % Sampling frequency

%% Calculate FFT
T = 1/Fs; % Sampling period
L = length(trace_test); % Length of signal
t = (0:L-1)*T; % Time vector
N = 2^nextpow2(L); % Next power of 2 from length of
trace
REF = fft(trace_test,N)/L; % double-sided amplitude
spectrum (complex: magnitude + phase)
f = Fs/2*linspace(0,1,N/2+1); %Fs/2 is the Nyquist
frequency

%% Plot single-sided amplitude spectrum.
figure;
amplitude = 2*abs(REF(1:N/2+1)); % first N/2+1 values
loglog(f,amplitude);
xlabel('Frequency (Hz)');
ylabel('RW Velocity (mm/s)'); %peak not rms
max_display_frequency = 12000;
xlim([60 max_display_frequency ]);
ylim([10e-5, 10]);
grid on;
hold on;

%% 100 dB equivalent RW motion
SoundTrace = METF.*2; %100dB = 2 Pa
p1 = loglog(frequency, SoundTrace, '.-r');
p1.MarkerSize=10;

%% 85 dB equivalent RW motion
SoundTrace = METF.*2*10^(-0.75); %100dB = 2 Pa
p2 = loglog(frequency, SoundTrace, '.-g');
p2.MarkerSize=10;
legend('Drilling', '100 dB sound', '85 dB sound');
```

B.2 Equivalent Sound Pressure Level

In this section, RW velocity in response to drilling is converted to equivalent sound pressure level using the METF values measured prior drilling across frequencies. To fully utilise the high-resolution frequency series of experimental data, instead of sacrificing the resolution to obtain a series of mean values at discrete points where METF values were measured, a METF curve is obtained via interpolation based on the discrete METF values. The MATLAB code for such implementation is shown below.

```
%% METF Interpolation
[~,I_lower] = min(abs(f-frequency(1)));
[~,I_upper] = min(abs(f-frequency(end)));
interpolationFrequency = f(I_lower: I_upper);
METF_interpolated =
spline(frequency,METF,interpolationFrequency);

%% Eq SPL calculation
Drilling = amplitude(I_lower: I_upper);
Eq_Drilling = Drilling./METF_interpolated'; % unit:Pa
Eq_DrillingdB = 20.*log10(Eq_Drilling./(2.0000e-05)); %
unit:dB
figure;
p3=semilogx(interpolationFrequency,Eq_DrillingdB);hold
on;grid on;
xlim([100 max_display_frequency ]);
ylim([40 110]);
xlabel('Frequency (Hz)');
ylabel('Equivalent Sound Pressure Level (dB)');
```

B.3 Equivalent Sound Pressure Level against Time

In this section, the algorithm to generate the time-varying equivalent sound pressure level is presented. A sliding window is applied on the time series experimental data, and within each window a equivalent sound pressure level is calculated using the METF curve obtained from Section B2.

The length of the sliding window along time axis is selected to be equal to one percent of the total length of a complete cochleostomy that has been validly recorded. This provides a common ground for comparing robotic and conventional drilling where only disturbance at the same operational stage is compared. Depending on the specific length of each cochleostomy drilling, the window size varies from 0.49s to 4.78s. A collection of window lengths and corresponding resolution in spectral analysis is listed in Table B.3-1. The lower end of the frequency range that is of interest is higher than the frequency resolution in all cases therefore the information is retained.

Table B.3 - 1 | Length of the sliding window in time domain and its corresponding frequency resolution in frequency domain for each measurement

Measurement #	Window Length of Time (s)	Frequency Resolution (Hz)
Conventional A	1.93	0.52
Robotic A	0.87	1.15
Conventional B	1.19	0.84
Robotic B	4.78	0.21
Conventional C	2.10	0.48
Robotic C	0.49	2.03

Short-time Fourier transform is the main methodology used to generate the time-resolved velocity measurement. An overlap of 2/3 of a window between adjoining sections is used in processing. This is to account for the tapering at the edge of the window, The MATLAB default hamming window was used to window the sections in order to minimise the effect of spectral leakage.

```
load('trace_var_filtered_driftCorrected.mat');
load('C_METFRW2L.mat');
trace_test = nonzeros(trace_test3);

Fs = 48000;
windowLength = round(length(trace_test)*0.01);
overlapPortion = 2/3;
overlapLength = round(windowLength*overlapPortion);

time = (windowLength*1: (windowLength-overlapLength):
length(trace_test))./Fs;
N = 2^nextpow2(windowLength);
f = Fs/2*linspace(0,1,N/2+1); %Fs/2 is the Nyquist
frequency

%% METF Interpolation
[~,I_lower] = min(abs(f-frequency(1)));
[~,I_upper] = min(abs(f-frequency(end)));
interpolationFrequency = f(I_lower: I_upper);
METF_interpolated =
spline(frequency,METF,interpolationFrequency);

%% STFT
s =
spectrogram(trace_test,windowLength,round(windowLength*
overlapPortion),N,Fs,'onesided');
dB_overtime = zeros(size(s,2),1);
dBA_overtime = zeros(size(s,2),1);
for i=1:size(s,2)
    amplitude = 2*abs(s(1:N/2+1,i))/windowLength;
    %% Eq SPL calculation, rms instead of peak to
obtain spectral sum
    Drilling_rms = amplitude(I_lower: I_upper)./sqrt(2);
    Eq_DrillingPa = Drilling_rms./METF_interpolated'; %
unit:Pa
```

```
    Eq_DrillingdB_sum =
10.*log10(sum(Eq_DrillingPa.^2)/(2.0000e-05)^2); %
unit:dB
    dB_overtime(i) = Eq_DrillingdB_sum;
end

figure;
time_normalised = time./(length(trace_test)/Fs)*100;
plot(time_normalised,dB_overtime);grid on;

xlabel('Time (% Cochleostomy Completion)');
ylabel('Sound Pressure Level (dB)');

n=sum(dB_overtime>120);
p=n/length(dB_overtime);
```

Appendix C

RW response and the Movement Measured at the Piezo Actuator Tip

In the assessment of TW's effect on RW response using a porcine cochlea – covered in Chapter 4, both sets of raw data of velocity magnitude measured on RW has dominant peaks located at 4 kHz. This resonance at 4kHz is not expected as part of the natural response of RW. It is possible though that the source of this resonance is within the stimulus part, i.e. the actuation setup. This was confirmed in a separate experiment where the velocity of the piezo tip was measured in isolation and resonance was found at a similar place at the same frequency band, as can be seen in Figure C-1. Apart from the non-linearity, the movement measured at the piezo actuator tip is not at a constant level across the frequency band of interest. It is therefore sensible to separate out the effect of the piezo

actuator movement on its own by normalising RW responses against the piezo actuator movement. The results can be shown in Figure 4.3-1 in Chapter 3.

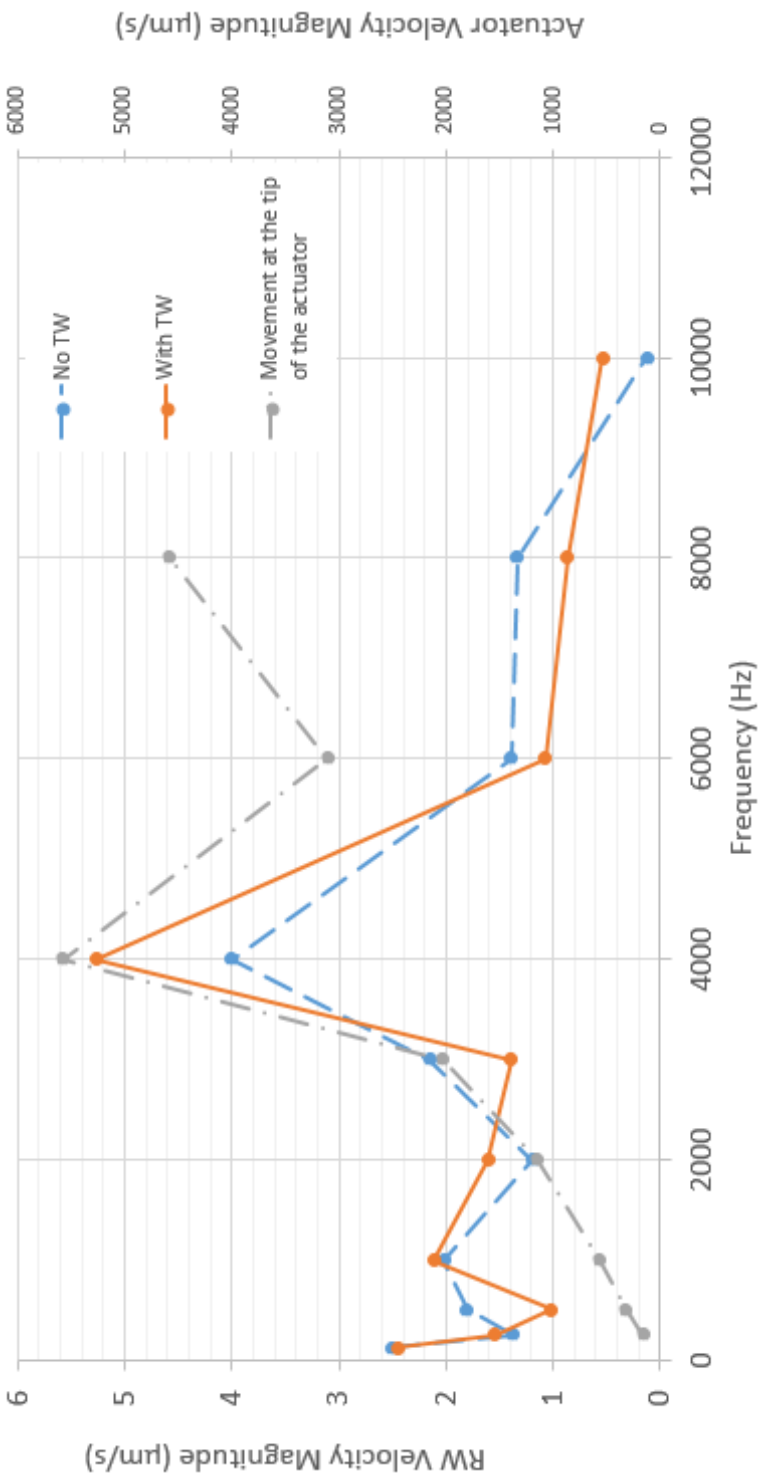

Figure C - 1 | Raw Cochlea RW Velocity Magnitude before (blue dashed line) & after (red solid line) the creation of a TW against the velocity measured at the tip of the cochlea (grey dash dotted line)

References

Action on Hearing Loss. (2012). Everything you need to know about getting hearing aids. The Royal National Institute for Deaf People.

Action On Hearing Loss. (2011). Taking action on hearing loss in the 21st century, 1–82.

Ahlbom, A., Bridges, J., De Jong, W., Hartemann, P., Jung, T., Mattsson, M.-O., … Thomsen, M. (n.d.). Scientific Committee on Emerging and Newly Identified Health Risks SCENIHR Potential health risks of exposure to noise from personal music players and mobile phones including a music playing function Health risks from exposure to noise from personal music players 3 ACKNOWLEDGMENTS. Retrieved from http://ec.europa.eu/health/ph_risk/risk_en.htm

Aibara, R., Welsh, J. T., Puria, S., & Goode, R. L. (2001). Human middle-ear sound transfer function and cochlear input impedance. *Hearing Research*, *152*(1–2), 100–109. https://doi.org/10.1016/S0378-5955(00)00240-9

Assadi, M. Z. (2011). *An Investigation of Cochlear Dynamics in Surgical and Implantation Processes*. Retrieved from http://bura.brunel.ac.uk/bitstream/2438/7966/1/FulltextThesis.pdf.

Assadi, M. Z., Du, X., Dalton, J., Henshaw, S., Coulson, C. J., Reid, A. P., … Brett, P. N. (2013). Comparison on intracochlear disturbances between drilling a manual and robotic cochleostomy. *Proceedings of the Institution of Mechanical Engineers. Part H, Journal of Engineering in Medicine*, *227*(9), 1002–1008. https://doi.org/10.1177/0954411913488507

ASTM F2504 - 05, Standard Practice for Describing System Output of Implantable Middle Ear Hearing Devices. (2005). West Conshohocken, PA: ASTM International. https://doi.org/10.1520/F2504-05

Benesty, J., Sondhi, M. M., & Huang, Y. (2007). *Springer Handbook of Speech Processing*. Springer Berlin Heidelberg. Retrieved from https://books.google.co.uk/books?id=Slg10ekZBkAC

Brant, J. A., & Ruckenstein, M. J. (2016). Electrode selection for hearing preservation in cochlear implantation: A review of the evidence. *World Journal of Otorhinolaryngology - Head and Neck Surgery*, *2*(3), 157–160. https://doi.org/10.1016/J.WJORL.2016.08.002

Brett, P. N., Taylor, R. P., Du, X., Proops, D., Griffiths, M. V, & Coulson, C. (2009). A Smart Generic Micro-drilling Tool Applied in Cochleostomy. In O. Dössel & W. C. Schlegel (Eds.), *World Congress on Medical Physics and Biomedical Engineering, September 7 - 12, 2009, Munich, Germany: Vol. 25/6 Surgery, Nimimal Invasive Interventions, Endoscopy and Image Guided Therapy* (pp. 314–316). Berlin, Heidelberg: Springer Berlin Heidelberg. https://doi.org/10.1007/978-3-642-03906-5_86

Cipolla, M. J., Iyer, P., Dome, C., Welling, D. B., & Bush, M. L. (2012).

Modification and comparison of minimally invasive cochleostomy techniques: A pilot study. *The Laryngoscope*, *122*(5), 1142–1147. https://doi.org/10.1002/lary.23231

Cohen-Mansfield, J., & Taylor, J. W. (2004). Hearing Aid Use in Nursing Homes, Part 2: Barriers to Effective Utilization of Hearing Aids. *Journal of the American Medical Directors Association*, *5*(5), 289–296. https://doi.org/10.1016/S1525-8610(04)70018-3

Coulson, C. J., Reid, A. P., Proops, D. W., & Brett, P. N. (2007). ENT challenges at the small scale. *The International Journal of Medical Robotics + Computer Assisted Surgery : MRCAS*, *3*(2), 91–96. https://doi.org/10.1002/rcs.132

Dalchow, C. V., Hagemeier, K. C., Muenscher, A., Knecht, R., & Kameier, F. (2013). Investigation of noise levels generated by otologic drills. *European Archives of Oto-Rhino-Laryngology*, *270*(2), 505–510. https://doi.org/10.1007/s00405-012-2012-9

de Boer, E. (1991). Auditory physics. Physical principles in hearing theory. III. *Physics Reports*, *203*(3), 125–231. https://doi.org/10.1016/0370-1573(91)90068-W

De Boer, E. (1996). Mechanics of the Cochlea: Modeling Efforts. In P. Dallos, A. N. Popper, & R. R. Fay (Eds.), *The Cochlea* (pp. 258–317). New York, NY: Springer New York. https://doi.org/10.1007/978-1-4612-0757-3_5

Dhanasingh, A., & Jolly, C. (2017). An overview of cochlear implant electrode array designs. *Hearing Research*, *356*, 93–103.

https://doi.org/10.1016/J.HEARES.2017.10.005

Escudé, B., James, C., Deguine, O., Cochard, N., Eter, E., & Fraysse, B. (2006). The Size of the Cochlea and Predictions of Insertion Depth Angles for Cochlear Implant Electrodes. *Audiology and Neurotology*, *11*(1), 27–33. https://doi.org/10.1159/000095611

Eze, N., Jiang, D., & Fitzgerald O'Connor, A. (2014). Inner ear energy exposure while drilling a cochleostomy. *Acta Oto-Laryngologica*, *134*(11), 1109–1113. https://doi.org/10.3109/00016489.2014.914245

Fettiplace, R., & Hackney, C. M. (2006). The sensory and motor roles of auditory hair cells. *Nature Reviews Neuroscience*, *7*(1), 19–29. https://doi.org/10.1038/nrn1828

Friedland, D. R., & Runge-Samuelson, C. (2009). Soft cochlear implantation: rationale for the surgical approach. *Trends in Amplification*, *13*(2), 124–138. https://doi.org/10.1177/1084713809336422

Gantz, B. J., & Turner, C. (2004). Combining acoustic and electrical speech processing: Iowa/Nucleus hybrid implant. *Acta Oto-Laryngologica*, *124*(4), 344–347. https://doi.org/10.1080/00016480410016423

Gantz, B. J., Turner, C., Gfeller, K. E., & Lowder, M. W. (2005). Preservation of Hearing in Cochlear Implant Surgery: Advantages of Combined Electrical and Acoustical Speech Processing. *Laryngoscope*, *115*(May), 796–802. https://doi.org/10.1097/01.MLG.0000157695.07536.D2

Gantz, B. J., Turner, C. W., & Correspondence, S. (2003). Combining Acoustic

and Electrical Hearing. *Laryngoscope*, *113*(October), 1726–1730. https://doi.org/10.1097/00005537-200310000-00012

Gerald, C. F., & Wheatley, P. O. (2004). *Applied Numerical Analysis*. Pearson/Addison-Wesley. Retrieved from https://books.google.co.uk/books?id=BiOZQgAACAAJ

Gifford, R. H., Dorman, M. F., Shallop, J. K., & Sydlowski, S. A. (2010). Evidence for the expansion of adult cochlear implant candidacy. *Ear and Hearing*, *31*(2), 186–194. https://doi.org/10.1097/AUD.0b013e3181c6b831

González-Prida, V. (2015). *Promoting Sustainable Practices through Energy Engineering and Asset Management*. IGI Global. Retrieved from https://books.google.co.uk/books?id=ay51CQAAQBAJ

Gross??hmichen, M., Salcher, R., Kreipe, H. H., Lenarz, T., & Maier, H. (2015). The Codacs??? direct acoustic cochlear implant actuator: Exploring alternative stimulation sites and their stimulation efficiency. *PLoS ONE*, *10*(3), 1–20. https://doi.org/10.1371/journal.pone.0119601

Guyer, P. (2009). *Engineering SoundBite: Fundamentals of Acoustics*. Guyer Partners. Retrieved from https://books.google.co.uk/books?id=u_DyySh9LwYC

HaiJin, Y., Weiwei, G., Lei, C., Na, W., JiaNa, L., LiLi, R., & ShiMing, Y. (2013). Microdissection of Miniature Pig Ear. *Journal of Otology*, *8*(2), 91–96. https://doi.org/10.1016/S1672-2930(13)50019-5

Hallmo, P., & Mair, I. W. S. (1996). Drilling in Ear Surgery: A Comparison of

Pre- and Postoperative Bone-conduction Thresholds in both the Conventional and Extended High-frequency Ranges. *Scandinavian Audiology*, *25*(1), 35–38. https://doi.org/10.3109/01050399609047553

Hardy, M. (1938). The length of the organ of Corti in man. *American Journal of Anatomy*, *62*(2), 291–311. https://doi.org/10.1002/aja.1000620204

Haynes, D. S., Young, J. a, Wanna, G. B., & Glasscock, M. E. (2009). Middle Ear Implantable Hearing Devices: An Overview. *Trends in Amplification*, *13*(3), 206–214. https://doi.org/10.1177/1084713809346262

Hickey, S. A., & O'Connor, A. F. (1991). Measurement of drill-generated noise levels during ear surgery. *The Journal of Laryngology and Otology*, *105*(9), 732–735.

Hosek, P. (2012). Algorithm for signal drop-out recognition in IC engine valve kinematics signal measured by laser Doppler vibrometer. *Optics & Laser Technology*, *44*(4), 1101–1112. https://doi.org/10.1016/J.OPTLASTEC.2011.09.034

Huebner, K. H. (2001). *The Finite Element Method for Engineers*. Wiley. Retrieved from https://books.google.co.uk/books?id=f3MZE1BYq3AC

International Electrotechnical Commission. (2002). Letter symbols to be used in electrical technology – Part 3: Logarithmic and related quantities, and their units. *IEC 60027-3 Ed. 3.0*.

James, C., Albegger, K., Battmer S. Deggouj, N. Deguine, O., R. B., Dillier, N., Gersdorff, M., Laszig, R., … Fraysse, B. (2005). Preservation of residual

hearing with cochlear implantation: how and why. *Acta Otolaryngol*, *125*(5), 481–491. https://doi.org/10.1080/00016480510026197

Jiang, D., Bibas, A., Santuli, C., Donnelly, N., Jeronimidis, G., & O'Connor, A. F. (2007). Equivalent noise level generated by drilling onto the ossicular chain as measured by laser Doppler vibrometry: a temporal bone study. *The Laryngoscope*. https://doi.org/10.1097/MLG.0b013e3180459a10

Jorge, J. R., Zenner, H. P., Hemmert, W., Burkhardt, C., & Gummer, A. W. (1997). Laser vibrometry. A middle ear and cochlear analyzer for noninvasive studies of middle and inner ear function disorders. *HNO*, *45 12*, 997–1007.

Kagawa, Y., Yamabuchi, T., Watanabe, N., & Mizoguchi, T. (1987). Finite element cochlear models and their steady state response. *Journal of Sound and Vibration*, *119*(2), 291–315. https://doi.org/10.1016/0022-460X(87)90456-1

Kale, S. S., & Olson, E. S. (2015). Intracochlear Scala Media Pressure Measurement: Implications for Models of Cochlear Mechanics. *Biophysical Journal*, *109*(12), 2678–2688. https://doi.org/10.1016/j.bpj.2015.10.052

Kemp, D. T. (1978). Stimulated acoustic emissions from within the human auditory system. *The Journal of the Acoustical Society of America*, *64*(5), 1386–1391. https://doi.org/10.1121/1.382104

Kiefer, J., Gstoettner, W., Baumgartner, W., Pok, S. M., Tillein, J., Ye, Q., & von Ilberg, C. (2004). Conservation of low-frequency hearing in cochlear implantation. *Acta Oto-Laryngologica*, *124*(3), 272–280.

https://doi.org/10.1080/00016480310000755a

Koshigoe, S., Kwok, W.-K., & Tubis, A. (1983). Effects of perilymph viscosity on low-frequency intracochlear pressures and the cochlear input impedance of the cat. *The Journal of the Acoustical Society of America*, *74*, 486–492.

Kwacz, M., Marek, P., Borkowski, P., & Mrówka, M. (2013). A three-dimensional finite element model of round window membrane vibration before and after stapedotomy surgery. *Biomechanics and Modeling in Mechanobiology*, *12*(6), 1243–1261. https://doi.org/10.1007/s10237-013-0479-y

Kylén, P., & Arlinger, S. (1976). Drill-generated noise levels in ear surgery. *Acta Oto-Laryngologica*, *82*(5), 402–409. https://doi.org/10.3109/00016487609120925

Kylén, P., Stjernvall, J.-E., & Arlinger, S. (1977). Variables Affecting the Drill-Generated Noise Levels in Ear Surgery. *Acta Oto-Laryngologica*, *84*(1–6), 252–259. https://doi.org/10.3109/00016487709123964

Lehnhardt, E. (1993). Intracochlear placement of cochlear implant electrodes in soft surgery technique. *Hno*, *41*(7), 356–359.

Lenarz, T., Stöver, T., Buechner, A., Lesinski-Schiedat, A., Patrick, J., & Pesch, J. (2009). Hearing Conservation Surgery Using the Hybrid-L Electrode. *Audiology and Neurotology*, *14*(1), 22–31. https://doi.org/10.1159/000206492

LePage, E. L. (1987). Frequency-dependent self-induced bias of the basilar

membrane and its potential for controlling sensitivity and tuning in the mammalian cochlea. *The Journal of the Acoustical Society of America*, *82*(1), 139–154. https://doi.org/10.1121/1.395557

Lunner, T., Rudner, M., & R??nnberg, J. (2009). Cognition and hearing aids. *Scandinavian Journal of Psychology*, *50*(5), 395–403. https://doi.org/10.1111/j.1467-9450.2009.00742.x

Luxenberger, W., Lahousen, T., & Walch, C. (2012). Suction-generated noise in an anatomic silicon ear model. *European Archives of Oto-Rhino-Laryngology*, *269*(10), 2291–2293. https://doi.org/10.1007/s00405-012-2090-8

Lyon, R. F. (1990). AUTOMATIC GAIN CONTROL IN COCHLEAR MECHANICS, 395–402. Retrieved from http://www.dicklyon.com/tech/Hearing/AGC_MOH1990-Lyon.pdf

Lyon, R. R., & Mead, C. A. (1989). Cochlear Hydrodynamics Demystified. *Caltech Computer Science Technical Report*.

Martarelli, M., & Revel, G. M. (2006). Laser Doppler vibrometry and near-field acoustic holography: Different approaches for surface velocity distribution measurements. *Mechanical Systems and Signal Processing*, *20*(6), 1312–1321. https://doi.org/10.1016/j.ymssp.2005.11.011

Mittmann, M., Ernst, A., Mittmann, P., & Todt, I. (2016). Insertional depth-dependent intracochlear pressure changes in a model of cochlear implantation. *Acta Oto-Laryngologica*, *6489*(September), 1–6. https://doi.org/10.1080/00016489.2016.1219918

Mittmann, P., Ernst, A., & Todt, I. (2014). Intracochlear pressure changes due to round window opening: A model experiment. *Scientific World Journal*, *2014*, 1–8. https://doi.org/10.1155/2014/341075

Nakajima, H. H., Dong, W., Olson, E. S., Merchant, S. N., Ravicz, M. E., & Rosowski, J. J. (2009). Differential Intracochlear Sound Pressure Measurements in Normal Human Temporal Bones. *Journal of the Association for Research in Otolaryngology*, *10*(1), 23–36. https://doi.org/10.1007/s10162-008-0150-y

Nam, J.-H., & Fettiplace, R. (2010). Force Transmission in the Organ of Corti Micromachine. *Biophysical Journal*, *98*(12), 2813–2821. https://doi.org/10.1016/j.bpj.2010.03.052

Neely, S. T. (1978). *Mathematical models of the mechanics of the cochlea*. California Institute of Technology. Retrieved from California Institute of Technology

Neely, S. T. (1981). Finite difference solution of a two-dimensional mathematical model of the cochlea. Retrieved from http://m.audres.org/cel/cochmod/JASA1981.pdf

Ni, G., Elliott, S. J., Ayat, M., & Teal, P. D. (2014). Modelling Cochlear Mechanics. *BioMed Research International*, *2014*(150637), 1–42. https://doi.org/10.1155/2014/150637

Öberg, M., Marcusson, J., Nägga, K., & Wressle, E. (2012). Hearing difficulties, uptake, and outcomes of hearing aids in people 85 years of age. *International Journal of Audiology*, *51*(2), 108–115.

https://doi.org/10.3109/14992027.2011.622301

Olson, E. S. (1998). Observing middle and inner ear mechanics with novel intracochlear pressure sensors. *The Journal of the Acoustical Society of America*, *103*(6), 3445–3463. https://doi.org/10.1121/1.423083

Parkin, J. L., Wood, G. S., Wood, R. D., & McCandless, G. A. (1980). Drill- and suction-generated noise in mastoid surgery. *Archives of Otolaryngology (Chicago, Ill. : 1960)*, *106*(2), 92–96.

Pau, H. W., Just, T., Bornitz, M., Lasurashvilli, N., & Zahnert, T. (2007). Noise exposure of the inner ear during drilling a cochleostomy for cochlear implantation. *The Laryngoscope*. https://doi.org/10.1097/MLG.0b013e31802f4169

Pennings, R. J. E., Ho, A., Brown, J., Van Wijhe, R. G., & Bance, M. (2010). Analysis of vibrant soundbridge placement against the round window membrane in a human cadaveric temporal bone model. *Otology and Neurotology*, *31*(6), 998–1003. https://doi.org/10.1097/MAO.0b013e3181e8fc21

Potter, J. L., VanKarsen, C. D., DeClerck, J. P., & Sklanka, B. J. (2012). Comparison of Modal Analysis Between Laser Vibrometry and NAH Measurements (pp. 471–480). Springer, New York, NY. https://doi.org/10.1007/978-1-4614-2425-3_45

Pracy, J. P., White, A., Mustafa, Y., Smith, D., & Perry, M. E. (1998). The comparative anatomy of the pig middle ear cavity: a model for middle ear inflammation in the human? *Journal of Anatomy*, *192*, 359–368.

https://doi.org/10.1017/S0021878298003379

Puria, S., & Allen, J. B. (1991). A parametric study of cochlear input impedance. *The Journal of the Acoustical Society of America*, *89*(1), 287–309. https://doi.org/10.1121/1.400675

Rhode, W. S. (1971). Observations of the Vibration of the Basilar Membrane in Squirrel Monkeys using the Mössbauer Technique. *The Journal of the Acoustical Society of America*, *49*(4B), 1218–1231. https://doi.org/10.1121/1.1912485

Rosowski, J. J., Chien, W., Ravicz, M. E., & Merchant, S. N. (2007). Testing a method for quantifying the output of implantable middle ear hearing devices. *Audiology and Neurotology*, *12*(4), 265–276. https://doi.org/10.1159/000101474

Rosowski, J. J., Davis, P. J., Donahue, K. M., Merchant, S. N., & Coltrera, M. D. (1990). Cadaver Middle Ears as Models for Living Ears: Comparisons of Middle Ear Input Immittance. *Annals of Otology, Rhinology & Laryngology*, *99*(5), 403–412. https://doi.org/10.1177/000348949009900515

Rothberg, S. J., Baker, J. R., & Halliwell, N. A. (1989). Laser vibrometry: Pseudo-vibrations. *Journal of Sound and Vibration*, *135*(3), 516–522. https://doi.org/10.1016/0022-460X(89)90705-0

Royal National Throat Nose and Ear Hospital: Cochleaer implants for adults. (2014). University College London Hospitals NHS Foundation Trust.

Russell, I. J. (2008). Cochlear Receptor Potentials. In *The Senses: A*

Comprehensive Reference (Vol. 3, pp. 319–358). Elsevier. https://doi.org/10.1016/B978-012370880-9.00030-X

Scheffer, C., & Girdhar, P. (2004). *Practical Machinery Vibration Analysis and Predictive Maintenance*. Elsevier Science. Retrieved from https://books.google.co.uk/books?id=tAvTO1t2mwkC

Schnupp, J., Nelken, I., & King, A. (2011). *Auditory Neuroscience: Making Sense of Sound*. MIT Press. Retrieved from https://books.google.co.uk/books?id=xbG4R8uHsG8C

Sikka, K., Kairo, A., Singh, C. A., Roy, T. S., Lalwani, S., Kumar, R., … Sharma, S. C. (2017). An Evaluation of the Surgical Trauma to Intracochlear Structures After Insertion of Cochlear Implant Electrode Arrays: A Comparison by Round Window and Antero-Inferior Cochleostomy Techniques. *Indian Journal of Otolaryngology and Head & Neck Surgery*, 1–5. https://doi.org/10.1007/s12070-017-1143-0

Silverthorn, D. U., & Johnson, B. R. (2010). *Human physiology : an integrated approach*. Pearson Benjamin Cummings. Retrieved from https://brunel.ent.sirsidynix.net.uk/client/en_GB/default/search/detailnonmodal/ent:$002f$002fSD_ILS$002f0$002fSD_ILS:473344/one?qu=DOC_ID%3D%22473344%22&te=ILS

Spencer, M. G., & Reid, A. (1985). Drill-generated noise levels in mastoid surgery. *The Journal of Laryngology and Otology*, *99*(10), 967–972.

Steele, C. R., & Taber, L. A. (1979). Comparison of WKB and finite difference calculations for a two-dimensional cochlear model, *65*(59), 1001–1007.

https://doi.org/10.1121/1.382569

Steele, C. R., & Zais, J. G. (1985). Effect of coiling in a cochlear model. *The Journal of the Acoustical Society of America*, *77*(77). https://doi.org/10.1121/1.392227

Stenfelt, S., Hato, N., & Goode, R. L. (2004a). Fluid volume displacement at the oval and round windows with air and bone conduction stimulation. *The Journal of the Acoustical Society of America*, *115*(2), 797–812. https://doi.org/10.1121/1.1639903

Stenfelt, S., Hato, N., & Goode, R. L. (2004b). Round window membrane motion with air conduction and bone conduction stimulation. *Hearing Research*, *198*(1–2), 10–24. https://doi.org/10.1016/j.heares.2004.07.008

Strömberg, A.-K., Yin, X., Olofsson, A., & Duan, M. (2010). Evaluation of the usefulness of a silicone tube connected to a microphone in monitoring noise levels induced by drilling during mastoidectomy and cochleostomy. *Acta Oto-Laryngologica*, *130*(10), 1163–1168. https://doi.org/10.3109/00016481003743050

Taylor, R., Du, X., Proops, D., Reid, A., Coulson, C., & Brett, P. N. (2010). A sensory-guided surgical micro-drill. *Proceedings of the Institution of Mechanical Engineers, Part C: Journal of Mechanical Engineering Science*, *224*(7), 1531–1537. https://doi.org/10.1243/09544062JMES1933

The American Hearing Research Foundation. (2008). Noise induced hearing loss. Retrieved January 1, 2016, from http://american-hearing.org/disorders/noise-induced-hearing-loss/

Tomita, M., Mann, W. C., & Welch, T. R. (2001). Use of assistive devices to address hearing impairment by older persons with disabilities. *International Journal of Rehabilitation Research. Internationale Zeitschrift Fur Rehabilitationsforschung. Revue Internationale de Recherches de Readaptation*, *24*(4), 279–289. Retrieved from http://www.ncbi.nlm.nih.gov/pubmed/11775032

Turner, C. W., Gantz, B. J., Karsten, S., Fowler, J., & Reiss, L. A. (2010). Impact of Hair Cell Preservation in Cochlear Implantation. *Otology & Neurotology*, *31*(8), 1227–1232. https://doi.org/10.1097/MAO.0b013e3181f24005

Urquhart, A. C., McIntosh, W. A., & Bodenstein, N. P. (1992). Drill-generated sensorineural hearing loss following mastoid surgery. *The Laryngoscope*, *102*(6), 689–692. https://doi.org/10.1288/00005537-199206000-00016

Verhaert, N., Walraevens, J., Desloovere, C., Wouters, J., & Gérard, J.-M. (2016). Direct Acoustic Stimulation at the Lateral Canal: An Alternative Route to the Inner Ear? *PLOS ONE*, *11*(8), e0160819. https://doi.org/10.1371/journal.pone.0160819

von Békésy, G., & Peake, W. T. (1990). Experiments in Hearing. *The Journal of the Acoustical Society of America*, *88*(6), 2905–2905. https://doi.org/10.1121/1.399656

vonIlberg, C., Kiefer, J., Tillein, J., Pfenningdorff, T., Hartmann, R., Stürzebecher, E., & Klinke, R. (1999). Electric-Acoustic Stimulation of the Auditory System. *ORL*, *61*(6), 334–340. https://doi.org/10.1159/000027695

Voss, S. E., Rosowski, J. J., Merchant, S. N., & Peake, W. T. (2000). Acoustic

responses of the human middle ear. *Hearing Research*, *150*(1–2), 43–69. https://doi.org/10.1016/S0378-5955(00)00177-5

Vuorialho, A., Karinen, P., & Sorri, M. (2006). Counselling of hearing aid users is highly cost-effective. *European Archives of Oto-Rhino-Laryngology*, *263*(11), 988–995. https://doi.org/10.1007/s00405-006-0104-0

Wilson, J. P. (1980). Evidence for a cochlear origin for acoustic re-emissions, threshold fine-structure and tonal tinnitus. *Hearing Research*, *2*(3–4), 233–252. https://doi.org/10.1016/0378-5955(80)90060-X

Wilson, J. P., & Johnstone, J. R. (1975). Basilar membrane and middle-ear vibration in guinea pig measured by capacitive probe. *The Journal of the Acoustical Society of America*, *57*(3), 705–723. https://doi.org/10.1121/1.380472

Yin, X., Strömberg, A.-K., & Duan, M. (2011). Evaluation of the noise generated by otological electrical drills and suction during cadaver surgery. *Acta Oto-Laryngologica*, *131*(11), 1132–1135. https://doi.org/10.3109/00016489.2011.600725

Yu, H., Tong, B., Zhang, Q., Zhu, W., & Duan, M. (2014). Drill-induced noise level during cochleostomy. *Acta Oto-Laryngologica*, *134*(9), 943–946. https://doi.org/10.3109/00016489.2014.927591